

A STUDY OF THE  
OPAQUE MINERALS  
IN THE  
WHITESTONE ANORTHOSITE,  
DUNCHURCH, ONT.

A STUDY  
OF THE OPAQUE MINERALS OF THE WHITESTONE ANORTHOSITE,  
Dunchurch, Ontario

By  
ULRICH HORST KRETSCHMAR, B.Sc. (McMaster)

A Thesis

Submitted to the Faculty of Graduate Studies  
in Partial Fulfilment of the Requirements  
for the Degree  
Master of Science

McMaster University

May 1968

"Bald wirst du das alles vergessen haben,  
bald von allen vergessen sein."

Selbstbetrachtungen, VII. Buch.

Marcus Aurelius

## ABSTRACT

A textural and mineralogical study of the magnetite, hemo-ilmenite and minor sulfide phases of the Whitestone anorthosite, Dunchurch, Ontario, was carried out. The composition of magnetite and hemo-ilmenite was determined by chemical analysis, X-ray diffraction and electron probe microanalysis. A modification of the solvus shape in the hematite-ilmenite system consistent with the composition of hemo-ilmenite lamellae, as well as a mechanism for formation of metamorphic magnetite porphyroblasts from ferrian-ilmenite is proposed. Buddington and Lindsley's experimental data cannot be used directly to obtain  $f_{O_2}$  and T of formation of the anorthosite because compositions fall in the highly oxidizing and as yet undetermined portion of their diagram.

## ACKNOWLEDGEMENTS

I wish to thank Dr. R. H. McNutt for his encouragement, directorship and the many benefits derived from his counsel during the course of this study.

To the graduate students at McMaster, particularly Ian Mason and Dave Jennings, whose incisive questions have helped clarify my own ideas, I extend special thanks.

I am grateful to Drs. D. H. Lindsley, A. J. Naldrett and H. P. Schwarcz for helpful discussions and advice at various stages during this study.

I acknowledge the liberal financial support of the Geological Survey of Canada.

Finally to Dianne, very special thanks for being such a critical editor, expert draughtswoman and constant helpful companion throughout this study.

## TABLE OF CONTENTS

	<u>Page</u>
I. Introduction	1
II. Brief Review of Pertinent Literature on Oxide Mineralogy	2
Terminology	2
Oxide Minerals in Igneous Rocks	5
Oxide Phases in Metamorphic Rocks	8
Electron Probe Analyses of Oxides	10
III. General Geology of the Area and Sample Localities	12
IV. Petrographic Description	
IV-1: Transmitted Light Microscopy	15
Introduction	15
Plagioclase	18
Pyroxene	18
Hornblende	19
Garnet	20
Opaques	20
Accessories and Alteration Products	22
Samples C-2, C-17, C-5A, C-5B and C-6	23
IV-2: Reflected Light Microscopy	
Introduction	25
Spinel Phase	25
Rhombohedral Phases	26
Relative Abundance of the Opaques	28
Microfabric of the Oxides	28
Samples C-2, C-17, C-5A, C-5B and C-6	31
Summary	33
V. Analytical Investigation	
V-1: Chemical Analyses of Oxide Concentrates and Whole Rock Samples	34
Discussion of the Chemical Analyses	37

TABLE OF CONTENTS (cont'd)

	<u>Page</u>
V-2: Electron Probe Analysis of Oxides	
Introduction	40
Operating Conditions	40
Composition of the Standards	41
Electron Probe Analyses	41
Qualitative Line Scan	50
Correction Procedures for Analyses	51
Discussion of the Electron Probe Analyses	53
V-3: X-Ray Diffraction Investigation	
A. Unit Cell Determination of the Magnetite	56
Discussion of the Unit Cell Data	58
B. Determination of Hemo-Ilmenite Composition	59
Discussion of Hemo-Ilmenite Composition	
Determinations	63
VI. Discussion and Interpretation of Results	
VI-1: Composition of the Opaque Minerals in the Whitestone	
Anorthosite	65
Magnetite	65
Rhombohedral Phases	68
Sulphides	73
Samples C-5A, C-5B and C-2	73
VI-2: Explanation of the Reaction Rims in Hemo-Ilmenite	
Adjacent to Magnetite	75
VI-3: Speculations About $f_{O_2}$ and T Conditions During	
Formation of the Oxides	81
VII. Suggestions for Further Work	83
<u>Appendices</u>	
<u>Appendix A: Mineral Separation Methods</u>	
I Crushing and Preliminary Separation	A1
II Heavy Liquid Separation	A3

TABLE OF CONTENTS (cont'd)

	<u>Page</u>
<u>Appendix B:</u> Sample and Standard Preparation for Electron Probe Microanalysis	B1
<u>Appendix C:</u> Description of Electron Probe Standards	C1
<u>Appendix D:</u> Description and Application of the CURVFT Fortran IV Program	D1
<u>Appendix E:</u> Recalculation Procedures for Electron Probe and Chemical Analyses	E1
<u>Appendix F:</u> Electron Probe Data Corrections and Evaluations of Errors	F1
I Example of Calculations for Hematite-Ilmenite Grain from Sample C-5B	F1
II Conclusions	F6
Bibliography	Z1

LIST OF TABLES

<u>Table</u>	<u>Page</u>
IV-1-1: Description of Handspecimens	16
IV-1-2: Modal Analyses of Gabbroic Anorthosite Samples	17
V-1-1: Chemical Analyses of Magnetite Concentrates (wt.%)	35
V-1-2: Chemical Analyses of Hemo-Ilmenite Concentrates and Whole Rock Samples (wt.%)	36
V-2-1: Composition of the Electron Probe Standards (wt.%)	42
V-2-2: Electron Probe Analyses of Magnetite	43
V-2-3: Electron Probe Analyses of Ilmenite Grains	44
V-2-4: Electron Probe Analyses of Hematite and Ilmenite Lamellae	46
V-2-5: Spectrographic Analysis of Magnetite and Ilmenite from Sample C-2	54
V-3-1: Unit Cell Determination of Magnetite	57
V-3-2: Unit Cell Dimensions of Pure Magnetites	58
V-3B-1: Composition of the Hemo-Ilmenite Separates Determined by X-Ray Diffraction	62
A-1: Silicate Contaminants in Oxide Separates	A4
C-1: Description of Electron Probe Standards	C1
E-1: Analysis of C-15 Hemo-Ilmenite Separate (wt.%) and Recalculation to mol.% Hem-Ilm	E3
F-1: Values of Critical Parameters for Absorption Correction	F4
F-2: Effect of Corrections on Original Concentration	F6

LIST OF FIGURES

<u>Figure</u>	<u>Page</u>
II-1: Phases in the System $\text{FeO-Fe}_2\text{O}_3\text{-TiO}_2$	4
II-2: Projection on to $f_{\text{O}_2}$ -T Plane of Conjugate Surfaces in $f_{\text{O}_2}$ -T-X Space	7
III-3: Sample Locations in Whitestone Anorthosite	14
V-2-1 A: Electron Beam Traverse of Hemo-Ilmenite Grain Adjacent to Magnetite	49
B: Nature of 2nd Generation Exsolved Ilmenite	49
V-3B-1: Relative Intensity ( $I_{(104)\text{Ilm}}/I_{(104)\text{Hem}}$ ) vs. wt.% Hematite	61
VI-1: Distribution of MnO Between Coexistent Titaniferous Magnetites and Ilmenite (or Ferrianilmenite)	66
VI-2: C. M. Carmichael's (1961) Solvus and Suggested Solvus Consistent with Composition of Hemo-Ilmenites in Whitestone Anorthosite	71
VI-3: Isothermal Sections Showing Tie Lines Between Coexisting $\text{Mte-Usp}_{\text{SS}}$ and $\text{Hem-Ilm}_{\text{SS}}$ for Several Buffers	79
A-1: Summary of Oxide Separation Procedure	A2
D-1 Listing of CURVFT Program	D5
D-2:: Sample Input for CURVFT Program	D9
D-3: Sample Output for Determination of $\text{TiO}_2$ in Rhombohedral Phases	D10

## I INTRODUCTION

This study is in part a response to Buddington and Lindsley's call for detailed studies of the oxide minerals from varied terrains. An attempt is made to obtain information about the intensive parameters, temperature and fugacity of oxygen, prevailing during the formation and subsequent metamorphism of the oxides in the foliated, gabbroic border facies of the Whitestone anorthosite.

To this end, a detailed textural, mineralogical and chemical study of the opaque minerals has been conducted, primarily by use of reflected light microscopy, X-ray diffraction and electron microprobe techniques.

Information obtainable from textural studies of minerals was limited until the fairly recent advent of the electron probe. Data gained by use of this instrument has supplemented information on exsolution textures of the oxide minerals in the anorthosite.

## II BRIEF REVIEW OF PERTINENT LITERATURE ON OXIDE MINERALOGY

### Terminology

Throughout this study, the terminology standardized by Buddington et al. (1963, p. 140) is used. The minor modifications which have been made for the sake of expediency are indicated below:

Titaniferous magnetite: a general term for a titanium bearing magnetite with no implications as to whether a one phase titanomagnetite or a magnetite with micro-intergrowths is involved.

Ilmeno-magnetite: magnetite with intergrowths of ilmenite.

Ferrianylmenite:  $\text{FeO.TiO}_2$  with 6 to 13%  $\text{Fe}_2\text{O}_3$  and up to perhaps 3 or 4% excess  $\text{TiO}_2$  in solid solution.

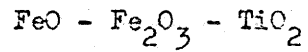
Hemo-ilmenite: ferrianylmenite with titanhematite or ilmeno-hematite in intergrowths (microintergrowths).

Titanhematite:  $\text{Fe}_2\text{O}_3$  with 10-25%  $\text{TiO}_2$  in solid solution (usually as  $\text{FeO.TiO}_2$  with a little excess  $\text{TiO}_2$ ).

Ilmeno-hematite: titanhematite with microintergrowths of ferrianylmenite or hemo-ilmenite.

As used in this study, 'ilmenite' indicates ferrianylmenite when homogeneous ilmenite is referred to, otherwise it is hemo-ilmenite. The context in which 'ilmenite' is used should leave little doubt as to its meaning. Similarly, hematite is used as a collective term for either titanhematite or ilmeno-hematite and again there should be no confusion as to which term is meant.

Fig. II-1: Composite figure of the system



Information for this figure has been summarized from Abdullah (1965), Akimoto, Nagata and Katsura (1957), Basta (1960), Buddington & Lindsley (1964), Carmichael (1961), Verhoogen (1962a). Accented phase boundaries indicate maximum extent of solid solution between end members or polymorphs at geologically reasonable temperatures (less than 1300°C). The information on this diagram is referred to in sections II & VI. ss = complete solid solution at temperatures above those indicated.

Fig. II-1

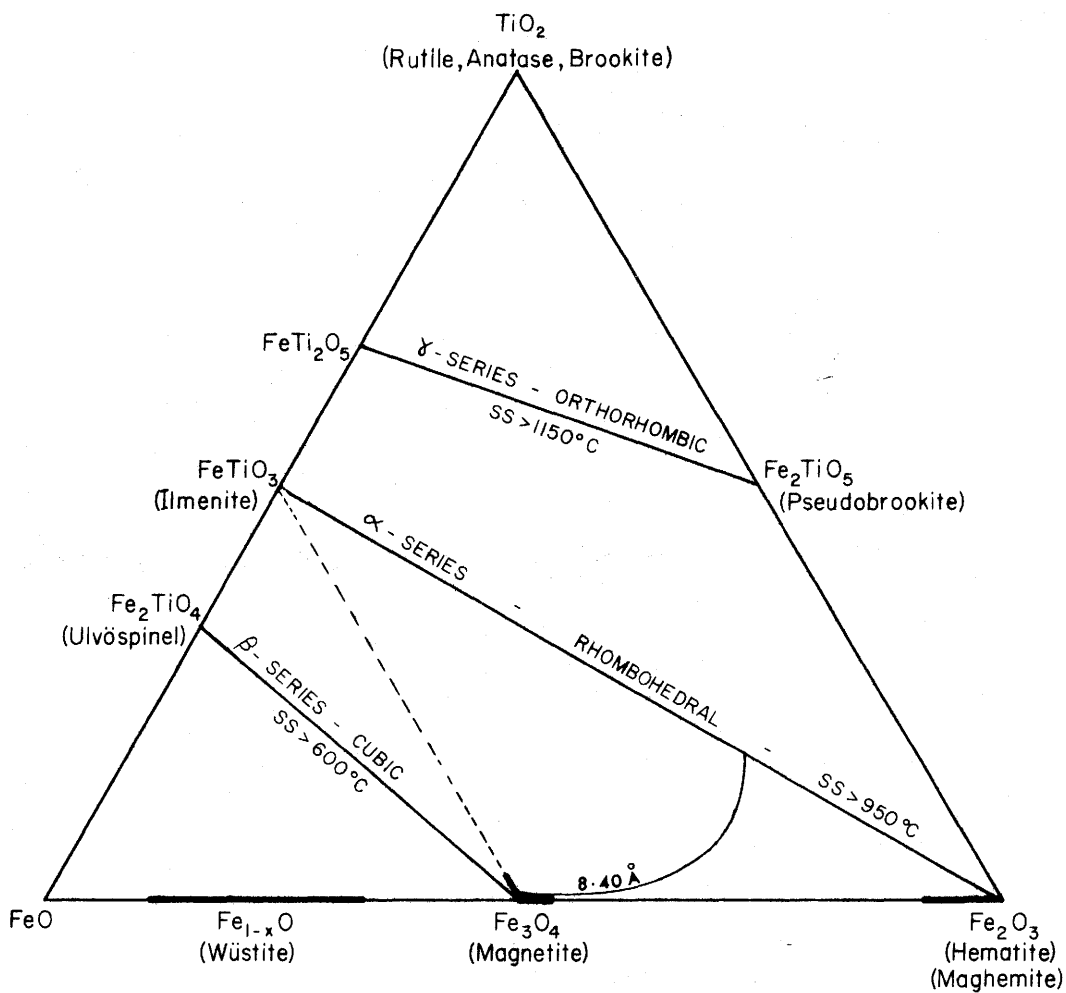


FIG. II-1: PHASES IN THE SYSTEM  $\text{FeO}-\text{Fe}_2\text{O}_3-\text{TiO}_2$

Mineral concentrates of the rhombohedral phases are sometimes referred to as hem-ilmenite concentrates.

Rhombohedral phases are minerals belonging to the hematite-ilmenite solid solution series and spinel phases belong to the magnetite-ulvospinel series.

### Oxide Minerals in Igneous Rocks

Phases in the  $\text{FeO-Fe}_2\text{O}_3\text{-TiO}_2$  system are of considerable interest in studies of rock magnetism, ore genesis and petrology. The geologically relevant portion of this system has been reproduced as Fig. II-1.

The important role of these minerals in determining the  $f_{\text{O}_2}$  and crystallization paths of igneous masses was first pointed out by Osborne (1959). Verhoogen's (1962a) summary of the changes that these minerals may undergo during oxidation was followed by Lindsley's experimental investigations of the geologically interesting phases in the  $\text{FeO-Fe}_2\text{O}_3\text{-TiO}_2$  system (Lindsley, 1962, 1963). Thus Buddington, who for many years had been investigating the chemical petrology of these minerals in the field (see Buddington et al., 1955; Buddington and Balsley, 1961; Buddington, 1964; Buddington, Fahey and Vlisidis, 1963), was able to collaborate with Lindsley to produce their 1964 paper (Buddington and Lindsley, 1964), which has proved to be of considerable import to petrology. Some of their results are briefly outlined below.

The composition of synthetically produced magnetite-ulvospinel<sub>ss</sub> and hematite-ilmenite<sub>ss</sub> in mutual equilibrium (where ss indicates solid

solution) is a function of temperature and  $f_{O_2}$ . For a given T, at successively higher  $f_{O_2}$ , magnetite-ulvospinel<sub>ss</sub> in equilibrium with hematite-ilmenite<sub>ss</sub> becomes successively lower in  $TiO_2$ . A summary of the experimental data is shown in Fig. II-2. The intersection of any two contours gives T and  $f_{O_2}$  at which the indicated titaniferous magnetite and rhombohedral phase can coexist.

This experimental data may be applied to coexisting magnetite and ilmenite from a wide variety of geological environments provided it is assumed that all  $TiO_2$  in magnetite is or was originally in the form of ulvospinel. There is convincing evidence that this is so. (see Buddington and Lindsley, 1964, p. 317, and Vincent et al., 1957, pp. 637-9). It must also be assumed that the commonly observed ilmenite lamellae in magnetite are the result of oxidation of ulvospinel, causing exsolution-like formation of ilmenite (see Buddington and Lindsley, 1964, p. 322), which will be called exsolution hereafter.

Recalculation procedures are presented that allow chemical analyses of naturally occurring oxides to be recalculated to molecular % hematite, ilmenite, ulvospinel and magnetite. In favourable circumstances these plot on Fig. II-2 and allow determination of T and  $f_{O_2}$  of formation. Uncertainties in the T and  $f_{O_2}$  determined arise mainly from the unknown effects of minor elements on the experimental data and the effect of "external granule" exsolution of ilmenite from magnetite (i.e. some ilmenite is lost from the magnetite by subsolidus oxidation and migration and the T

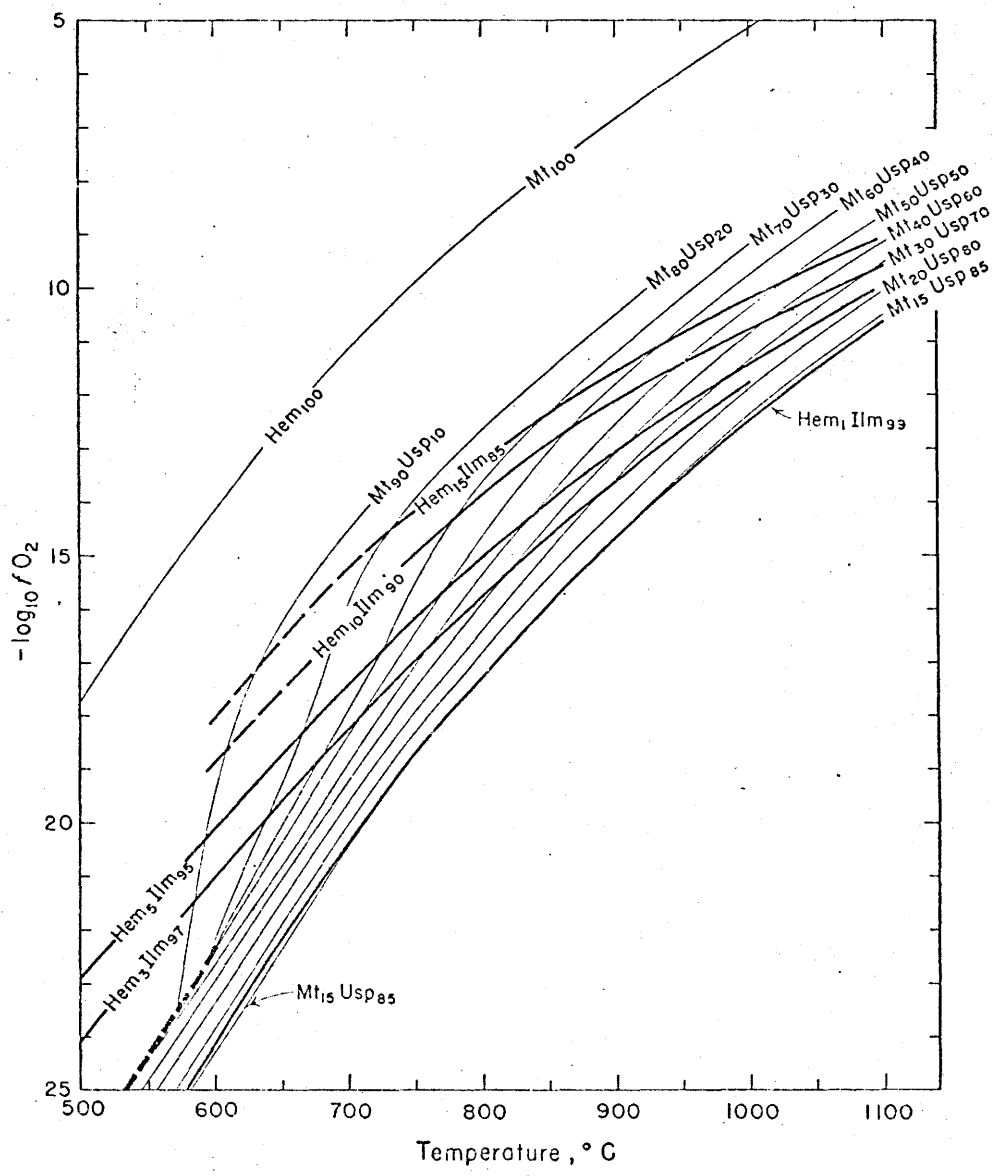


Fig. II-2: Projection onto  $f_{O_2}$ -T Plane of Conjugate Surfaces in  $f_{O_2}$ -T-X Space.

After Buddington and Lindsley, 1964, p. 316.

obtained is therefore lower than that existing at the time of formation). Secondary and deuteric alteration of the oxides will also increase uncertainties in the values of the extensive parameters determined.

Buddington and Lindsley apply their method to a wide variety of igneous and metamorphic rocks and obtain temperatures that generally compare favourably with those obtained by independent methods.

The bulk composition of most magmas is such that (titano-) magnetite and ilmenite are among the phases to crystallize together. In such instances,  $T$  and  $f_{O_2}$  determined are those obtaining during the last one quarter of the crystallization sequence of these magmas (Buddington and Lindsley, 1964, p. 329).

#### Oxide Phases in Metamorphic Rocks

Little work has been done on the behaviour of oxide minerals during metamorphism, although Eugster (1959) has discussed the effect of  $f_{O_2}$  and  $T$  changes on iron biotite, using mainly experimental data.

Buddington and Lindsley (1964) state that under dry conditions of metamorphism where the  $f_{O_2}$  is essentially that of the oxide minerals, and under 'wet' reducing conditions, an exchange reaction between exsolved ilmenite in magnetite takes place, the magnetite gaining  $Fe_2TiO_4$  and the ilmenite gaining  $Fe_2O_3$ . This is equivalent to a rotation of tie lines about a fixed bulk composition.

Abdullah and Atherton (1964) and Abdullah (1965) show magnetites from metamorphic rocks to be non-stoichiometric (containing excess  $\text{Fe}_2\text{O}_3$ , often due to late stage alteration) and low in  $\text{TiO}_2$  and  $\text{MnO}$ . The amount of  $\text{TiO}_2$  in magnetites coexisting with ilmenite shows a distinct sympathetic relationship to metamorphic grade (i.e.  $\text{TiO}_2$  is higher in magnetites from high grade rocks.) Gjelsvik (1957) showed metamorphic magnetites to contain less than 0.02 wt.%  $\text{MnO}$  and Wright (1965) found such magnetites to be 'very pure' .

The  $\text{MnO}$  contents of coexisting magnetite and ilmenite from a variety of rocks has been plotted by Buddington and Lindsley, 1964, p. 353 (reproduced here as Fig. VI-1). A well defined field of metamorphic rocks near the origin shows magnetites and ilmenites to contain less than 0.1 and 1.0 wt.%  $\text{MnO}$  respectively.

Studies of changes in oxide mineralogy with progressive metamorphism of a given rock unit have not been undertaken, but a start has been made in this direction by Schwarczy (1966), who found decreasing  $\text{Fe}_2\text{O}_3$  content in ilmenites with increasing metamorphic grade (corresponding to increasingly reducing conditions) in an arkosic quartzite.

Chinner (1960) concluded on the basis of unit cell data that magnetites from rocks with oxidation ratios varying from 6-75 showed little variation in composition. Abdullah (1965) found that considerable variation in  $\text{Fe}^{2+}/\text{Fe}^{3+}$  ratio in magnetites can occur with no corresponding change in the unit cell. Chinner's data should thus be

treated with caution.

### Electron Probe Analyses of Oxides

Electron microprobe analysis has proven particularly suited to the study of the fine grained oxides of volcanics. One of the earliest attempts in this direction was that of Ade-Hall (1964) who determined the composition of a number of ulvospinel-rich titanomagnetites from the Deccan traps. Wright and Lovering (1965) studied elemental distribution and oxidation products of some Fe-Ti sands in New Zealand. In a recent paper I.S.E. Carmichael (1967) presents some excellent quantitative analyses of coexisting magnetites and ilmenites from salic volcanic rocks.

There are a number of other recent papers (e.g. Anderson, 1965; Reed, 1965), in which the electron probe is used to determine the composition of oxides, but the above three aptly illustrate the variety of recalculation procedures in use. Ade-Hall (1964) recalculated the Fe and Ti of his titanomagnetites to wt.% ulvospinel in some unspecified manner, seemingly by simply using the Ti content plotted on a curve vs. wt.% ulvospinel. (His paper was written before Buddington and Lindsley's work was published.)

Wright and Lovering (1965) used norm calculations to apportion oxygen between  $\text{Fe}^{2+}$  and  $\text{Fe}^{3+}$  in order to recalculate the analyses to utilize Buddington and Lindsley's data. Limiting  $\text{Fe}_3\text{O}_4$  contents were calculated by assuming that all  $\text{Fe}_2\text{O}_3$  was combined with FeO as magnetite (cf. Vincent et al., 1957). The bulk compositions of his phases were obtained by the clever ruse of cutting up microphotographs of exsolved

grains and weighing them.

I.S.E. Carmichael (1967) innovated an ingenious recalculation technique which is described in Appendix E.

### III GENERAL GEOLOGY OF THE AREA AND SAMPLE LOCALITIES

Samples for this study were collected from the oxide-rich mafic aggregates in the strongly foliated, gabbroic border facies on the eastern edge of the Whitestone anorthosite near Dunchurch, Ont. (Fig. III-1). The sample localities were chosen because of the abundance of oxides and accessibility. A description of the appearance of the oxide segregations in handspecimen is presented in Table IV-1-1.

The geology of the anorthosite and immediate surroundings were the subject of a study by Lacy (1960). The following brief description is taken in part from his paper.

The anorthosite forms an elongate, dome-shaped body 6.5 km. wide and 16 km. long extending in a northeasterly direction. Near its contact with metasediments it becomes gneissose with narrowing bands and streaks richer in ferromagnesian minerals, that are concentrated in some exposures into coarse knots, notably rich in oxides. Since the contact between the border facies and the country rock is not well exposed, the geological relations are somewhat obscure.

The metamorphic history of the area is complex, a characteristic of the Grenville province. Upper amphibolite and granulite facies metamorphism is indicated and Lacy suggests that retrogressive

metamorphism has also occurred. Microtextures showing crushing and regrowth of minerals in the anorthosite are additional evidence of a complex geological history. The tectonic setting of anorthosites in the western Grenville structural province, similar in occurrence to the Whitestone anorthosite, has been described by Kranck (1961).

At present, the Whitestone anorthosite is the subject of an extensive mineralogic and petrographic investigation by I. M. Mason of McMaster University and further details of the geology will be described in his Ph.D. thesis. The geological map used for Fig. III-1 was constructed by I. M. Mason.

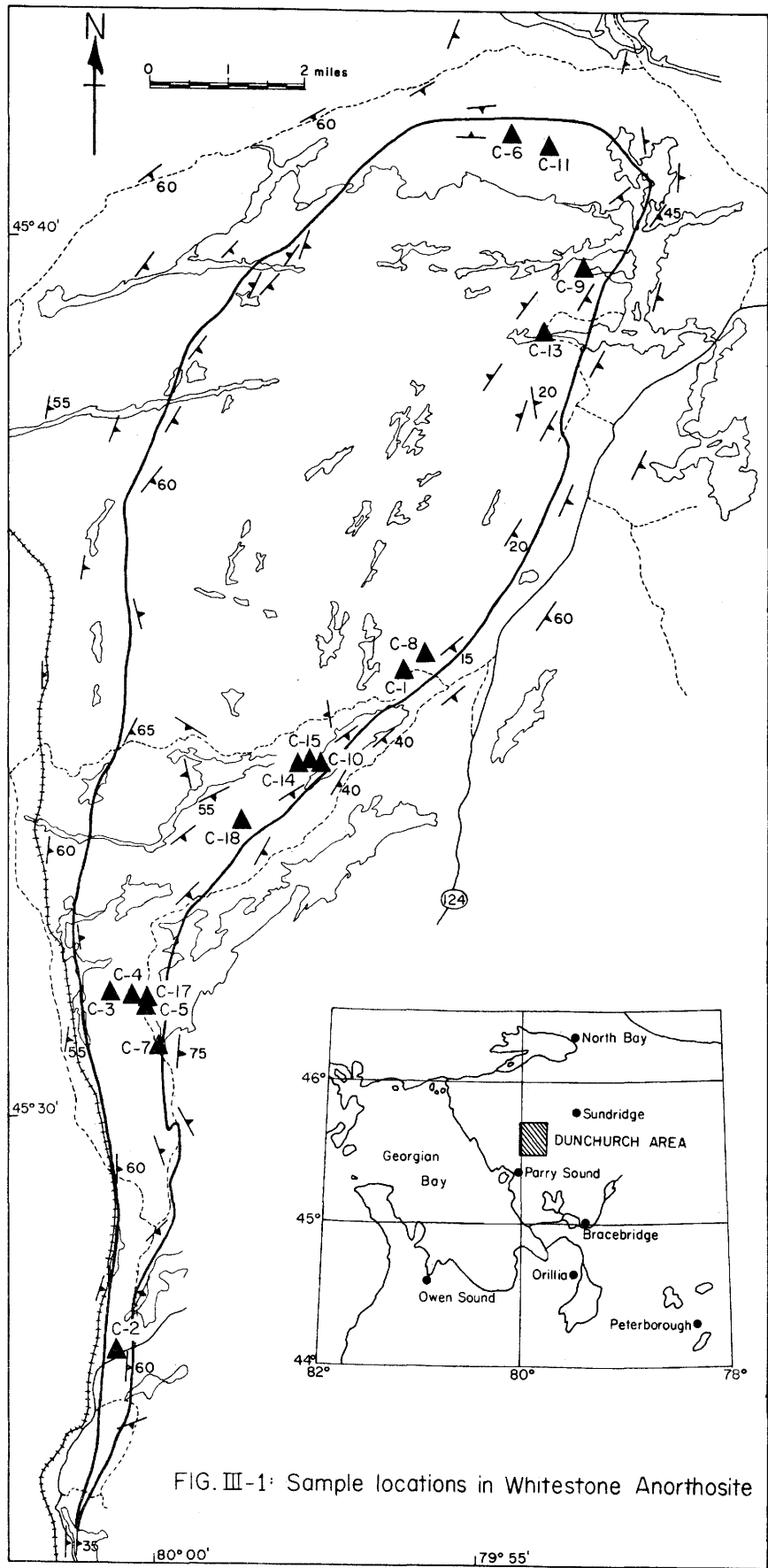


FIG. III-1: Sample locations in Whitestone Anorthosite

#### IV. PETROGRAPHIC DESCRIPTION

##### IV-1: Transmitted Light Microscopy

###### Introduction

The following description is based on the study of 53 thin sections and polished thin sections which were prepared from hand-specimens collected in the mafic-rich (gabbroic) border facies of the Whitestone anorthosite at the locations in Fig. III-1. In handspecimen the appearance of the samples varies widely as indicated in Table IV-1-1. However, microscopic study disclosed marked similarity of petrographic and textural relationships. A generalized description of mineralogic and petrographic properties as presented below is feasible, since varying proportions of plagioclase, clinopyroxene, amphibole, garnet and oxides comprise 98% of all specimens.

The specimens were collected primarily in order to study the oxides. The modes indicated in Table IV-1-2 cannot be considered to be truly representative of the border facies. Only oxide segregations were collected for C-9, C-14, and C-18.

Specimens to which special reference is made (e.g. samples C-2, C-17, C-6 and C-5A and C-5B) are described separately at the end of this section.

Photomicrographs for the plates were taken with a Leitz Ultraphot microscope and high speed Ektachrome film.

Table IV-1-1: Description of Handspecimens \*

Sample No.	C-1	C-2	C-3	C-4	C-5A	C-5B	C-6	C-7	C-8	C-10	C-11	C-13	C-15	C-17
mean grain size of rocks (mm)	10	10	8-10	8	2-3	8-10	10-20	2-3	5	5	5	10-15	2-5	10
massive or dense	m	h	m	m	m	m	s	m	m	m	m	m	m	h
foliated, gneissoid	m	s	s	m	m	h	m	m	s	m	m	s	m	s
colour index (= % mafics)	30	60	40	90	80	60	5	70	80	90	80	50	60	60
average dimension of mafic segregation (cm)														
maximum	3	2.0-3.0	5	m	m		1.0	1	m	2	m	3	10	2-3
minimum	2	1	5	s	s	5**	$\frac{1}{2}$	$\frac{1}{2}$	s	2	s	3	5	1
				s	s				s		s			
				i	i				i		i			
				v	v				v		v			
				e	e				e		e			

h = highly  
m = moderately  
s = slightly

\* All specimens are holocrystalline, medium to coarse grained and have allotriomorphic-granular texture

\*\* Average width of bands

Table IV-1-2: Modal Analyses of Gabbroic Anorthosite Samples

Sample No.	C-1*	C-2	C-3*	C-4	C-5A	C-5B*	C-6*	C-7	C-8	C-10	C-11	C-13	C-15*	C-17
plagioclase	82	33	15	19	22	26	-	48	10	8	28	28	58	31
pyroxene	3	19	12	-	15	-	-	16	80	60	26	13 <sup>+</sup>	23	31
amphibole	1	22	35	57	28	52	-	-	5	3	24	-	3	28
garnet	5	15	5	7	25	12	-	25	-	7	11	48	13	6
opaques	1	8	22	12	9	8	15	11	5	21	9	11	3	4
scapolite	9	tr	5	tr	-	-	-	-	-	tr	tr	tr	-	tr
biotite	tr	1	5	tr	$\frac{1}{2}$	2	5	-	-	-	-	2	-	-
epidote	tr	-	tr	-	-	-	-	-	-	tr	tr	-	-	-
quartz	tr	tr	tr	tr	tr	tr	80	tr	tr	tr	tr	tr	tr	tr
other <sup>++</sup>	tr	tr	3 <sup>++</sup>	tr	-	tr	-	-	-	-	tr	-	-	tr
% An in plagioclase	58-64	38-44	58-66	37-44	54	49	-	30	44	57	44	66	63-65	49

\* These samples are inhomogeneous and the modes must be treated with caution.

+ Consists mostly of heavily altered pyroxene.

++ Includes minor muscovite, calcite sphene and apatite.

### Plagioclase

As indicated in Table IV-1-2, the plagioclase composition of the gabbroic facies is more varied than that of the main body of the anorthosite, which ranges between An<sub>55</sub> and An<sub>60</sub> (I. Mason, personal communication, 1967). With few exceptions, distinct evidence of cataclasis or late consolidation stage movement is observed in the feldspar. This consists of scattered relics of larger crystals showing undulatory extinction, bent twin lamellae and fractured margins. The grain-size of the plagioclase ranges from less than 1 mm. to 10 mm. or more and is quite variable within a section. The individual grains are anhedral and generally show intricately sutured borders. Zoned crystals are not uncommon.

Minute rounded grains of unidentifiable oxides occur scattered throughout the feldspar in varying proportions, sometimes giving it a dusty appearance (Plate 1, Fig. 1). Alteration to secondary deuteric minerals is not common and seems to be directly related to the degree of weathering of the outcrop.

### Pyroxene

The clinopyroxene, which is the only pyroxene observed in the border facies, is pale greenish to almost neutral in thin sections and is sometimes slightly pleochroic. It displays high relief and moderate birefringence. Maximum extinction angle in longitudinal sections is approximately 40°. Typical short prismatic habit and pyroxene cleavage are generally present. It is biaxial (+ve) and has 2V of approximately 60°. These properties suggest that the

pyroxene is augite. Chemical analyses of pyroxenes from the Whitestone anorthosite recalculate to  $Wo_{48}En_{33}Fs_{19}$  (salite-augite), confirming this identification (I. M. Mason, personal communication, 1968).

Alteration of the augite to a green hornblende is ubiquitous and has progressed to varying stages. Incipient alteration is characterized by discolouration and hornblende formation at the edges of pyroxene aggregates and grains. As alteration progresses, more pyroxene is consumed at the edges of grains and along interior cleavage planes. Concomitantly, minute oxide blebs consisting mainly of magnetite begin to form in the cleavage planes. As described below, these increase in size as alteration proceeds, finally coalescing to elongate grains and irregular blebs, leaving the pyroxene matted and dusty in appearance. In the final stages a poikilitic or sieve texture forms in the hornblende alteration. The interstices of the hornblende then frequently contain minute anhedral grains of quartz.

Some pyroxene contains abundant minute rodlets of oxides (Plate 2, Fig. 1).

Relict exsolution lamellae are occasionally observed in the augite and one instance of hourglass zoning was seen.

#### Hornblende

The hornblende shows typical strong pleochroism from dark battle green to olive green to yellowish green. Interference colours are masked by its strong primary colour. It often displays prismatic habit and pseudo-hexagonal outline. Typical rhombohedral amphibole cleavage is commonly present.

This mineral occurs as optically continuous rims around oxides or pyroxene grains. It also forms reaction rims consisting of separate grains around clusters or elongate segregations of pyroxene grains. Often it has a sieve texture, being intergrown with quartz and feldspar. Its obvious and invariable reaction or rimming relationship to pyroxene or oxide must be emphasized. It generally appears fresh and unaltered.

### Garnet

Garnet is a major constituent of almost all sections. Semi-quantitative probe analysis and chemical analysis (I. M. Mason, personal communication, 1968) confirmed that the garnet in the gabbroic portion of the Whitestone anorthosite is comparatively pure almandine (less than 1% MnO and 5% MgO). It occurs in three distinct habits. Most frequently it is found as small euhedra, scattered throughout the section. In such cases it is generally associated with hornblende and plagioclase or with oxide. When garnet forms a narrow rim around oxide, it frequently has a myrmekitic-graphic habit and appears to be intergrown with plagioclase. Occasionally large sieved garnets containing almost all of the other constituents are found. Generally, garnet has a fresh appearance, only occasionally being slightly altered to chlorite and calcite along fractures. In sections from somewhat weathered rocks it appears slightly cloudy.

### Opagues

The opaques consist mainly of hemo-ilmenite, ilmenite and magnetite. Magnetite frequently displays euhedralism, but hemo-

ilmenite and ilmenite are generally in the form of rounded anhedral blebs or trails of grains. Often the oxides are rimmed by amphibole or garnet which seems to have formed by reaction with oxides. In some sections (e.g. C-3), considerable amounts of oxides, generally magnetite, occur as small anhedral blebs scattered throughout the pyroxene, growing in size and quantity as the intensity of alteration to amphibole increases. When alteration has been very extensive, trains of oxide blebs form and often coalesce to larger aggregates.

In pyroxene grains, oxides also occur as minute rods which are oriented perpendicular to each other but are inclined randomly (Plate 2, Fig. 1).

Two lines of evidence indicate that the oxides have been remobilized:

1. Injection of oxides along prominent partings or cleavage planes of silicates has taken place (Plate 1, Fig. 2 and Plate 6, Fig. 1).

This is most common where oxide segregations are large.

2. Frequently, interesting and unusual dendritic growths of opaque material in cleavage planes and cracks of silicates were observed under very high magnification (Plate 2, Fig. 2). They occur scattered through all the silicates, but are particularly noticeable in feldspar because of the contrast in colour. The size of these dendrites increases with proximity to oxide blebs, which strongly suggests that they formed by remobilization of oxide.

In addition to the oxides, minor amounts of pyrite, pyrrhotite and chalcopyrite are found in most sections. They are located in

minute, late stage, secondary veinlets that also contain hydrous oxides.

Composition and textural relationships of opaques are fully described in section IV-2.

#### Accessories and Alteration Products.

Scapolite is the major alteration product, having formed from plagioclase. Progressive scapolitization has been described by Haughton (1967) for samples from the Whitestone anorthosite and is illustrated in his Plates 2 to 5.

A neutral, slightly pleochroic variety of epidote, having a myrmekytic-graphic texture occurs in trace amounts in the more altered sections especially where scapolitization is extensive.

Biotite is almost exclusively associated with oxide in C-3 and C-6, where it forms reaction rims in which laths of dark brown (Ti rich?) strongly pleochroic biotite radiate from oxide blebs. Rarely is it associated with hornblende.

Contrary to expectations, sphene is not an abundant accessory in the border facies. Where it does occur it always rims oxide (ilmenite) or is closely associated with oxide.

Quartz is poikilitically intergrown with hornblende and occasionally occurs as interstitial anhedral in feldspar (e.g. C-5). There is a little in each section, but it is quite minor in abundance.

Muscovite, calcite, and chlorite have been observed as alteration products of garnet in section C-1. They are rare otherwise.

Small euhedra of apatite occur in minor amounts in most sections, but C-2 contains rather more than the other samples. It is generally

contained within or closely associated with hornblende.

Samples C-2, C-17, C-5A, C-5B and C-6.

With the exception of sample C-6, which is a quartz-ilmenite stringer with some biotite, the above mineralogic and textural descriptions aptly describe these samples also.

Geologic relations suggest that samples C-2 and C-17 may be xenoliths (I. Mason, personal communication, 1967). In handspecimen, both have very similar appearance, being very dark and dense and fresh. They contain sufficient magnetite to deflect a compass needle and the only rhombohedral phase is homogeneous ilmenite. Exsolved hematite is very rare or absent (see Section IV-2). The degree of alteration of pyroxene to hornblende in C-2 is slightly more than in C-17. The former also contains more garnet. These petrographic differences are slight and could be the result of differences in degree of metamorphism due to their relative positions in the anorthosite. Thus, they appear to be sufficiently similar that the notion of a common origin for both can be entertained.

Samples C-5A and B came from the same outcrop and seem to be the same rock type, except for a difference in texture. C-5A is a dense, massive, mafic, fine-grained, rusty weathering, garnetiferous gneiss. Gneissosity is not marked.

C-5B was collected from an immediately adjacent area (within 1 ft.) where an abrupt transition to a coarsely banded gneiss with marked foliation occurs over a distance of 1 cm. Feldspathic and mafic components are segregated in bands up to 5 cm wide. The mafic

bands are largely amphibole and oxide. Garnet is visible only on a weathered surface. These samples were collected with a view to determining what changes in oxide mineralogy and rock chemistry took place during the separation of the mafic constituents from a massive into a strongly banded gneiss.

## IV-2. Reflected Light Microscopy

### Introduction

The following description of the opaque minerals in the gabbroic facies of the anorthosite is based upon the study of 35 polished sections and polished thin sections with Leitz M.O.P. and Ultraphot microscopes. The photomicrographs were taken with the latter instrument.

The rhombohedral phases are ilmenite and hemo-ilmenite with coarsely exsolved ilmeno-hematite. Magnetite is the only spinel phase present. Ubiquitous but minor pyrite, pyrrhotite and chalcopyrite were also found.

### Spinel Phase

Homogeneous, isotropic, unaltered magnetite occurs in sections from all sample localities. The magnetite appears fresh and uniformly grey and has reflectivity intermediate between ilmenite and hematite. Minor martitization along weathered cracks occurs in the magnetite of some sections. This alteration appears as a very slightly anisotropic rim with a bluish tinge.

Magnetite occurs mainly as subhedral to anhedral rounded blebs but well developed euhedral grains showing octahedral outline are not uncommon (e.g. Plate 3, Fig. 1). This "primary" magnetite varies in size from small specks (0.1 mm) to large grains (10 mm or more). The "secondary" magnetite in pyroxene (described in Section IV-1) is much finer (less than 0.1 mm) and always shows anhedral outlines.

Occasional long thin slivers of magnetite were observed to penetrate large hemo-ilmenite grains in the (001) direction parallel to the exsolved ilmeno-hematite. Plate 3, Fig. 2 shows that the ilmenite which this magnetite penetrates contains no exsolved hematite. A similar relationship has been observed in the Allard L. ilmenite ores where it has been interpreted as magnetite replacement of ilmeno-hematite (Maucher and Rehwald, 1961, p. 193).

Evidence of solid solution with rhombohedral or spinel phases is very rare. During the entire study only two magnetite grains with some ilmenite as sandwich intergrowths were discovered. Relict ilmenite lamellae were not observed.

Irregular cracks were found in most of the magnetite grains. Their orientation did not seem to be crystallographically determined except where minute fractures, oriented perpendicularly and thus forming small crosses could be seen at high magnification. This was found only in one instance. A. J. Naldrett (personal communication, 1968) suggested that these crosses might contain spinel but none was observed under maximum obtainable magnification (2500X).

#### Rhombohedral Phases

Ilmenite with varying amounts of hematite in solid solution is the only rhombohedral phase present. It occurs in two distinct manners.

Samples from location C-2 show completely homogeneous ilmenite grains. This ilmenite has no visible exsolved hematite under any magnification. Its occurrence is more fully described below with samples C-2 and C-17.

At other locations in the oxide-rich portions of the gabbroic facies, ilmeno-hematite exsolution lamellae are found in hemo-ilmenite. These oxide concentrations consist primarily of aggregates of individual, rounded to elongate, 5-10 mm long, interlocking hemo-ilmenite grains, in which the ilmeno-hematite is exsolved in the basal (001) plane. Homogeneous ilmenite and hemo-ilmenite never coexist. A brief description of the reflected light properties of these phases follows.

Ilmenite (hemo-ilmenite) is a dull light brownish grey colour in air. In oil, reflectivity is considerably lower and the colour is definitely more brown. Ilmenite lamellae show distinct pinkish to light brown reflective pleochroism which is more marked in oil than in air. Strong anisotropism, ranging from light greenish grey to brownish grey, is less distinct in oil than in air. These properties, particularly a pinkish reflective pleochroism, suggest that considerable hematite is in solid solution in the ilmenite.

Hematite (ilmeno-hematite) has a much higher reflectivity, appearing almost white, with a slight bluish tinge which is accented and somewhat greyer in oil than in air. The lamellae display only a weak reflective pleochroism. Anisotropism is distinct, ranging between greyish blue and greyish both in air and in oil. In most sections a faint trace of pinkish colour suggests considerable ilmenite in solid solution.

Hematite has a somewhat greater hardness than ilmenite and the hematite lamellae occasionally retained some polishing relief.

(Hardness is G for the former and F for the latter on the Talmadge

scale).

Alteration of the hemo-ilmenite aggregates was observed only in specimens from weathered outcrops, where it was of minor extent. Buddington's "meta-ilmenite" (Buddington et al., 1963), which appears to be a commonly observed phenomenon where deuteric or secondary reworking of the rhombohedral phase has taken place, was not found.

Rutile was not seen in any of the polished sections.

Skeletal-graphic intergrowths of hemo-ilmenite with silicates is a commonly observed habit for ilmenite deposits and was also seen occasionally in the oxide-rich portion of the Whitestone anorthosite. An example of such a texture is illustrated in Plate 5, Fig. 1, where hemo-ilmenite is intergrown with garnet.

#### Relative Abundance of the Opaques

Volumetrically, hemo-ilmenite greatly predominates over magnetite in all samples except C-2 and C-17. Magnetite constitutes 5-20% of the oxide minerals in any given locality and is never completely absent. The amount of magnetite was not observed to be systematically related to the amount of hemo-ilmenite.

Sulfides constitute up to a maximum of about 3% of the opaques, and are present in all polished sections.

#### Microfabric of the Oxides

The amount and size of exsolved ilmeno-hematite lamellae in hemo-ilmenite varies considerably, but does not seem to correlate with any other single factor such as quantity of oxides or magnetite present, grain size or gneissosity of the host rock. In some local-

ities ilmenite with only very fine (3 to 5  $\mu$  wide) trellis or spindle shaped hematite lamellae is found. These lamellae are parallel to sub-parallel and generally constitute only 5-10% of the grain. These same well-defined, discontinuous, crystallographically oriented hematite lamellae may also be up to 25  $\mu$  wide (Plate 4, Fig. 1). There is no second set of exsolved ilmenite lamellae in this hematite. Where fine hematite lamellae are offset or at grain boundaries, occasional broadening of the lamellae occurs. A. J. Naldrett (personal communication, 1968) has suggested that this is simply due to nucleation at the boundary.

In the other major type of exsolution, which is more complex, hematite may constitute up to 50% of hemo-ilmenite grains. Hematite is roughly parallel and crystallographically oriented and forms large irregular patches and discontinuous lamellae in ilmenite--and in turn contains a second set of exsolved ilmenite lamellae. Variations in texture and shape of the exsolved ilmeno-hematite are illustrated in Plates 3, 4 and 6.

Both of the major exsolution types may occur in grains from a single handspecimen, and/or at any given locality. Gradation between these types is primarily a function of crystallographic orientation.

Evidence of cataclasis is ubiquitous in the oxides and cataclastic texture is also found in the feldspar. Frequently offset exsolution lamellae in the hemo-ilmenite and trails of rhombohedral phases injected along cleavage planes of surrounding silicates ( as illustrated in Plate 6, Fig. 1 ) are strongly suggestive

of late-stage or post-consolidation movement and remobilization of the oxides. Magnetite showed much less evidence of remobilization than did hemo-ilmenite. It is generally only slightly elongated rather than being as ragged and irregular in shape as hemo-ilmenite. In Stanton's (1964a, b) terminology, compared to other silicates and oxides, magnetite has a greater tendency to show euhedralism as a result of relative surface energies, rather than paragenetic sequence.

The most interesting textural relationship observed is undoubtedly the thinning and eventual disappearance of exsolved hematite lamellae in hemo-ilmenite grains adjacent to magnetite. The hematite-poor rim, which is apparently 50  $\mu$  wide, is illustrated in Plate 3, Fig. 1, Plate 4, Fig. 1 and Plate 6, Fig. 2. It was observed in all samples where magnetite and hemo-ilmenite are in contact. Under high magnification, hematite lamellae that gradually thin towards the magnetite grain are seen to persist in their original crystallographic direction to within 5 to 10  $\mu$  of the boundary, then disappear completely. These observations are true for any orientation of the hematite exsolution plane relative to the magnetite contact. This interesting reaction relationship was the subject of extensive study with the electron probe, and is described further in section V-2.

Sulfides show no tendency to occur in any one particular manner, but are scattered throughout the silicates and oxides either as single subhedral to euhedral (e.g. pyrite) grains or as multiphase aggregates. Sometimes they are completely enclosed in single hemo-ilmenite or magnetite grains or are interstitial (e.g. Plate 3, Fig. 1).

They are generally altered (e.g. Plate 5, Fig. 2) to secondary iron minerals (limonite?). Occasionally, they display growth-in-cavity textures (euhedral to subhedral crystals projecting into a cavity). In several instances they were observed to be concentrated primarily in small veinlets that transgress all other minerals. The sulfides are generally less than 0.5 mm in maximum dimension.

Sulfides show no antipathetic relations--pyrite may be in contact with pyrrhotite and/or chalcopyrite. The latter however, is generally closely associated with pyrrhotite and may have exsolved from it.

#### Samples C-2, C-17, C-5A, C-5B and C-6

The similarity of samples C-2 and C-17 as noted from their silicate mineralogy is echoed in the mineralogy of the opaques. In both C-2 and C-17 magnetite amounts to 40 to 50% of the oxides. In C-2 homogeneous ilmenite is the only rhombohedral phase. In C-17, minor exsolved hematite is found in the ilmenite. In samples from both localities, magnetite is intimately associated with the ilmenite and is often enclosed in it. Euhedralism of magnetite is not frequently observed; magnetite and ilmenite have very similar shapes which range from rounded to irregular and elongate.

Optically, the magnetite closely resembles that from other locations in the gabbroic facies. The ilmenite appears slightly less pink than that in exsolved hemo-ilmenite from other localities, suggesting that it contains somewhat less hematite in solid solution.

Unaltered pyrrhotite is the predominant sulfide phase and

amounts to 2 to 3% of the opaques. Pyrite and chalcopyrite occur less frequently in samples from localities C-2 and C-17 than anywhere else.

In samples from locality C-5A, hemo-ilmenite and sulfide are evenly distributed throughout the rock. The shapes of these grains is quite varied and highly irregular, varying from elongate wisps and trails to minute equi-dimensional rounded blebs. Many of these grains are compound magnetite and hemo-ilmenite grains with very fine scale (only several  $\mu$  wide) exsolution lamellae of the hematite phase. Grains with more than 20 to 30% exsolved hematite lamellae are rare.

At locality C-5B, immediately adjacent to C-5A, these oxides have coalesced to stringers composed of larger individual hemo-ilmenite grains that now contain plates of exsolved hematite and ilmeno-hematite 50-100  $\mu$  wide. These stringers are up to 3-4 cm long and 1 cm wide and are completely enclosed in amphibole. Magnetite, wholly or partly contained in the stringers has a strong tendency to occur as euhedra (e.g. Plate 3, Fig. 1).

In the quartz stringer, at locality C-6, the predominant oxide is an extremely finely exsolved ilmenite with hematite lamellae less than one  $\mu$  wide. It occurs as individual grains that have coalesced to form stringers up to 5 cm long. Magnetite occurs infrequently as small euhedra, up to 0.5 cm in diameter that are partially or completely surrounded by ilmenite. Weathering of this ilmenite along cracks has produced minor alteration.

### Summary

The most significant points arising from study of the oxide mineralogy can be listed as follows:

1. Exsolution textures of hematite in ilmenite are complex and varied, both within a handspecimen and overall; the apparent magnetite-hemo-ilmenite zoning is found wherever magnetite and hemo-ilmenite are in contact.
2. Volumetrically, hemo-ilmenite greatly predominates over magnetite. Pyrite, pyrrhotite and chalcopyrite are ubiquitous but minor phases.
3. Evidence of remobilization of the oxides is widespread.
4. The oxide mineralogy and exsolution textures are remarkably similar to those of major ilmenite deposits of the world, such as Abu Ghalaga and Allard L. as evidenced from photos and descriptions of these deposits by Hammond (1952), Carmichael (1959, 1961), Maucher and Rehwald (1961) and Krause (1965).

## V. ANALYTICAL INVESTIGATION

### V-1. Chemical Analyses of Oxide Concentrates and Whole Rock Samples

Selected magnetite and hematite-ilmenite concentrates, separated by methods outlined in Appendix A, were analyzed by J. Muysson, McMaster University, using rapid wet chemical methods.

Selection of oxide samples for chemical analysis was based on the following considerations:

1. Polished section study indicated that the maximum amount of information could be gained from a chemical analysis.
2. The oxide concentrates were of high purity.
3. The outcrop from which the sample was obtained showed little weathering.

On this basis, seven magnetite concentrates and two hematite-ilmenite samples were analyzed. A homogeneous magnetite from the Blue Mountain Nepheline Syenite body with optical properties very similar to the magnetites under investigation was also included with the samples, because a large quantity of high purity concentrate was available. The results of the chemical analysis of the magnetites are indicated in Table V-1-1.

Considerable difficulty was experienced in determination of the ferrous content of some of the concentrates. A black magnetic residue (later identified as pyrrhotite) remained, regardless of the dissolution method used (J. Muysson, personal communication). Because of this the FeO content of some of the magnetites is doubtful,

Table V-1-1: Chemical Analyses of Magnetite Concentrates (wt %)

Sample No.	MAGNETITE							
	B.M.	C-2	C-3	C-18	C-5B	C-14	C-15	C-17
SiO <sub>2</sub>	00.45	1.14	1.23	4.88	2.80	3.06	4.32	2.65
TiO <sub>2</sub>	0.12	0.89	2.24	14.08	1.73	15.87	13.43	1.79
Al <sub>2</sub> O <sub>3</sub>	0.77	0.55	0.70	0.59	0.88	1.13	0.69	0.82
Fe <sub>2</sub> O <sub>3</sub>	69.18	+	61.10	39.23	51.25	43.10	33.45	56.38
FeO	29.15	34 **	34.00 **	41.26	40.23	35.41	45.03	36.33
MnO	0.54	0.03	0.06	0.08	0.03	0.06	0.06	0.03
MgO	0.05	0.20	0.21	0.72	0.45	0.58	0.73	0.44
CaO	0.01	0.12	0.15	0.31	0.31	0.21	0.38	0.32
Na <sub>2</sub> O	0.00	.021	.009	.022	.047	.002	.004	.049
K <sub>2</sub> O	.027	.019	.019	.020	.024	.014	.015	.029
S	0.00	5.87	0.25	0.00	2.38	0.30	1.81	1.71
Cr <sub>2</sub> O <sub>3</sub>	0.00	0.00	0.09	0.02	0.16	0.11	0.06	0.14
Sum	100.30	106.51	100.06	101.21***	100.29	99.85	99.98	100.69
Less O=S	0.00	2.57	0.11	0.00	1.04	0.05	0.79	0.75
Total	100.30	103.94*	99.95	101.21	99.25	99.80	99.19	99.94
Total Fe <sup>+</sup>	101.58	97.67	98.89	85.09	95.96	82.45	83.50	96.76

as Fe<sub>2</sub>O<sub>3</sub>

\* includes oxygen of FeO as Fe<sub>2</sub>O<sub>3</sub>

\*\* doubtful

\*\*\* a good deal of elemental iron appears to be present in this sample

Analyst: J. Muysson, McMaster University.

Table V-1-2: Chemical Analyses of Hemo-Ilmenite Concentrates  
and Whole Rock Samples (wt.%) \*

Sample No.	HEMO-ILMENITE		W H O L E R O C K		
	C-2	C-15	C-2	C-5A	C-5B
SiO <sub>2</sub>	0.72	1.05	44.54	44.91	47.06
TiO <sub>2</sub>	47.57	28.07	4.55	2.78	2.35
Al <sub>2</sub> O <sub>3</sub>	0.10	0.46	12.36	14.56	14.77
Fe <sub>2</sub> O <sub>3</sub>	55.53	70.65	1.88	3.66	3.32
FeO	Fe det. as Fe <sub>2</sub> O <sub>3</sub>		16.84	14.81	10.84
MnO	0.48	0.86	.36	.27	.20
MgO	not determined		4.50	5.29	6.16
CaO	0.12	0.25	10.06	10.24	10.46
Na <sub>2</sub> O	not determined		2.18	2.25	2.69
K <sub>2</sub> O	not determined		.42	.25	.51
P <sub>2</sub> O <sub>5</sub>	not determined		2.11	.10	.28
H <sub>2</sub> O+ 110°C	not determined		.35	.50	.81
H <sub>2</sub> O- 110°C	not determined		.07	.10	.10
CO <sub>2</sub>	not determined		.10	.23	.20
Less Fe=Fe <sub>2</sub> O <sub>3</sub>	4.75	2.81			
Total	99.87	98.67	100.32	99.95	99.75
Total Fe as Fe <sub>2</sub> O <sub>3</sub>	55.53	70.65	20.60	20.12	15.37

\* Analyst: J. Muysson, McMaster University

as indicated in the table.

Whole rock samples of the ilmenite-rich inclusion C-2 and the two C-5 samples described in section IV were also analyzed. The analyses of the hemo-ilmenites and the whole rock samples are shown in Table V-1-2.

#### Discussion of the Chemical Analyses

An unusual amount of difficulty was encountered during the separation of the oxides as was found also by Buddington & Lindsley, (1964), p. 326; Vincent et al. (1957); Duchesne, (1966) and Aoki, (1966). The separation methods outlined in Appendix A are not entirely satisfactory. This is largely due to the occurrence of magnetite or ilmenite in cleavage planes of the pyroxene (see Plate 6, Fig. 1). Often this resulted in a large pyroxene contamination of the magnetite concentrate. Because of the extreme toxicity of Clerici solution and other liquids with specific gravity similar to magnetite (5.2) it was decided to use Methylene Iodide, despite the disadvantage of its low specific gravity.

Visual checks for iron contamination from the jaw crusher were made at all stages of the separation. No ragged, malleable iron particles were found and it was concluded that contamination from the crusher is negligible. Separation of minor pyrrhotite impurity from the magnetite could not be achieved. The amount of pyrrhotite in the concentrate can be estimated from the amount of sulfur indicated by the chemical analysis.

Electron probe analyses, optical properties and unit cell

parameters indicate that the magnetite contains essentially no titanium. Consequently, the high titanium content of magnetite concentrates C-14 and C-15 as seen from the chemical analysis must be due to contamination by ilmenite and hemo-ilmenite. X-ray diffraction traces and polished grain mounts confirmed the presence of considerable ilmenite in magnetite concentrates C-14 and C-15 and small amounts in all other magnetite separates except C-2, C-3, C-17 and B.M. Further grinding and repetition of the separation steps improved the quality of the concentrates only slightly. Plate 3, Fig. 1 indicates that it might indeed be difficult to obtain a clean magnetite separate when magnetite is completely enclosed by hemo-ilmenite. Since several independent methods indicate that the magnetites are essentially Ti free, and the Ti in the magnetite analyses is known to be due to contamination, recalculation of the chemical analyses to mol.% ulvospinel is incorrect. Therefore, with the exception of B.M. and perhaps C-2, the chemical analyses are of limited value for indicating magnetite compositions.

X-ray diffraction traces of hemo-ilmenite concentrates showed no magnetite peaks and therefore the separates of rhombohedral phases are considered to be purer.

Since FeO was not determined for ilmenite C-2 and hemo-ilmenite C-15, it was necessary to use I.S.E. Carmichael's procedure (described in detail in Appendix E) rather than Buddington and Lindsley's method to recalculate the chemical analyses, as well as the probe analyses. This is unfortunate because this scheme of computation to some extent vitiates direct comparison with the result of Buddington and Lindsley.

Calculations carried out by both methods show the numerical difference to be very small. Using Carmichael's method, C-2 recalculated to Hem<sub>7.7</sub>Ilm<sub>92.3</sub> and C-15 to Hem<sub>43.6</sub>Ilm<sub>56.4</sub> (mol.%). C-15 was shown to contain 44 mol.% hematite from the X-ray diffraction intensities (section V-3B). The X-ray method seems to give results that are in excellent agreement with the chemical analysis.

## V-2. Electron Probe Analysis of Oxides

### Introduction

An Acton Microprobe analyzer, model MS-64 was used throughout this study. For details of electron optics, electronics, detector geometry, etc., Haughton (1967) should be consulted.

Oxide grains in polished thin sections of the samples were analyzed, using the spot analysis technique described by Klemm (1965). Grains of interest were located by reference to polaroid photos of the polished thin sections on which phases identified by reflected light microscopy had been labelled. Qualitative line scan traces were obtained for the magnetite-hemo-ilmenite reaction relationship described in section IV.

### Operating Conditions

Conditions of analysis for all elements determined were: 16 KV accelerating voltage, 150 microamps beam current runoff on pure Fe and 80 nanoamps specimen current. The analyzing crystals used were  $10\bar{1}1$  quartz and  $10\bar{1}0$  quartz for Fe, Ti and Mn and K.A.P. for Mg and Al. Three separate detectors allowed coincident analysis of any two of the elements Fe, Ti, Mn with either Al or Mg. Sealed counters were used for the heavy elements and flow proportional counters for the light elements. A constant counting time of 10 seconds was used throughout. The beam width, in general 1-2 microns, was minimized by focusing on plagioclase in the polished thin sections and utilizing its natural fluorescence to indicate beam size. For some ilmenite grains

containing very fine hematite exsolution (e.g. C-6) a beam width of 5-10 microns was used, because individual lamellae could not be resolved.

#### Composition of the Standards

Standards suitable for EPMA must satisfy fairly rigorous requirements. They should be homogeneous and free of inclusions and should cover a wide range of compositions so that satisfactory working curves can be established. Their composition should be accurately known.

After considerable searching, the standards listed in Table V-2-1 were found to be suitable. They satisfy the above criteria with the exceptions noted in Appendix C.

#### Electron Probe Analyses

Replicate analyses of all unknowns were carried out. At least three separate locations on each grain were analyzed to test for homogeneity or zoning. Between 5 and 10 ten-second counts have been averaged to arrive at the composition of each oxide. All the magnetite analyses given in Table V-2-2 are of homogeneous, physically distinct, euhedral to subhedral magnetite grains. Analyses reported in Table V-2-3 were carried out on homogeneous-appearing grains or large lamellae of ilmenite. All analyses in Table V-2-4 refer to single lamellae of hematite or ilmenite. These may occur adjacent to each other, or in separate grains in the same section.

Standards were analyzed at least once each half hour on the same spot of the same grain. Drift was also monitored by frequently repeated analyses of a pure metal standard.

Table V-2-1: Composition of the Electron Probe Standards (wt.%) \*

Std. No.						LHD	LHD					LHD
	64019	R1993	A 3	L 20	L 31	mte-usp	ilm.	R1958	R1959	A 1	A 2	hem-ilm
FeO	30.35	28.88	44.86	51.4	51.0	46.69	47.35	41.12	42.25	38.31	38.36	13.69
Fe <sub>2</sub> O <sub>3</sub>	67.14	68.52	28.08	21.4	21.2	36.47	---	3.65	4.90	4.07	9.89	71.06
TiO <sub>2</sub>	1.34	0.89	20.56	26.6	27.0	16.84	52.65	49.25	48.25	51.68	49.71	15.24
MnO	0.37	0.14	0.39	0.6	0.6	---	---	3.15	1.74	0.55	0.85	---
Al <sub>2</sub> O <sub>3</sub>	0.00	0.48	3.16	---	---	---	---	0.93	1.94	1.28	0.37	---
CaO	0.09	---	0.11	---	0.1	---	---	---	---	0.06	---	---
MgO	---	---	2.64	---	---	---	---	0.43	0.24	4.01	1.00	---
Cr <sub>2</sub> O <sub>3</sub>	---	---	0.19	---	---	---	---	---	---	0.03	---	---
SiO <sub>2</sub>	0.43	---	---	---	---	---	---	1.13	0.72	---	0.08	---
Sum	99.72	98.91	99.99	100.0	99.9	100.00	99.99	99.66	99.54	99.99	100.26	99.99

\* for locality, donor, detailed description of standards and deficiencies in the analyses see Appendix C.

In theoretical magnetite, FeO = 31.03, Fe<sub>2</sub>O<sub>3</sub> = 68.96.

Table V-2-2 Electron Probe Analyses of Magnetites \*

Sample No.	Grain No.	Wt. % Fe as FeO $\pm$ 1.0%	Comments
C-1	IV	91.4	
C-2	V	86.2	inferior analyses, because only 3 standards
	VI	88.6	
	VIII	86.4	
	IX	88.2	
C-3	I	95.5	Fe counts high on standards
	II	94.4	
	III	95.3	
C-4A	IV	90.3	
C-4C	I	91.2	
	II	90.3	
C-5A	XI	99.5	Fe counts high on standards
C-5B	I	93.0	
C-6	I	93.0	
C-7	II	89.8	Fe counts low on standards
	IV	88.2	
C-8	I	93.4	
	II	92.0	
	III	94.0	
	IV	90.9	
C-9	VII	96.9	
C-10	I	89.2	
	II	90.1	
C-11	I	88.8	
	III	90.4	
	VIII	91.2	
C-13	no magnetite observed		
C-14	no magnetite observed		
C-15	IX	93.6	
C-17	VII	96.4	
	VIII	96.3	
C-18	XV	95.8	
	III	88.9	

\* TiO<sub>2</sub>, MgO, Al<sub>2</sub>O<sub>3</sub>, MnO were all consistently below the detection limit.

All Fe as FeO in pure magnetite = 93.1 wt.%.

Table V-2-3: Electron Probe Analyses of Ilmenite Grains\*

Column No.**	I	II	III	IV	V	VI	VII	VIII
		weight percent				molecular percent		
Sample No.	Fe as FeO ± 0.7	Ti as TiO <sub>2</sub> ± 1.0	Recalculated FeO FeO'      Fe <sub>2</sub> O <sub>3</sub> '		Sum	Hem	Hem	Ilm
C-1	47.1	46.0	41.4	6.4	93.8	12.6	6.5	93.5
	49.9	46.8	42.1	8.7	97.6	11.1	8.5	91.5
	49.0	44.0	39.0	10.5	94.1	16.4	10.7	89.3
C-2	52.7	45.2	40.6	16.6	102.4	14.2	15.5	84.5
	51.0	46.8	42.1	9.9	98.8	11.1	9.5	90.5
	51.4	47.1	42.4	10.1	99.6	10.5	9.6	90.4
	51.7	44.5	40.0	13.0	97.5	15.5	12.7	87.3
C-3	no suitable		ilmenite seen					
C-4A	49.0	45.9	41.3	8.6	95.8	12.8	8.6	91.4
	49.0	45.0	40.5	9.5	95.0	14.5	9.5	90.5
	47.0	48.4	43.5	3.9	95.8	8.0	3.8	96.2
C-4C	no suitable		ilmenite seen					
C-5A	50.7	47.5	42.7	8.9	99.1	9.8	8.6	91.4
	52.7	43.5	39.1	15.1	97.7	17.4	14.8	85.2
	52.2	45.7	36.1	12.3	99.1	13.2	11.9	88.1
	52.3	44.5	39.1	13.7	97.3	15.5	13.3	86.7
	53.1	43.5	39.1	15.5	98.1	17.4	15.2	84.8
C-5B	no suitable		ilmenite seen					

\* for MnO, MgO, Al<sub>2</sub>O<sub>3</sub> see text.

\*\* Column number; I and II wt.% FeO and TiO<sub>2</sub> from probe analysis; III and IV FeO reappportioned to FeO' and Fe<sub>2</sub>O<sub>3</sub>' according to scheme outlined in Appendix E; V sum of FeO' and Fe<sub>2</sub>O<sub>3</sub>' and TiO<sub>2</sub>; VI mol. % Hem obtained from wt. % TiO<sub>2</sub> and equation E-1; VII and VIII mol % Hem and Ilm, calculated by method of Appendix E.

Table V-2-3 (continued)

Column No.	I	II	III	IV	V	VI	VII	VIII
C-6	52.8	44.9	40.4	13.7	99.0	14.7	13.3	86.7
	58.0	41.3	37.1	23.2	101.6	21.6	21.9	78.1
	48.2	49.7	44.7	3.9	98.3	5.6	3.8	96.2
	51.2	46.3	41.6	10.6	98.5	12.1	10.3	89.7
	50.1	48.8	43.9	6.9	99.6	7.3	6.6	93.4
C-7	48.4	46.1	41.5	7.7	95.3	11.3	7.7	92.3
	46.2	48.6	43.7	2.8	95.1	7.7	2.8	97.2
C-8	49.5	46.6	41.9	8.4	96.9	11.5	8.3	91.7
	49.2	46.8	42.1	7.9	96.8	11.1	7.8	92.2
C-9	52.4	47.1	42.4	11.2	100.7	10.5	10.6	89.4
C-10	49.3	44.4	39.9	10.1	94.5	15.7	10.2	89.8
	49.8	44.7	40.2	10.7	95.6	15.1	10.7	89.3
C-11	48.7	44.8	40.3	9.4	94.5	14.9	9.5	90.5
	49.0	46.7	42.0	7.8	96.5	11.3	7.7	92.3
	48.5	45.7	41.1	8.2	95.0	13.2	8.3	91.7
	50.4	46.3	41.6	9.7	97.5	12.1	9.5	90.5
C-13	54.7	48.9	44.0	11.9	104.8	7.1	9.2	90.8
	52.6	49.5	44.5	9.0	102.9	6.0	8.3	91.7
	50.9	50.6	45.5	6.0	102.1	3.9	5.6	94.4
C-14	48.7	48.2	43.3	6.0	97.5	8.5	5.8	94.2
	49.9	45.0	40.5	10.5	96.0	14.5	10.4	89.6
	48.3	47.9	43.1	5.8	96.8	9.0	5.7	94.3
C-15	50.9	46.6	41.9	10.0	98.5	11.5	9.7	90.3
	49.9	44.8	40.3	10.7	95.8	14.9	10.7	89.3
C-17	51.6	46.6	41.9	10.8	99.3	11.5	10.4	89.6
	52.3	46.2	41.5	12.0	99.7	12.3	11.5	88.5
	53.4	45.0	40.5	14.4	99.9	14.5	13.8	86.2
	50.5	47.7	42.9	8.5	99.1	9.4	8.2	91.8
C-18	51.8	43.1	38.8	14.5	96.4	18.2	14.4	85.6
	51.2	43.3	38.9	13.6	95.8	17.8	13.6	86.4

Table V-2-4: Electron Probe Analyses of Hematite and Ilmenite Lamellae

Column No.*	I	II	III	IV	V	VI	VII	VIII
	weight percent				molecular percent			
Sample & Ident. No.	Fe as FeO ± 0.7	Ti as TiO <sub>2</sub> ± 1.0	Recalculated FeO FeO'      Fe <sub>2</sub> O <sub>3</sub> '		Sum	Hem	Hem	Ilm
C-1 I	59.3	40.6	36.5	25.3	102.4	22.8	23.8	76.2
II	79.3	23.2	20.9	38.9	103.0	55.9	55.9	44.1
C-4 A II	77.9	12.1	10.9	74.5	97.5	77.0	75.5	24.5
III	73.5	20.0	18.0	61.7	99.7	62.0	60.7	39.3
C-4 C I	79.7	14.4	13.0	74.2	101.6	72.6	72.0	28.0
II	79.5	14.4	12.9	74.0	101.3	72.6	72.0	28.0
C-5 A IV	57.6	40.1	36.1	23.9	100.1	23.8	23.0	77.0
VII	60.7	35.3	31.7	32.2	99.2	33.0	31.3	68.7
V 1	80.8	14.7	13.2	74.2	102.1	72.1	71.6	28.4
2	51.8	46.1	41.5	11.5	99.1	12.4	11.1	88.9
VI 1	60.8	35.3	31.7	32.3	99.3	33.0	31.4	68.6
2	68.8	23.6	21.2	52.6	97.4	55.2	52.9	47.1
3	67.0	29.2	26.3	44.4	99.9	44.5	43.3	56.7
4	53.0	44.2	39.7	14.7	98.6	16.0	14.3	85.7
5	72.8	25.0	22.5	55.9	103.4	52.5	52.8	47.2
6	57.0	39.3	35.3	24.0	98.6	25.4	23.5	76.5
C-5B I	50.8	46.7	42.0	9.8	98.5	11.3	9.5	90.5
II	50.3	44.1	39.7	11.8	95.6	16.2	11.8	88.2
III	50.5	46.1	41.7	9.8	97.6	12.4	9.6	90.4
IV	77.1	15.1	13.6	70.6	99.3	71.3	70.1	29.9
V	77.6	14.7	13.2	71.5	99.4	72.1	70.9	29.1

\*See footnote in Table V-2-3 for explanation of columns

Table V-2-4 (continued)

Column No.		I	II	III	IV	V	VI	VII	VIII
S. & I. No.									
C-9	V	83.3	12.8	11.5	79.8	104.1	75.7	75.7	24.3
	VI	83.3	12.3	11.1	80.8	104.2	76.6	76.7	23.3
C-11	VII	76.4	14.4	12.9	70.5	98.8	72.7	71.0	29.0
C-13	I	54.7	49.7	44.7	11.1	105.5	5.6	10.1	89.9
	II 1	55.1	46.7	42.0	14.6	103.3	11.3	13.5	86.5
	2	55.2	49.0	44.0	12.4	105.4	6.9	11.2	88.8
	3	60.3	43.4	39.0	23.6	106.0	17.6	21.4	78.6
	4	51.0	51.2	46.0	5.5	102.7	2.7	5.1	94.9
	5	57.0	46.0	41.4	17.4	104.8	12.6	15.9	84.1
	6	51.0	51.1	46.0	5.6	102.7	2.9	5.2	94.8
	III	68.9	33.5	30.1	43.1	106.7	36.4	39.2	60.8
	IV	50.7	51.1	46.0	5.3	102.4	2.9	4.9	95.1
	V 1	67.3	34.2	30.8	40.6	105.6	35.0	31.3	62.7
	2	70.2	26.3	23.6	51.8	101.7	50.0	49.7	50.3
	3	72.7	17.8	16.0	63.0	97.4	66.2	63.9	36.1
C-14	I	76.3	15.9	13.9	63.7	93.5	69.8	66.8	33.2
	II	74.7	17.8	16.0	65.2	99.0	66.2	64.7	35.3
C-15	I	69.8	29.8	26.8	47.8	104.4	43.3	44.5	55.5
	IV	54.5	44	39.6	16.6	100.2	16.4	16.9	83.1
	V	78.4	12	10.8	75.3	98.1	77.2	75.8	24.2
	V	77.1	15.9	14.3	69.8	100.0	69.8	68.7	31.3
	IV	62.6	20.3	18.3	49.3	87.9	61.4	54.8	45.2
	VII	79.7	13.4	12.0	75.2	100.6	74.5	73.7	26.3
C-17	II	82.6	11.1	10.0	80.1	101.2	78.9	78.3	21.7
	VI 1	86.9	6.7	6.0	89.9	102.6	87.3	87.0	13.0
	2	79.0	15.1	13.6	72.7	101.4	67.1	70.7	29.3
	3	72.6	21.8	19.6	58.9	100.3	58.6	57.5	42.5
	4	74.5	19.1	17.2	63.7	100.0	63.7	62.5	37.5
		83.3	10.4	9.4	82.2	102.0	80.2	79.8	20.2

Fig. V-2-1

A. Electron Beam Traverse of Hemo-ilmenite grain adjacent to magnetite.

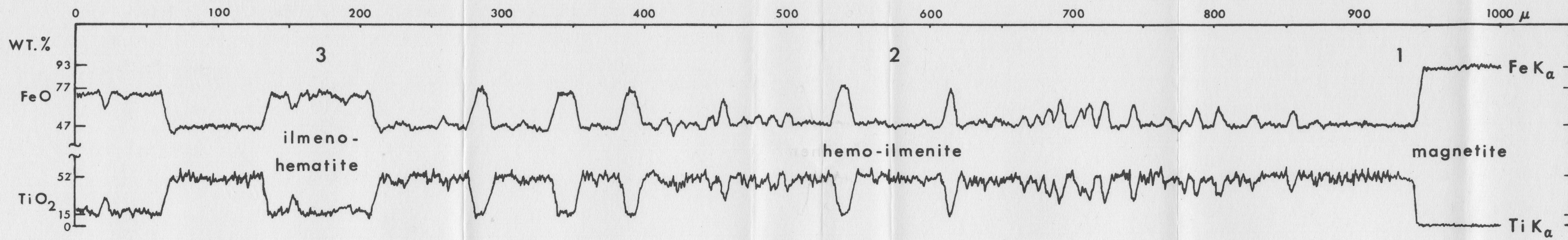
- Area:
1. Magnetite-ferrianilmenite boundary.
  2. Incomplete resolution of ilmeno-hematite lamellae.
  3. Ilmeno-hematite with 2nd generation ilmenite.

- Note:
1. The  $\text{TiO}_2$  content of the magnetite is 0 wt.%. .
  2. Magnetite is homogeneous.
  3. Hematite lamellae increase in size with increasing distance from the magnetite grain.
  4. Traverse is across grains from Sample C-3, but very similar profile is obtained wherever this phenomenon is observed, e.g. Plate 3, Fig. 1 .

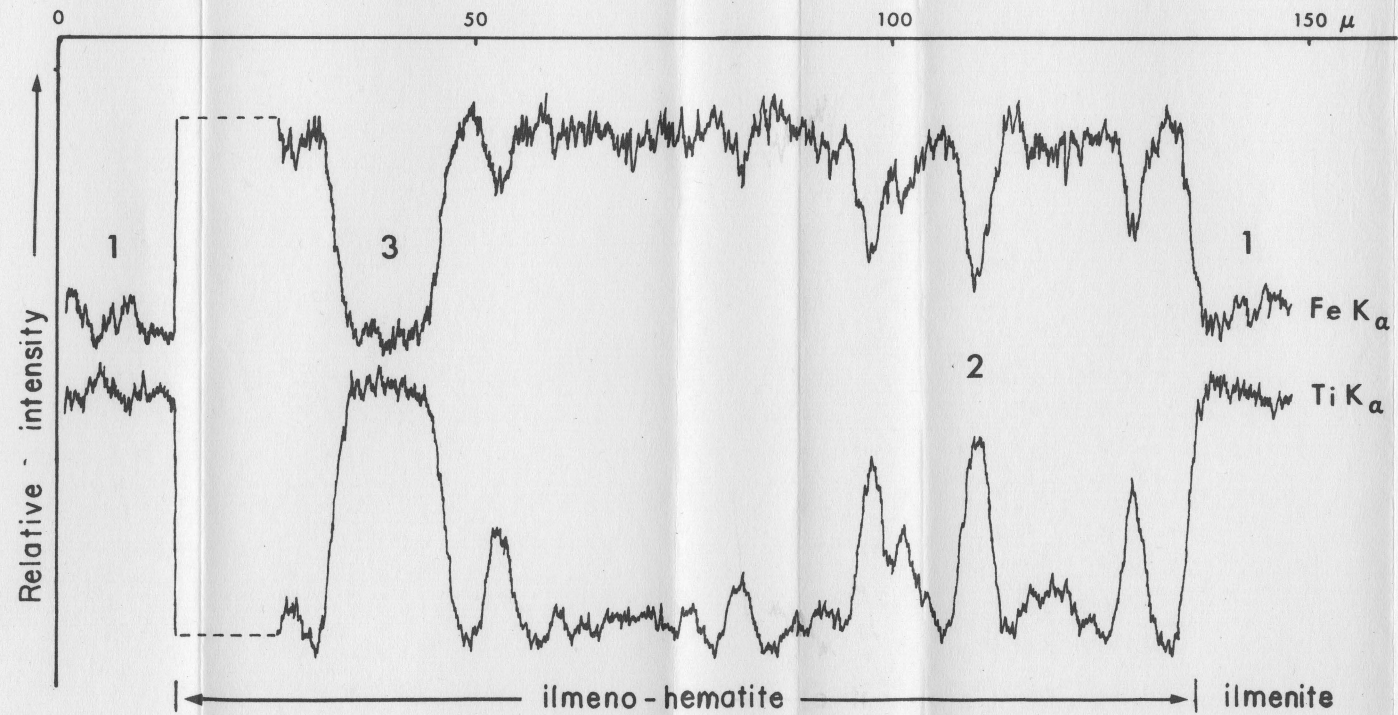
B. Nature of the second generation exsolved ilmenite.

- Note: Composition of second generation ilmenite lamellae (3) is closely similar to that of adjacent primary exsolved ilmenite (1). Area (2) shows second generation ilmenite which is not completely resolved.

Fig. V-2-1



A: Electron beam traverse of hemo-ilmenite grain adjacent to magnetite



B: Nature of 2nd generation exsolved ilmenite

Results of analyses are reported in wt.% oxide, although strictly speaking, atom % of Fe and Ti were being determined. Curves of wt.% TiO<sub>2</sub> vs. counts and atom % Ti vs. counts were drawn by the CURVFT program described in Appendix D. The values for the unknowns obtained in the latter case were converted to wt.% TiO<sub>2</sub> (by multiplying by the factor TiO<sub>2</sub>/Ti = 1.6680). These values corresponded exactly to those obtained for the unknown using the curve of TiO<sub>2</sub> vs. counts. Subsequently all results were obtained from curves of wt.% oxides vs. counts in order to minimize manipulation required. Fe is reported as FeO.

Columns VII and VIII in Tables V-2-3 and V-2-4 show probe analyses recalculated to mol.% hematite and ilmenite according to I.S.E. Carmichael's (1967) method, outlined in Appendix E. For comparative purposes, column VI of these tables shows the hematite content of each grain or lamella obtained directly from the curve of wt.% TiO<sub>2</sub> vs. molecular % hematite, as described in Appendix E.

#### Qualitative Line Scan

Investigation of the distribution of elements between coarsely exsolved hemo-ilmenite grains and magnetite was carried out using the line scan method described by Keil (1967, p. 18). A typical trace produced from an electron beam traverse of a reaction rim (similar to that shown on Plate 3, Fig. 1, but actually from sample C-3) has been reproduced as Fig. V-2-1A. The boundary between magnetite and hemo-ilmenite is sharp, with no change in the concentration of either Ti or Fe; however, for a distance of approximately 50  $\mu$  from the boundary

there is apparently no hematite in the ilmenite.

The nature of the second generation exsolved ilmenite in hematite is shown in the area marked 3 in Fig. V-2-1A, and a traverse at a slower scanning rate to reveal the exact composition of these ilmenite lamellae has been reproduced in part B of the figure. This figure and its implications to the formation of the oxide minerals are discussed more fully in section VI.

Although the variations in the concentrations of Mn and Mg on the line scans are barely above background, it was observed that these elements are enriched in the ilmenite-rich phase relative to the hematite-rich phase. This is in accord with the observations of Anderson (1966 b), but at variance with those of Bolfa et al. (1961), who report a higher Mn content in the hematite lamellae than in the ilmenite lamellae of a grain of hemo-ilmenite.

By comparison with standard A1, the MgO content of the hemo-ilmenite lamellae in C-3 is estimated to be a maximum of 1%. The MgO content of the hemo-ilmenite was never observed to exceed this amount in any sample analyzed, since MgO was generally below the detection limit (estimated to be approximately 1% for the operating conditions of the probe). MnO content was determined to be approximately 0.4 wt.% (also the detection limit) in the hemo-ilmenite lamellae of sample C-3.

#### Correction Procedures for Analyses

It is well known that in order to minimize absorption, fluorescence and atomic number corrections, it is imperative that the

standards used be as similar in composition to the unknown minerals as possible (Smith, 1965; Keil, 1967; Adler, 1966).

In order to evaluate the maximum effect that these corrections can have on the final composition of iron-titanium oxides analyzed under the above conditions with the Acton microprobe, detailed calculations were carried out using pure metals as reference standards (Appendix F).

Comparison of corrected compositions with those obtained by simple proportionality and/or the computer (CURVFT) fitted least squares curves of counts versus composition described in Appendix D, shows that the various corrections tend to cancel each other. The composition of oxides obtained after corrections were applied are within 1-2 wt.% of the uncorrected values. This difference decreases considerably if the correction calculations are carried out using ilmenite or hematite-ilmenite standards rather than pure Fe. Further proof that absorption and fluorescence are negligible for both Fe and Ti in the Fe-Ti oxides is provided by the fact that the second order coefficient of the least squares line of counts versus composition for the standards was very small, varying in magnitude between  $10^{-3}$  and  $10^{-38}$ . If fluorescence or absorption were significant, some curvature of the line would be expected. Only for systems having unusual compositions (e.g. Al determination in Al-U alloys) are corrections expected to be significant.

It was concluded that under the outlined conditions of analysis, the effect of fluorescence, absorption and atomic number corrections

is small; therefore, these corrections were not applied to the data obtained.

#### Discussion of the Electron Probe Analyses

The probe analyses of magnetite indicate that the Fe content calculated as FeO is within  $\pm 5$  wt.% of that observed for pure magnetite (93.1 wt.%). While this is a rather large deviation overall, the better quality analyses (e.g. C-5B, C-6) indicate a composition closer to that of pure magnetite. Ample additional evidence has indicated that the magnetite is comparatively pure. A spectrographic analysis on the magnetite and ilmenite separated from sample C-2 gives an order of magnitude indication of the minor element content of these phases (Table V-2-5). Some of the Ti indicated in magnetite C-2 may be due to ilmenite contamination.

The error in FeO indicated in column I of Table V-2-2 and in FeO and TiO<sub>2</sub> indicated in columns I & II of tables V-2-3 and V-2-4 is the standard deviation of the composition arising from recalculation and use of the CURVFT program (see Appendix D). Inherently, the TiO<sub>2</sub> values are slightly more precise than the FeO values because fluorescence and absorption effects by Ti radiation tend to cancel each other (see Appendix F). For Fe, only absorption with no fluorescence of iron radiation takes place. However, the small range of TiO<sub>2</sub> values that the ilmenite and hemo-ilmenite standards display results in a larger degree of uncertainty in the unknown TiO<sub>2</sub> compositions than in the corresponding FeO compositions, when the CURVFT program is utilized.

Table V-2-5: Spectrographic Analysis of Magnetite  
and Ilmenite from Sample C-2\*

Element	Concentration (ppm)	
	Magnetite	Ilmenite
Be	34	12
Ga	84	tr.
Ti	0.90 % (?)	too much
Cr	tr.	not found
V	2315	815
Ni	74	tr.
Co	330	55
Cu	300	28
Y	not found	tr.
Mn	190	1965
Sc	tr.	tr.
Zr	1.25	90
Mg	0.455 %	0.15 %

\* Analyst: F. C. Campbell, McMaster University

The main source of uncertainty in Fe and Ti for all analyses arises from random experimental errors (Appendix F). Errors due to counting statistics (amounting to  $\sqrt{N}$  where  $N$  = no. of counts) also account for a significant source of variation because count rates were comparatively low (never exceeding 3000 counts/sec. on Fe in magnetite under the most favourable conditions). Both FeO and  $TiO_2$  are estimated to be precise to within a least 5 wt.%. Generally the values are better than this ( $\pm 2\%$ ).

The sum of FeO,  $Fe_2O_3$  and  $TiO_2$  for all analyses tends to be low. This is due mostly to the presence of minor elements such as V, Mn, Mg, Cr and Al, which were not detected. The sum of these elements is estimated to amount to approximately 2 wt.%. In the case of sample C-13, which is an early analysis, the high values for the sum are thought to be due to abnormally high counts on standards and these analyses must be considered inferior.

It is estimated that the final recalculated mol.% values for hematite-ilmenite are precise to within 10 mol.%. This estimate takes into consideration all sources of error, including unanalyzed elements, random experimental error and error inherent in the recalculation procedure.

### V-3. X-Ray Diffraction Investigation

#### A. Unit Cell Determination of the Magnetite

Several investigators have shown that a systematic change in unit cell dimensions accompanies change in composition of one-phase Fe-Ti spinels resulting from experimental oxidation (Akimoto et al., 1957; Lindsley, 1962). Buddington and Lindsley (1964) state that unit cell data alone cannot be used to determine the compositions of natural Fe-Ti spinels because there may be a wide variation in the composition and degree of oxidation of the magnetic minerals for the same value of lattice parameter (see Buddington and Lindsley, 1964, p. 348 and Abdullah, 1965, p. 275). In addition Abdullah (op. cit. p. 278) suggests that low grade metamorphic rocks commonly contain non-stoichiometric magnetite.

An investigation of the unit cell dimensions of the separated magnetites was carried out in order to determine the relationship between lattice parameters and chemical composition of the magnetites as determined on the probe.

Aliquots of magnetite separates were ground in a mechanical mortar for 45 minutes; a small quantity of pure, finely ground NaCl was added as internal standard to the mixture which was then homogenized and mounted on a glass slide with clear nail polish and acetone. Mn filtered  $\text{FeK}_\alpha$  radiation was used to obtain X-ray traces of each sample. ( $\text{CoK}_\alpha$  radiation which gives a higher intensity to the same

peak than  $\text{FeK}_\alpha$  radiation was not available). The magnetite (311) peak was scanned repeatedly at  $\frac{1^\circ}{4}$ /min. and the values of the unit cell dimensions were averaged and their standard deviation calculated. The results are shown in Table V-3-1.  $8.3956\text{\AA} \pm 0.0041$  is the average for all the magnetites determined.

Table V-3-1: Unit Cell Determination of Magnetite

Sample No.	Unit Cell ( $a_0$ in $\text{\AA}$ )	Standard Deviation ( $\text{\AA}$ )	No. of scans of (311) peak
C-1	8.404	0.005	18
C-2	8.398	0.003	5
C-3	8.393	0.000	2
C-4A	8.393	0.001	5
C-4B	8.394	0.001	7
C-5A	8.399	0.001	5
C-5B	8.397	0.001	5
C-6	8.387	0.001	7
C-9	8.396	0.002	4
C-13	8.399	0.006	8
C-14	8.396	0.003	5
C-15	8.392	0.003	2
C-17	8.393	0.002	2
C-18	8.391	0.003	2

Average of 14 determinations  $8.3956\text{\AA} \pm 0.0041\text{\AA}$

Discussion of the Unit Cell Data

Table V-3-2 shows the unit cell dimensions that have been reported in the literature for pure magnetite.

Table V-3-2: Unit Cell Dimensions of Pure Magnetites

Size of Unit Cell (a <sub>o</sub> in Å)	Description of Magnetite	Reference
8.396	v. pure natural mte from Bisberg, Sweden	Basta (1957)
8.395	"generally accepted" value for pure natural magnetite	Zeller & Babkine (1965)
8.395	pure synthetic magnetite	Lindsley (1962), Akimoto et al. (1957)
8.395	pure natural magnetite from Mineville, N. Y.	Deer, Howie & Zussman (1966)

The unit cell values determined are considered to be accurate to within the standard deviation indicated. They might be improved somewhat by use of  $\text{CoK}_\alpha$  radiation, which was not available. Powder photos, which would also allow a more accurate determination, could not be taken with the Fe tube available. The unit cell value of  $8.396\overset{\circ}{\text{Å}}$  in conjunction with the very low  $\text{TiO}_2$  content of the magnetites (as demonstrated by probe analyses shown in Table V-2-2) uniquely determines that the magnetites are very close to "pure" and stoichiometric (see Fig. 10, p. 348, Buddington and Lindsley, 1964). The effect of small quantities of minor elements on the unit cell dimensions seems to be negligible as shown by Zeller and Babkine (1965) who were able to derive an equation that adequately describes the variation of unit cell dimen-

sions of magnetite with variation in  $\text{TiO}_2$  content.

#### B. Determination of Hemo-Ilmenite Composition

The theory of X-ray diffraction analysis of mixtures was developed by Klug and Alexander (1954) and applied by Petruk (1964) to the analysis of binary mixtures of some rock-forming minerals. He measured the peak intensity of a characteristic reflection from a pure phase (e.g. quartz), then noted the attenuation due to absorption of this intensity caused by admixture of a second mineral (e.g. pyrrhotite). An unsuccessful attempt was made to apply this method to determination of the amount of hematite in the hemo-ilmenite separates. The major problem encountered lay in the difficulty of making reproducible mineral mounts for intensity determination. Also, the binary standard mixtures of hematite and ilmenite in varying proportions did not seem to behave according to theoretical predictions.

On the suggestion of H. D. Grundy (personal communication, 1968), the peak intensity ratio  $I_{(104)} \text{ ilm} / I_{(104)} \text{ hem}$  was utilized, eliminating several of the variables attendant to sample preparation that require close control. Construction of an empirical calibration curve eliminates the requirement of theoretical behaviour.

Five standard mixtures [ $\text{Hem}_{18.07}$ ,  $\text{Hem}_{37.43}$ ,  $\text{Hem}_{50.00}$ ,  $\text{Hem}_{67.77}$  and  $\text{Hem}_{90.53}$  (wt.%) ] were prepared from a pure hematite specimen from the Mesabi range and ilmenite separated from sample C-17. Although no chemical analysis of the Mesabi hematite was available, the X-ray

trace showed it to be very pure. In addition, peak positions and intensities of the (104) peaks were entirely comparable with those of spec-pure hematite. All available evidence, including microscopic observations, electron probe work and unit cell determination, suggests that the composition of ilmenite C-17 is similar to ilmenite C-2, for which a chemical analysis is shown in Table V-1-2. Insufficient amounts of the C-2 separate remained for it to be used to prepare the standard mixtures.

One gram samples of hematite and ilmenite standards and hemo-ilmenite separates were ground in a power mortar. Tatlock (1966) states that crushed mineral samples (in which crystallite size of all constituents is less than 100 $\mu$ ) can readily be ground to the optimum 40 $\mu$  size in 15-30 min. All samples were ground for 45 minutes. Weighed amounts of hematite and ilmenite powders for standard mixtures were then mixed in plastic vials for 3 minutes in a spectroscopic mixer. All powders were mounted on a glass slide with clear nail polish and acetone.

FeK $_{\alpha}$  radiation and the strongest peak (the (104) peak) of both hematite and ilmenite were used. Generally the X-ray scan rate was 1/4 $^{\circ}$   $\theta$ /minute, but comparable results were obtained from more rapid scan rates. All intensities referred to are intensities above background.

The ratio I ilm/I hem was found to be exponentially related to the wt.% hematite of the five standards (Fig. V-3B-1)\*. The ratios

---

\* The curve can be represented by the equations:  $\log (I \text{ ilm}/I \text{ hem})_{\text{unknown}} = -0.017959 x + 0.6990$  or  $x = 54.821 \log 5.0/(I \text{ ilm}/I \text{ hem})_{\text{unknown}}$  where  $x = \text{wt.}\% \text{ hematite}$ .

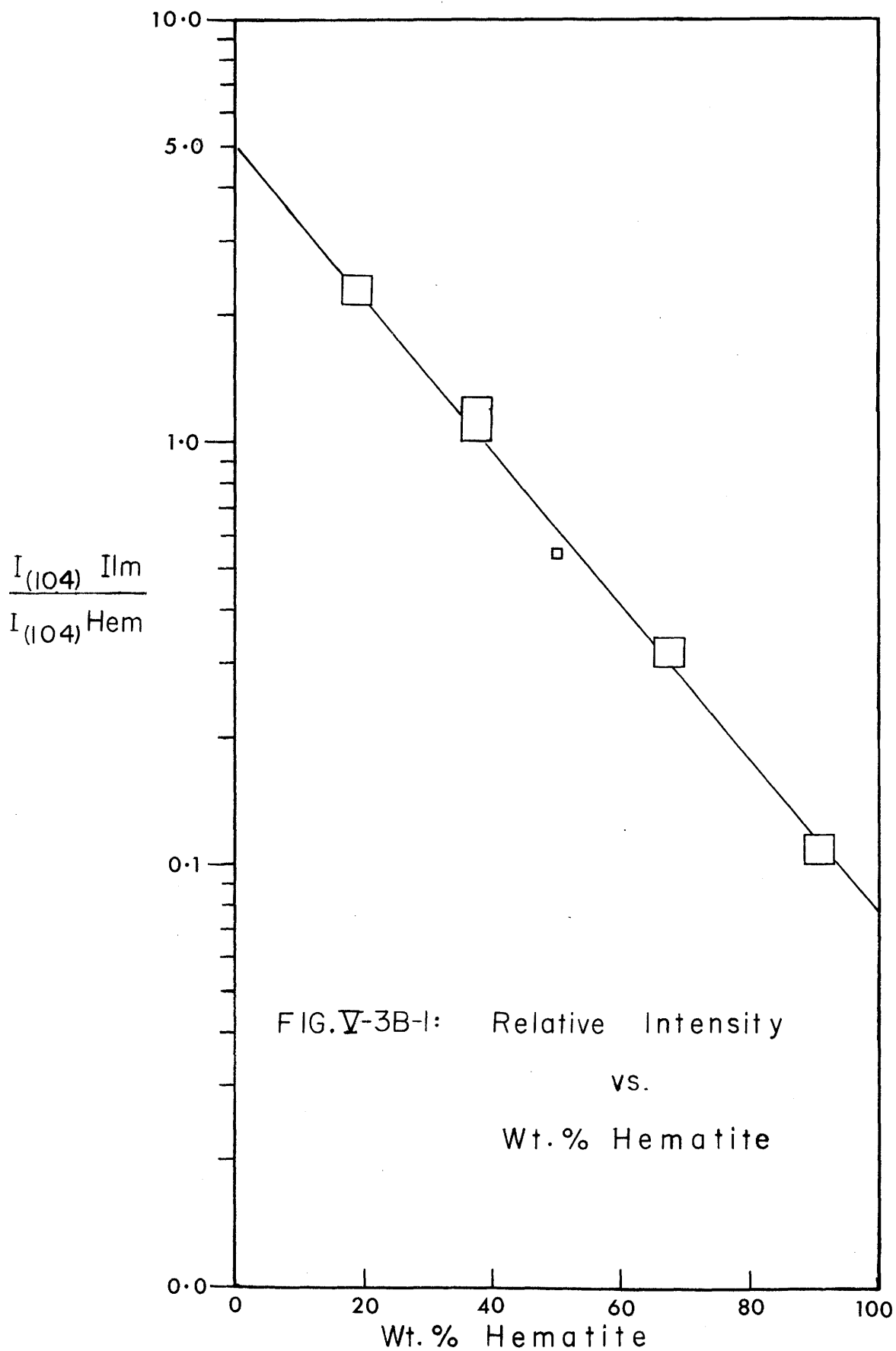


Table V-3B-1: Composition of the Hemo-Ilmenite Separates Determined  
by X-Ray Diffraction

Sample No.	$I_{(104) \text{ ilm}} / I_{(104) \text{ hem}}^+$	Wt.% Hematite $\pm$ 5 wt.%
C-1	1.06	37
C-3	1.63	27
C-4A	3.49	9
C-4B	1.29	33
C-5A	2 <sup>++</sup>	20
C-5B	2.40	18
C-6	5	pure ilm <sup>+++</sup>
C-9	1.02	37
C-13	1.36	31
C-14	0.66	48
C-15	0.81	44
C-18	2.10	20

+ These are averages of three independent determinations. The error (one standard deviation of the ratio) in this column is between 0.10 and 0.15 relative units.

++ Uncertain because of the large amount of garnet impurity in the separate. Note however that the proportion of hematite to ilmenite can be estimated independently from Fig. V-2-1 to be a minimum of Hem<sub>35-40</sub>.

+++ The method is insensitive to 5% hematite or less. Microscopic observation shows minute lamellae of hematite throughout. There also is up to 10% hematite in solid solution (see section VI).

plotted in the figure are the averages of between 20 and 50 scans of the (104) peaks of hematite and ilmenite and the size of the boxes indicates 1 standard deviation of the ratio.\*\* The composition of the hematite-ilmenite separates shown in Table V-3B-1 was determined from Fig. V-3B-1 by averaging three independent analyses and referring them to the curve.

#### Discussion of Hemo-ilmenite Composition Determinations

There are numerous sources of uncertainty in this method. They are mainly related to the difference between the standard mixtures and the samples. The former are mechanical mixtures of end members while the latter are exsolved from an originally homogeneous phase. If exsolution is complete and large lamellae of the exsolving phases are formed, the samples will closely resemble the standard mixtures upon the same degree of comminution. For incomplete or partial exsolution of the phases, the similarity will not be as close.

The electron probe analyses in section V-2 indicate that the 'pure' ilmenites C-17 and C-2 contain between 10 and 15 mol.%  $\text{Fe}_2\text{O}_3$ . These values may be somewhat high, since chemical analysis of C-2 ilmenite (Table V-1-2) indicated 8 mol.% hematite and unit cell parameters plotted on Lindsley's (1963) Fig. 2 show 5 mol.% hematite. The uncertainty in the composition of the standards and the effect of

---

\*\* If  $z = f(x, y)$ :  $s_z = \left( \left( \frac{dz}{dx} \right)^2 s_x^2 + \left( \frac{dz}{dy} \right)^2 s_y^2 \right)^{\frac{1}{2}}$

where  $s_x$ ,  $s_y$ ,  $s_z$  are the standard deviations of  $x$ ,  $y$  and  $z$  res-

pectively. Thus for unknown C-4B,  $I_{\text{ilm}}/I_{\text{hem}} = \frac{21.08 \pm 1.08}{16.4 \pm 1.1} = 1.285 \pm 0.108$

Baird (1962)

silicate impurities on the peak intensities of the unknowns suggests that the wt.% hematite values in Table V-3B-1 are only good to  $\pm 5$  wt.% hematite.

Recalculation of these wt.% values to mol.% hematite thus serves little purpose since the two differ only by one or two percent (e.g. Hem<sub>44</sub> Ilm<sub>56</sub> wt.% equals Hem<sub>42.3</sub> Ilm<sub>57.7</sub> mol.%). Subsequently, they will be treated as mol.% values.

## VI. DISCUSSION AND INTERPRETATION OF RESULTS

### VI-I. Composition of the Opaque Minerals in the Whitestone Anorthosite

#### Magnetite

The electron probe analyses of magnetites from all localities indicate a Ti content below the limit of detection of the probe (i.e., less than 1%, see Table V-2-2). Chemical analyses of magnetite concentrates (Table V-1-1), show varying amounts of  $\text{TiO}_2$ , which must be considered to be largely due to contamination. Unit cell data also suggest a very low  $\text{TiO}_2$  content (section V-3A).

The low  $\text{TiO}_2$  and MnO content of the magnetites supplements textural and geological evidence of metamorphic recrystallization of magnetite. In an early paper, Buddington et al. (1955) suggested a possible thermometric significance for the  $\text{TiO}_2$  content of magnetites. The low Ti content of metamorphic magnetite has been noted by several authors (e.g., Heier, 1956; Marmo, 1959; Abdullah and Atherton, 1964; Abdullah, 1965). The MnO contents of the magnetite and ilmenite from localities C-2 and C-15 clearly plot on Fig. VI-1 in the field of metamorphic gneisses and metamorphic ilmenite-titaniferous magnetite ores, very near the origin.

Unit cell determination on the magnetite from all localities indicated an average  $a_0$  value of  $8.396 \text{ \AA} \pm 0.004 \text{ \AA}$ . Buddington and Lindsley's Fig. 10 (p.348), which is a plot of compositions and lattice parameters of one-phase spinels from volcanic rocks, indicates that the determined magnetites should be stoichiometric. However, recent work

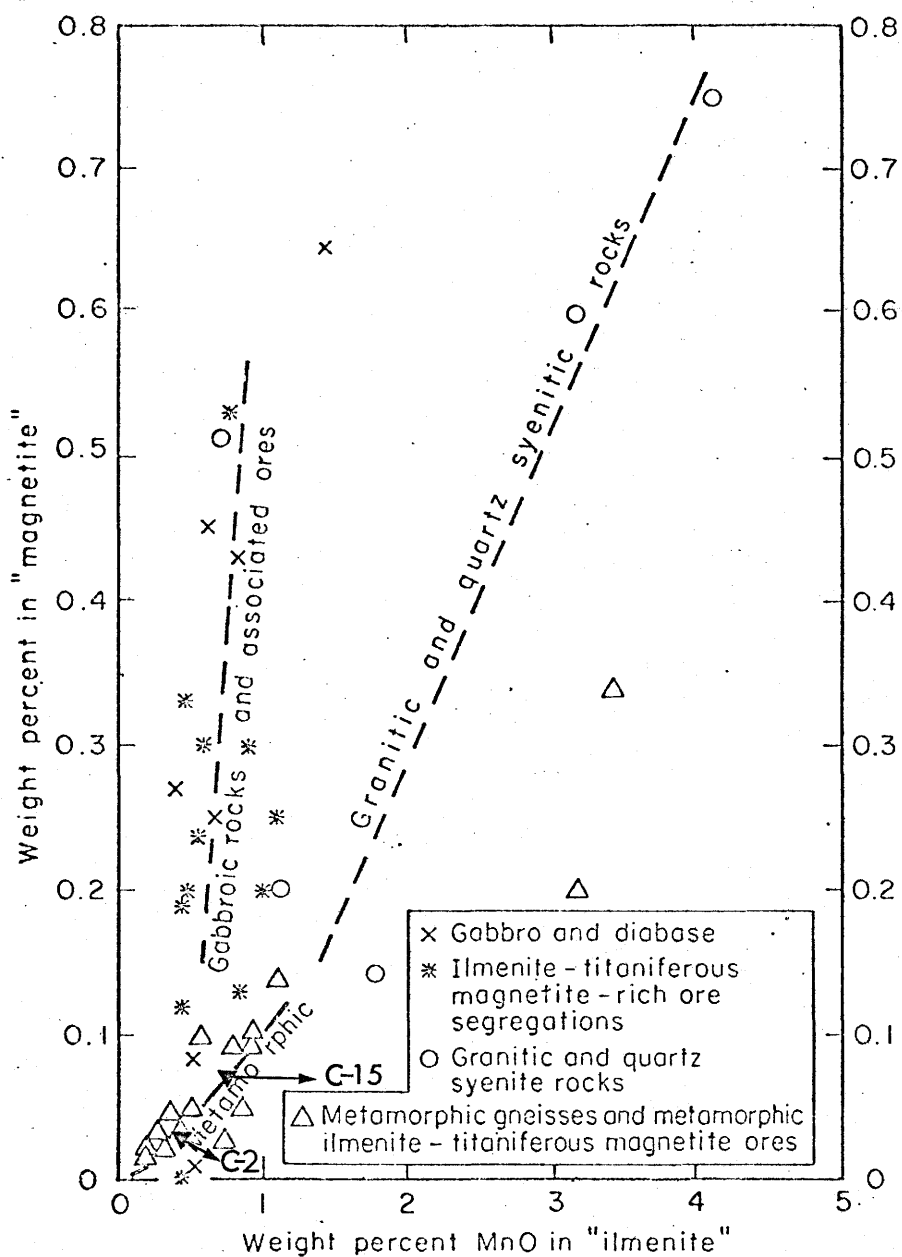


Fig. VI-1: Distribution of MnO Between Coexistent Titaniferous Magnetites and Ilmenite (or Ferri-ilmenite).

After Buddington and Lindsley, 1964, p. 353.

by Abdullah on metamorphic magnetites (Abdullah, 1965) has suggested that the 8.40 Å line of equal unit cell edge is in a different position than in Buddington's figure. As shown in Fig. II-1 of the system FeO-Fe<sub>2</sub>O<sub>3</sub>-TiO<sub>2</sub>, the 8.40 Å line emanates from pure magnetite and parallels the magnetite-hematite join for some distance. Abdullah also presents a number of analyses of metamorphic magnetites which show an excess of Fe<sub>2</sub>O<sub>3</sub> above that required by stoichiometry. Lindsley (1962) found a maximum solubility of 8% Fe<sub>2</sub>O<sub>3</sub> in magnetite at low oxygen pressure and 1075°C (also indicated in Fig. II-1). These observations suggest that the assumption of stoichiometry of the magnetites from the Whitestone anorthosite should be examined more closely.

In pure stoichiometric magnetite, the ratio FeO/Fe<sub>2</sub>O<sub>3</sub> (wt.%) is 0.45. For the "better" magnetite analyses of Table V-1-1 (i.e., low Ti indicated) this same ratio varies from a low of 0.55 (C-3) to a high of 0.78 (C-5B), indicating excess FeO rather than Fe<sub>2</sub>O<sub>3</sub>. In part, this may be contamination of the concentrate by rhombohedral phases.

The stoichiometry of the magnetite must be questioned on other grounds, pertaining to the reaction relationship between magnetite and hemo-ilmenite. This point will be dealt with below.

Both Anderson and Hargraves have observed low TiO<sub>2</sub> contents in the magnetites of anorthosite. The Labrieville anorthosite (Anderson, 1966a) contains magnetite with minor exsolved ilmenite lamellae and TiO<sub>2</sub> contents ranging between 1 and 5 wt. %. The magnetite in the Allard L. anorthosite suite (Hargraves, 1962) shows no exsolved ilmenite and 0.8 to 3.3 wt. % TiO<sub>2</sub>.

It seems that magnetite from anorthosites in general tends to

have substantially lower  $\text{TiO}_2$  contents than the magnetite of quickly cooled volcanic rocks. Note that both the Allard L. and Labrieville anorthosites are also in the Grenville province and therefore probably have had a similar metamorphic history.

#### Rhombohedral Phases

The analyses of ilmenite grains presented in Table V-2-3 indicate that ilmenite generally contains between 8 and 12 mol.% or an average of 10 mol.% hematite in solid solution. The "grains" for analysis were carefully selected, large, apparently homogeneous areas of ilmenite (either lamellae or discs) in hemo-ilmenite, as well as reaction rims adjacent to magnetite (see section V-2). However, as was discussed in section IV-2, only sample C-2 contains separate homogeneous grains of ilmenite (which also contains 8 mol.% hematite in solid solution and is thus ferrianilmenite).

The analyses of coarse hematite and ilmenite lamellae (Table V-2-4), on the other hand, show a wider range of compositions, between approximately  $\text{Hem}_{70}$  and  $\text{Hem}_{10}$ , respectively. Analyses of hematite lamellae indicating compositions closer to pure hematite than  $\text{Hem}_{70}$  are inferior (i.e., sum of  $\text{FeO}$ ,  $\text{Fe}_2\text{O}_3$  and  $\text{TiO}_2$  is less than 97 or greater than 102 wt. %). It is concluded that the ilmeno-hematite lamellae have a maximum hematite content of 70 mol.%. This value was also observed by Anderson, in ilmeno-hematite from an unspecified locality, presumably the Labrieville anorthosite (Anderson, 1966b).

The entire range in composition of lamellae listed in Table V-2-4 can be explained by reference to Fig. V-2-1, which is a typical electron

beam traverse of hemo-ilmenite grains. The composition determined will be a function of crystallographic orientation to some extent (lamellae making a shallow angle with the surface of the specimen will tend to increase electron beam penetration of near surface boundaries), but will primarily be a function of the width of the exsolution lamellae and of the electron beam. Incomplete resolution of exsolved lamellae by the electron beam will result in a chemical analysis which combines both guest and host phase. For example, in the area between the numbers 1 and 2 (part A of Fig. V-2-1) the exsolved hematite lamellae are too fine to be completely resolved and seem to be ilmenite-rich compared to those further from the magnetite. As the lamellae become larger (area 3), the exsolved hematite phase is completely resolved but the second generation ilmenite lamellae in this hematite are not.

The composition of this second generation ilmenite as well as the limiting compositional values for the primary exsolved phases is of paramount importance to the shape of the solvus in the hematite-ilmenite system. In Fig. V-2-1 B, a trace of a typical traverse across a large exsolved ilmeno-hematite lamellae is illustrated, with part of the adjacent hemo-ilmenite lamellae also shown (areas marked 1 on either side). All the second generation ilmenite lamellae in this hematite lamella are completely enclosed by hematite and closely resemble those illustrated by C. M. Carmichael (1961, p. 511, Fig. 1C). In the area marked 2, this secondary ilmenite is not completely resolved by the electron beam, but in area 3, a 10-15  $\mu$  wide secondary lamella is completely resolved and has an identical composition to the

adjacent primary ilmenite lamellae (Hem<sub>10</sub>).

C. M. Carmichael (op. cit., p. 523) showed that the second generation hematite is richer in Fe<sub>2</sub>O<sub>3</sub> than the primary hematite in the Allard L. ilmenite ores. His experiments involved homogenizing and exsolving specimens and inferring compositions by X-ray diffraction and Curie point methods. On this basis he fitted a solvus to: "those points which should be closest to the equilibrium composition using all of the available information". The composition of the second generation exsolved ilmenite was not determined and the ilmenite-rich limb of the solvus below 700°C was inferred on the basis of one Curie point determination and one point determined by Uyeda (1958), both from natural specimens at room T. It resembles that inferred by Nichols (1955). C. M. Carmichael's solvus as redrawn by Lindsley (1963) is shown in Fig. VI-2. The fact that the composition of both the first and second generation ilmenite in the hemo-ilmenite of the Whitestone Anorthosite are the same suggests that the ilmenite-rich side portion of the solvus curve is almost vertical. A solvus consistent with the composition observed in the hemo-ilmenites is shown in Fig. VI-2.

The hematite composition determined (Hem<sub>70</sub>) may be the result of equilibrium cooling to 450°C (or lower) along the hematite limb of the author's suggested solvus, or it may be the result of cessation of exsolution at approximately 875°C in a system with Carmichael's solvus. The latter possibility seems highly unlikely since Carmichael was able to observe exsolution in his charges after 100 days at 400°C. In the absence of more detailed knowledge about the hematite-rich limb (which could be obtained by probing the second generation hematite

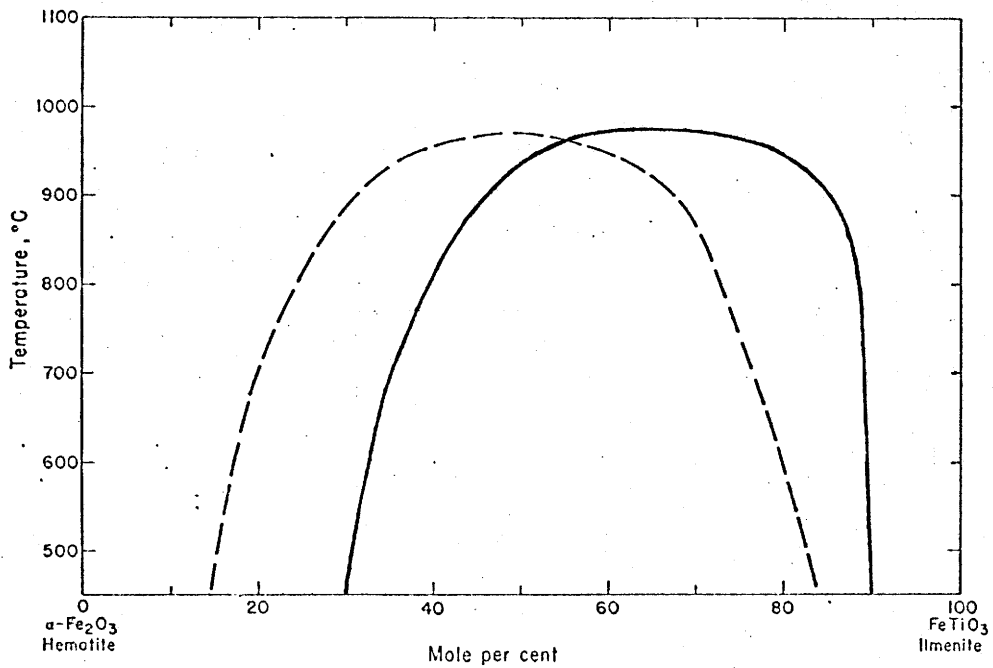


Fig. VI-2: C. M. Carmichael's (1961) Solvus (dashed line) and Suggested Solvus Consistent with Composition of Hematite and Ilmenites in Whitestone Anorthosite (solid line).

After Lindsley, 1963, p. 62.

lamellae) and the kinetics of exsolution, the suggested modification of the hematite-rich limb must be considered tentative.

To account for the two generations of mutually exsolved phases, C. M. Carmichael (op. cit., p. 523) states that there was a very long period during the formation of the Allard L. deposit at which the temperature was between 575 and 600°C:

"It is quite possible that this was the constant temperature at the depth of burial of the deposits in the roots of the pre-Cambrian mountains. The smaller lamellae, both of ilmen-haematite in the haemo-ilmenite, and haemo-ilmenite in the large lamellae have exsolved at the progressively lower temperature produced by erosion that brought the deposits to the surface. The extremely small lamellae that are richest in hematite, and can only be identified by their Curie point, may have separated in relatively recent geological time. It does not appear that room temperature equilibrium has been reached yet."

The importance of kinetics in the formation of the Allard L. textures seems certain. However, the occurrence of this same exsolution type in ilmenites from a wide variety of environments, e.g., in other ilmenite deposits (see Rose, 1960, 1961) in the charnockites of Vohibarika, Madagascar described by Bolfa et al. (1961) and in gabbro (Krause, 1965), makes C. M. Carmichael's two-stage cooling process seem unlikely.

The bulk composition of the rhombohedral phase in the Whitestone anorthosite varies markedly throughout the area sampled, -- between about Hem<sub>50</sub> and Hem<sub>10</sub> (Table V-3B-1). The values in this table are low, if anything, because the ilmenite standard used contained some exsolved hematite, and of course, about 8% hematite in solid solution (section V-3B). Local variation in oxygen fugacity seems likely for the Whitestone anorthosite on the basis of this observed variation in bulk composition of the ilmenite phase and the hemo-ilmenite reaction rim with magnetite

described below.

### Sulfides

The sulfides pyrite, pyrrhotite and chalcopyrite occur as minor interstitial constituents in the oxide-rich segregations of the Whitestone anorthosite as in many anorthosites (Hargraves, 1962; Rose, 1960, 1961 and Anderson, 1966a). This would seem to suggest that one is dealing with phases in the as yet undetermined system Fe-Ti-O-S in the ores of these deposits. However, no reference was found describing sulfides that constituted more than about 4% of the opaques, which suggests that  $f_{S_2}$  was very low indeed during formation of the bulk of the oxides.

Recent investigations in the system Fe-S-O (Naldrett, 1968) have shown that equilibrium coexistence of magnetite and pyrrhotite requires at least 30% S at liquidus temperatures. Only during the very latest differentiation stages could such conditions have existed in the Whitestone anorthosite. Furthermore, there is textural evidence (veins containing sulfides) that some of the observed sulfides were introduced later than the oxides. This suggests that sulfides need not be considered in a discussion of the phase relations.

### Samples C-5A, C-5B and C-2

C.I.P.W. norms were calculated from chemical whole rock analyses of samples C-2, C-5A and C-5B using a computer program written by I. M. Mason.

The norm for C-2 showed 3% magnetite, 9% ilmenite and 5% apatite. The high apatite is somewhat unusual and may be pertinent to the selection of theories for the origin of the oxides. Philpotts (1967)

suggested on the basis of experimental and field work that oxide-apatite rocks, commonly associated with anorthosite, formed by immiscibility of apatite-oxide and silicate liquids, citing Allard L. as an example. Hargraves (1962, p. 169) shows the maximum apatite content of the mafic-rich rocks associated with the Allard L. ores to be 9.8 volume %. Thus, the requisite composition (approximately 33% apatite and 66% magnetite) for formation by segregation of an apatite-oxide liquid is not observed either at Allard L. or at Dunchurch. Philpotts' theory thus does not hold, unless it is postulated that such a segregation product has been considerably modified.

The bulk composition of rhombohedral phases (Table V-3B-1) is not significantly different in C-5A (Hem<sub>20</sub>) and in C-5B (Hem<sub>18</sub>) even though metamorphic differentiation in C-5B has been extensive. Chinner's oxidation ratios are 18 for C-5A and 22 for C-5B -- only a slight difference. C.I.P.W. norms further reflect the similarity of C-5A and C-5B. The norms for both rocks show approximately 5% magnetite, 5% ilmenite, 0.5% apatite and no hematite.

These points indicate that metamorphic differentiation between samples C-5A and C-5B has not been accompanied by significant oxidation, reduction or change in bulk composition at handspecimen size. This is so despite the fact that all pyroxene in C-5A (15% by volume) has been altered to hornblende in C-5B. Bowes and Park (1966) also reported no change in bulk composition of handspecimens from adjacent outcrops.

## VI-2 Explanation of the Reaction Rims in Hemo-Ilmenite Adjacent to Magnetite

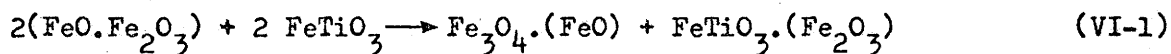
Reaction rims between hemo-ilmenite and adjacent minerals are not uncommon. They have also been observed in the Labrieville anorthosite, in the Allard L. and Egersund, Norway ilmenite ores, in the Abu Ghalaga ilmenite deposit in Egypt and in ilmenite ores from Espeland, Norway. The excellent photos of Allard L. ores in the Bildkartei der Erzmikroskopie (Maucher and Rehwald, 1961) show reaction rims in hemo-ilmenite adjacent to a silicate phase. Freund (1966, p. 214) illustrates a hemo-ilmenite grain bordering on magnetite with "marked little hematite in the outer portions" (of the ilmenite) from Espeland near Bergen, Norway.

Several explanations of this zoning relationship have been presented. In the ilmenite ores of Abu Ghalaga, Krause (1965) found a reaction rim consisting of homogeneous ilmenite in hemo-ilmenite where this phase was in contact with either silicate, magnetite or sulfide minerals. These secondary minerals were formed by a later hydrothermal-pneumatolytic phase of mineralization. By means of an electron beam traverse across the secondary minerals and ilmenite rim, he demonstrated that diffusion of Fe into the secondary mineralizing phase is the cause of this hematite-poor rim (Krause, 1967). A marked increase in Ti content in the bordering ilmenite and a corresponding decrease in Fe content is observed as the "guest" phase is approached. Krause attributes the diffusion of Fe to the higher temperature prevailing during introduction of the second ("guest") phase of mineralization.

In Basta's work on the  $\text{Fe}_3\text{O}_4$ - $\text{FeTiO}_4$ - $\text{FeTiO}_3$  system (Basta, 1960), an early work by Evrard is referred to:

"Evrard (1944) observed in the Egersund ore, at the contact of an ilmenite grain with a magnetite one, a small area where hematite exsolution lamellae disappear and which he attributed to a migration phenomenon."

A similar relationship in the Egersund ores has been illustrated by Hubaux (1956). Basta (1960) explains this phenomenon by a process similar to that produced on heating magnetite-ilmenite intergrowths; a process which results in the enrichment of magnetite in FeO and which he depicts as follows:



Basta also presents recalculated analyses of the Egersund Ti-poor, FeO-rich magnetites which make his proposed process plausible for the Egersund ores. For the Whitestone anorthosite oxides, this process does not seem to be valid because although there is some possibility of excess FeO in the magnetite,  $\text{Fe}_2\text{O}_3$  decreases in the ilmenite reaction rim adjacent to the magnetite. It should be noted however, that the ilmenite adjacent to the magnetite does contain 10% excess  $\text{Fe}_2\text{O}_3$ .

In his study of the Labrieville anorthosite, Anderson (1966, p. 1677) states:

"Relict zoning of hemo-ilmenite adjacent to magnetite indicates extremely local influence of oxidation-reduction agents. Apparently, the proportion of titaniferous magnetite to water will determine how much reduction of ferrian ilmenite takes place during subsolidus cooling of ferrian ilmenite and titaniferous magnetite assemblages. The selective zoning of hemo-ilmenite grains adjacent to ilmeno-magnetite suggests that ferrian ilmenite served as oxidizing agent, at least during the final stages of oxidation of the titaniferous magnetite."

The zoning relationship observed in the Whitestone anorthosite

oxides appears to differ from Krause's zoning in that he found the Fe concentration in the ilmenite to drop markedly and the Ti concentration to rise correspondingly in the vicinity of the guest phase. Fig. V-2-1A demonstrates that while there is less Fe in the ilmenite within 50  $\mu$  of the magnetite grain (due to depletion in hematite) the Fe concentration does not drop below that required for ferrian-ilmenite, with about 10% excess  $\text{Fe}_2\text{O}_3$  in solid solution (corresponding to approximately 47% FeO and 52%  $\text{TiO}_2$  by weight).

The electron probe trace also shows that the composition of the homogeneous ferrianilmenite directly adjacent to the magnetite has a composition identical to that observed for exsolved ilmenite throughout the grain. Plate 6, Fig. 2 illustrates depletion of  $\text{Fe}_2\text{O}_3$  in the hemo-ilmenite directly adjacent to the magnetite.

Two possible explanations for the observed zoning relations may be entertained:

1. Heating of the exsolved hemo-ilmenite occurred during metamorphism to a temperature in the vicinity of 700°C (below the temperature required for complete homogenization) permitting diffusion of  $\text{Fe}^{3+}$  to occur. Any magnetite present and nucleated at the grain boundary of the hemo-ilmenite could then grow at the expense of the hematite close to the grain boundary, but diffusion equilibrium throughout the hemo-ilmenite could not be reached because dropping temperatures increasingly inhibited molecular motion. Growth of magnetite by this process requires reduction of some of the  $\text{Fe}_2\text{O}_3$  to FeO. However, local  $f_{\text{O}_2}$  must have been sufficiently high

to inhibit formation of a Ti-rich magnetite. Possibly local buffering of  $f_{O_2}$  was achieved by the rhombohedral phases themselves. A pervasive fluid phase, reducing relative to ferriannilmenite, does not appear to have caused reduction of the  $Fe_2O_3$  since hematite lamellae adjacent to silicates were not reduced (as they were at Allard L.). However, the presence of a fluid phase of some sort is required for formation of amphibole from pyroxene during metamorphism.

2. During his experiments in the system  $FeO-Fe_2O_3-TiO_2$ , Lindsley (1963) found a strong T dependence of magnetite-ulvospinel<sub>ss</sub> in equilibrium with ilmenite-hematite<sub>ss</sub> for the NNO (Ni-NiO) buffer. Lindsley's isothermal sections for a portion of this system are shown as Fig. VI-3. A possible explanation of the phenomenon observed in this study is as follows:

As the oxide assemblage cooled at oxygen fugacities in excess of the NNO or even the  $MnO-Mn_2O_3$  buffers, ilmenite became impoverished in hematite and magnetite in ulvospinel. As can be seen from Fig. VI-3, this corresponds to a rotation of tie lines between coexisting magnetite<sub>ss</sub> and ilmenite<sub>ss</sub> about a fixed bulk composition.

At  $600^\circ C$  and  $f_{O_2}$  of the NNO buffer, ilmenite contains about 8 mol.% hematite and magnetite about 4 wt.%  $TiO_2$  (10 mol.% ulvospinel). At the same T but under somewhat more oxidizing conditions, the isothermal sections suggest that magnetite will contain less  $TiO_2$ , but that ilmenite composition will not differ

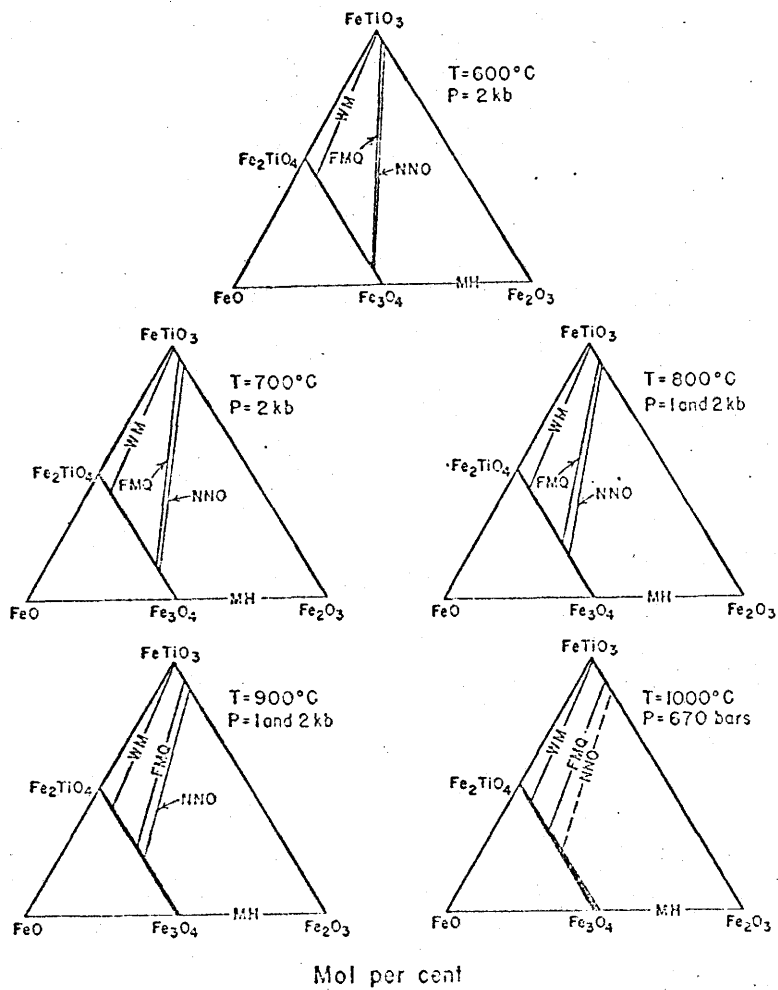


Fig. VI-3: Isothermal Sections Showing Tie Lines Between  
Coexisting  $\text{Mte-Usp}_{\text{SS}}$  and  $\text{Hem-Ilm}_{\text{SS}}$  for Several Buffers.

After Lindsley, 1963, p. 63.

significantly.

At some point during this cooling, the fall in temperature essentially stops diffusion of Ti from and infusion of  $\text{Fe}^{3+}$  into the magnetite. The observed zoning represents this process "frozen-in". The relict Ti content expected in magnetite if this mechanism is valid was not observed with the probe, but may, in fact, be present at concentrations too low for probe determination.

The first hypothesis proposed is particularly suited as an explanation of the marked euhedralism of many of the magnetite grains, which suggests growth by accretion during metamorphism, and is therefore favoured by the author.

### VI-3 Speculations About $f_{O_2}$ and T Conditions During Formation of the Oxides

The genesis of the titaniferous iron ores of anorthosites is closely connected to the genesis of the anorthosite itself. The question of anorthosite genesis is not definitely settled, but the magmatists seem to have the upper hand (Buddington, 1957; Anderson, 1966a).

In recent studies, the major hemo-ilmenite deposits have been considered as examples of high T, late stage magmatic differentiates (e.g., Hammond, 1952; Rose, 1960, 1961). Immiscibility between silicate and Fe-Ti oxide liquids has been proposed by Hargraves (1962), Anderson (1966a) and Philpotts (1966, 1967) in order to best reconcile field observations.

On the basis of marked similarity between Fe-Ti oxides in the Whitestone anorthosite and other well-described anorthosites, it seems safe to assume that a major portion of the oxides originally formed at magmatic temperatures between  $1100^{\circ}\text{C}$  and  $900^{\circ}\text{C}$ . The upper T was deduced from the 2 per mil primary fractionation of oxygen isotopes between ilmenite and plagioclase in the Labrieville anorthosite by Anderson (1965) and the lower T was estimated by Buddington (1957) from phase petrology of anorthosites in general.

Subsequent to the differentiation of the Whitestone anorthosite and formation of the oxides, at least one episode of prograde metamorphism caused formation of low Ti magnetite and almandine and hornblende rims around the oxides. This metamorphism was of the upper amphibolite or granulite facies grade (I. M. Mason, personal communication,

1968). Metamorphism apparently occurred under "wet" oxidizing conditions since pyroxene was altered to amphibole and hemo-ilmenite with up to 50% hematite was stable. If conditions had been more oxidizing than they were, say at the  $f_{O_2}$  of the MH buffer, rutile or pseudobrookite should have been observed as these are stable phases under these conditions (Lindsley, 1963).

The composition of the observed oxide assemblages thus restricts oxygen fugacities during metamorphism to values between the MH and NNO buffers. These are precisely the conditions under which the solvus in the hematite-ilmenite system occurs. When Lindsley performed his experiments, buffers were not available to allow accurate location of the solvus; consequently, his curves cannot be used to determine  $f_{O_2}$  and T of formation of the oxide assemblage in the Whitestone anorthosite from the mol.% compositions of hematite, ilmenite, magnetite and ulvospinel. However, at 700°C, which is approximately the temperature prevailing during upper amphibolite facies metamorphism (Fyfe, Turner and Verhoogen, 1958) the restrictions imposed by the compositions of the oxides and the metamorphic mineralogy can be used to indicate a  $-\log_{10} f_{O_2}$  of  $16.5 \pm 2.5$  (Fig. II-2).

## VII. SUGGESTIONS FOR FURTHER WORK

The following is a list of suggestions based on problems encountered or speculated upon either directly or indirectly during this study. It is hoped that they may provide guidelines for further research. They are not necessarily in order of importance.

1. Determine experimentally the position of the solvus in the hematite-ilmenite system using recently developed oxygen fugacity buffers (Eugster and Skippen, 1967).
2. Determination of the shape of the solvus in the hematite-ilmenite system by electron probe analysis of lamellae in exsolved rhombohedral phases from rocks that contain two coexisting rhombohedral phases (i.e., one hematite-rich and one ilmenite-rich). These rocks are rare (D. H. Lindsley, personal communication, 1968).
3. Study the kinetics of the hematite-ilmenite exsolution by homogenization experiments similar to C. M. Carmichael's (1961), but under controlled  $f_{O_2}$ . Composition of the exsolved phases could be determined by electron probe analysis. Kinetics of such exsolution might be speeded up by doping phases with minor elements to induce strain in the lattices.
4. Experimental determination of the variation in distribution coefficients of minor elements (especially Mn, Mg) with T for coexisting magnetite-ilmenite and hematite-ilmenite might provide the basis of a geothermometer.

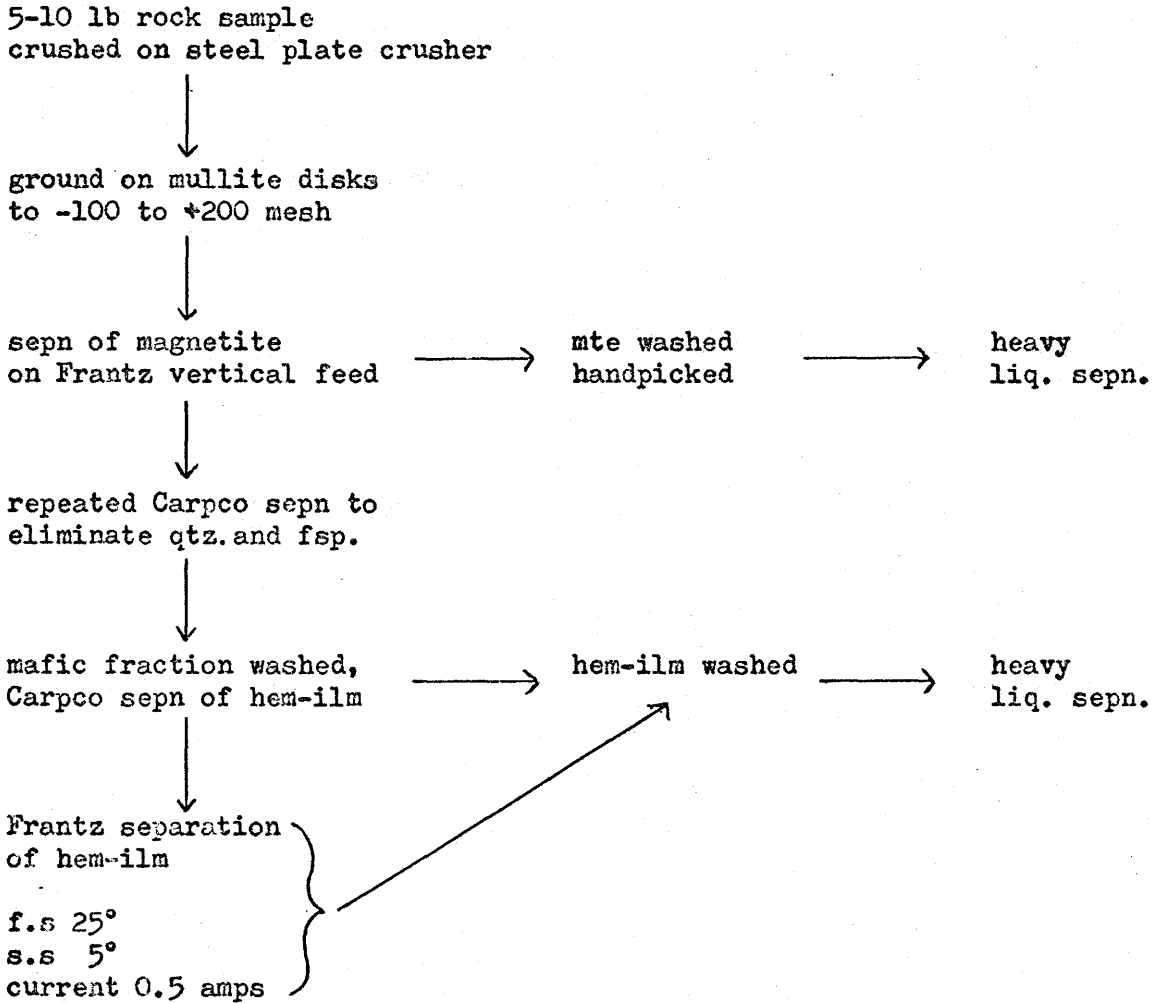
5. Probe analysis or chemical analysis of carefully separated oxides from a progressively metamorphosed oxide-rich igneous body to allow deductions about  $f_{O_2}$  - T conditions during metamorphism (regional or thermal).
6. Determination of the phase relations in the system Fe-Ti-O-S.
7. Correlation between host rock oxidation ratios and the compositions of metamorphic magnetite.
8. Verification of Verhoogen's (1962b) predictions about  $TiO_2$  distribution between coexisting silicates and oxides.
9. Extension of the work of Speidel (1965) on the determination of the effect of minor elements on  $f_{O_2}$  relations in the Fe-Ti oxide system.
10. Investigate the effect of  $P_{total}$  and  $P_{H_2O}$  on the oxide solvi in cubic and rhombohedral oxide solid solution systems.
11. Evaluation of the stoichiometry assumption made to recalculate chemical and probe analyses in order to come up with a single recalculation procedure for oxides to mol.% end members. (see e.g., Vincent et al., 1957; Lindsley, 1963; Wright and Lovering, 1965; Buddington and Lindsley, 1964; Aoki, 1966 and I. S. E. Carmichael, 1967).
12. Development of better separation methods for the oxides.

## Appendix A: Mineral Separation Methods

### I Crushing and Preliminary Separation (see Fig. A-1).

1. 5-10 lb. of sample were crushed in a steel plate jaw crusher.
2. The entire sample was powdered on Bico mullite disks to pass through -100 (149 $\mu$ ) to +200 (74 $\mu$ ) mesh sieves.
3. The most magnetic fraction was effectively separated from the sample by Frantz isodynamic separator, set for vertical feed and a current of 0.1 amps. The trough of the electromagnet was lined with aluminum foil to prevent the magnetite from sticking to it.
4. The magnetite concentrate was washed with water and acetone several times and further concentrated by handpicking with a horseshoe magnet on an inclined sheet of paper.
5. The magnetite free separate was cleaned of the quartzo-feldspathic fraction using a high current (2.5 amps) and rapid rotation rate of the magnet (setting 90 on the dial) on a Carpc magnetic separator. The remaining mafic fraction consisted mainly of pyroxene, amphibole, garnet and hemo-ilmenite.
6. The hemo-ilmenite was separated from this fraction on the Carpc separator using the same magnet rotation rate as in step 5 with a somewhat lower current. Since some hemo-ilmenite remained in the mafics, this residue was passed through the Frantz separator with a side slope of 5°, a front slope of 25° and a current of 0.5 amps. The two hem-ilm separates were combined, washed with water and acetone and dried.

Fig. A-1: Summary of oxide separation procedure.



## II Heavy liquid separation

Remaining silicate contaminants of the oxide concentrates were removed by use of methylene iodide (sp.G. 3.325 at 20°C, Handbook of Physics and Chemistry, 1963). The oxides were shaken with MeI in a separatory funnel using a circulatory motion. The slight centrifugal force that resulted, in addition to the greater density of the oxides, caused them to settle out first. When most of the oxides had settled out, they were tapped off. The lighter fraction was discarded. The oxide fraction was washed several times in acetone and dried under a heat lamp placed at a sufficient distance to prevent oxidation of  $\text{Fe}^{+2}$ . At every stage the purity of the concentrates was estimated under a binocular microscope. The final purity of the concentrates was determined by counting 1000 grains under transmitted light which allowed identification of the silicate impurities. The results are shown in Table A-1.

Table A-1: Silicate Contaminants in Oxide Separates \*

Sample No.	Separate	Oxide	Volume percent	
			Pyroxene	Garnet
C-1	mte	96.0	3.4	0.6
	hem-ilm	95.8	1.8	2.4
C-2	mte	97.8	2.2	---
	hem-ilm	98.7	1.3	---
C-3	mte	98.0	2.0	---
	hem-ilm	95.0	3.4	1.6
C-4A	mte	87.2	12.8	---
	hem-ilm	90.4	9.0	0.6
C-4B	mte	95.0	4.9	0.1
	hem-ilm	96.6	2.8	0.6
C-5A	mte	95.8	4.2	---
	hem-ilm**	80	---	20
C-5B	mte	92.6	7.0	0.4
	hem-ilm	95.4	4.6	---
C-6	mte	90.4	9.6	---
	hem-ilm**	95	3	2
C-9	mte	95.0	4.8	0.2
	hem-ilm	99.0	0.6	0.4
C-13	mte	72.6	27.2	0.2
	hem-ilm	96.8	2.0	1.2
C-14	mte**	97	3	---
	hem-ilm	97.4	0.2	2.4
C-15	mte	94.8	4.4	0.8
	hem-ilm	97.6	1.4	1.0
C-17	mte	94.0	6.0	---
	hem-ilm	94.4	3.6	2.0
C-18	mte	98.5	0.5	1.0
	hem-ilm	98.4	1.6	---

\* based on 1000 grains counted

\*\* visually estimated

## Appendix B: Sample and Standard Preparation for Electron Probe

### Microanalysis

The method used is similar to that recommended by Smith (1965) and has also been used by Haughton (1967). Because of the low takeoff angle on the Acton probe, considerable care must be taken during sample preparation.

Rock sections containing oxide-rich segregations were sliced with a diamond saw and ground using Buehler Ltd. coarse, medium and fine diamond impregnated aluminum disks. The sections were polished with nine  $\mu$  diamond paste and Metadi polishing oil on a rotating nylon cloth lap. A final polish with 1  $\mu$  diamond paste was found to give an excellent, high quality polish to all specimens. An ultrasonic probe with acetone was used to clean specimens between steps during polishing.

Thin sections of the specimens polished in the above manner were prepared by Don Falkiner. The polished surface was glued onto a glass slide with Canada Balsam, trimmed to size and ground with 600 mesh  $\text{Al}_2\text{O}_3$  to thin section thickness. In order to transfer the rock slice, the perimeter of the thin section was coated with vaseline and the section was glued onto another glass slide with epoxy cement which was allowed to harden. On subsequent heating, the C.B. softened and the first glass slide was easily removed. The polished surface was carefully cleaned of C.B. and polishing oil with acetone or methanol.

Grains of the minerals used as electron probe standards were

set with epoxy in holes drilled into a special brass sample holder to fit the Acton probe. The polishing procedure and sequence used was as above, with the final polish being provided by the one  $\mu$  diamond paste. This assures that the quality of the polish on sample and standard is the same.

Samples and standards were coated simultaneously with carbon in a vacuum deposition apparatus until the brass sample holder was purple in colour. This colour is easy to attain visually and gives a good conducting coat (Smith, 1965). Despite the carbon coat, which completely changed the optical properties of the oxides, it was found that the oxides could be easily distinguished from each other after some practice.

## Appendix C

Table C-1: Description of Electron Probe Standards

Standard No.	Donor and/or Source	Locality	Description	Analyst	Reference
64019	McMaster University Standard	Princess Sodalite Quarry, Bancroft, Ontario	very pure, homogeneous magnetite	J. Muysson, McMaster U. Dept. of Geol. (1964)	James, (1965)
A 1	A. T. Anderson, U.S.G.S., Washington D. C.	unknown Anderson's std. no. K 13-131. 81L	pure, Mg-rich ilmenite	Katzendorfer and Boileau, Quebec, Dept. of Nat. Res. (1964)	Anderson (1966a, b)
A 2		A128			
A 3		La Blache magnetite deposit, Quebec, Anderson's No. L4.175	mte with very finely ex-solved ulvospinel		Girault (1953) Anderson (1966a, b)
R 1993	P.W. Weiblen, Department of Geology, Univ. of Minnesota	unknown A.F. Buddington's field No. B 193	pure, homogeneous magnetite	C.O. Ingamells Univ. of Minnesota, (1953)	
R 1959		?	homogeneous ilmenite		
R 1958		ED 1924			

Table C-1 (continued)

Standard No.	Donor and/or Source	Locality	Description	Analyst	Reference
LHD ilm	D.H. Lindsley, Geophysical Laboratory, Washington, D.C.	synthetic minerals	pure ilmenite	composition in Table V-2-1 derived assuming mol composition is correct, then calculat- ing wt.% oxides.	Lindsley (1963, 1962)
LHD hem-ilm			hem <sub>70</sub> ilm <sub>30</sub> (mol %)		
LHD mte-usp			mte <sub>52</sub> usp <sub>48</sub> (mol %)		
L 20  L 31	C.M. Carmichael, Department of Geo- physics, Univ. of Western Ontario	Deccan basalt flows, India	homogeneous magnetite, with high ulvospinel content	Ade-Hall, (1964) Evans, (1965) *	Carmichael (1965)  Ade-Hall (1964)  Evans (1967)

\* see appended section

\*  
L 20, L 31

No chemical analyses of these minerals are available. Their compositions were determined independently, and on different electron-probes by Ade-Hall and B. W. Evans (University of California, Berkeley). Ade-Hall's results show a consistently higher percentage ulvospinel for these minerals than do Evans' (see Table 1, Carmichael, 1965). Ade-Hall's probe was an early model. Evans' data also agrees closely with the amount of ulvospinel expected from unit cell determinations. Therefore, more weight was given to his data. Thus, L20 was considered to contain 73% usp and L31, 74%. Ade-Hall (1964) reports that there should be no major amounts of Mg or Al because the total Fe and Ti contents are close to the expected value. However, by direct proportionality with standard R 1959, 2.3%  $Al_2O_3$  and 2.7%  $Al_2O_3$  were found in L20 and L31 respectively. Mg was not detected.

#### Appendix D: Description and Application of the CURVFT Fortran IV Program

During the first part of this study, when only three standards, two ilmenites and one magnetite-ulvospinel were available, the composition of oxides was obtained by simple proportionality, after the counts had been corrected for drift and background. Only counts from standards analysed immediately before or after the specimen, were used to calculate composition by proportionality.

As more suitable standards became available, covering a large range of possible compositions, CURVFT, a Fortran IV program for the McMaster IBM 7040 computer was utilized to analyse the results for Fe and Ti. The program was obtained from N. D. McRae, University of Western Ontario. Mg, Mn, and Al were obtained by proportionality from standards throughout.

The computer program establishes a calibration curve similar to that shown by Keil (1967, p. 24) by plotting standard counts, corrected for drift and background, against composition.

Each input card contains the composition of one oxide standard (in wt.%) and the counts per ten second interval (up to 10 separate ten second counts can be accommodated on one card) for the element (or oxide) of interest. Column 2 on standard and data card indicates the number of separate 10 second counts taken at each locality on the specimen or standard. The data cards contain only the number of counts per 10 seconds obtained from the unknowns for the same element as

above. Fig. D-1 is a listing of the program. Fig. D-2 shows input for a sample run and Fig. D-3 is the output for this same data.

The program fits data to the following equation:

$$C_i = A_0 + A_1 N_i + A_2 N_i^2 \quad (D-1)$$

where  $C_i$  = comp. of the  $i$ th standard.

$N_i$  = average no. of counts for the  $i$ th standard.

The method of fit is by minimizing the sum of the squares of the weighted errors.

$$E_i^2 = W_i (C_i - A_0 - A_1 N_i - A_2 N_i^2) \quad (D-2)$$

The "Error Sum of Squares" comes from this equation.

The resulting equations are:

$$\begin{aligned} 1. \quad & A_0 \sum_i W_i + A_1 \sum_i W_i N_i + A_2 \sum_i W_i N_i^2 = \sum_i W_i C_i \\ 2. \quad & A_0 \sum_i W_i N_i + A_1 \sum_i W_i N_i^2 + A_2 \sum_i W_i N_i^3 = \sum_i W_i C_i N_i \\ 3. \quad & A_0 \sum_i W_i N_i^2 + A_1 \sum_i W_i N_i^3 + A_2 \sum_i W_i N_i^4 = \sum_i W_i C_i N_i^2 \end{aligned} \quad (D-3)$$

This set of linear equations is then solved for  $A_0$ ,  $A_1$  and  $A_2$ .

The associated errors in these calculations are denoted "std. dev." and should be as small as possible. From the calibration curve drawn with  $A_0$ ,  $A_1$  and  $A_2$ , the composition of an unknown can be calculated. The error in the composition of the unknown is a combined result of error in the fit of the curve and of deviation of replicate analyses from the average.

The sample computer run given below is for a determination of  $TiO_2$  in hemo-ilmenite and ilmenite.

For each run \* several combinations of standard analyses were

tested in order to establish the best calibration curve i.e. the curve which minimizes the difference between known and calculated compositions in the back calculation step of the program.

For determination of the composition of the unknown magnetites, magnetite standards alone were sufficient to fix the calibration curve. Excellent curves were obtained, the difference between known and back calculated Fe content of the standards being consistently less than 1%. However, the range of Fe-Ti content of the ilmenite and hematite-ilmenite standards was not large enough to give a satisfactory calibration curve for determination of rhombohedral phases. When all the standards (mte, ilm, and hemo-ilmenite) analysed in a run were combined, an excellent calibration curve was obtained; consequently, unknown sample compositions were determined from the computer-drawn curve of all standards unless the difference between calculated and unknown compositions for the standards was greater than 2 wt.%. In such instances, the composition of the unknowns was obtained by simple proportionality with standards analysed immediately before or after the unknowns. The error in composition obtained by grouping magnetite and rhombohedral phases is considered to be negligible.

When counts from standards and/or pure metals varied only within 10% on successive days they were averaged. The resulting curve was better because it was drawn on the basis of a larger number of individual determinations (up to 50).

---

\* a run contains all the analyses between standard determinations when the counts on the standards do not vary by more than 10%, i.e. when drift can be assumed to be linear.

Often, there was considerable drift in the beam current, particularly during warmup of the microanalyser. Counts from standards determined at this time could not be averaged with the rest and composition of the unknowns was determined by proportionality. Despite this, some inferior analyses were obtained (e.g. ilmenite and hematite lamellae for sample C-13, Table V-2-4).

Before it was realized that the same detector crystals must be used to analyse for an element each time, different crystals were used and counts obtained were not comparable.

```

$JOB   WATFOR  000922 U KRETSCHMAR  030  010  030
$IBJOB          NODECK
$IBFTC
COMMENT          CODED 1966 BY L. W. FINGER
COMMENT          CURVFT PROGRAM, COURTESY N. D. MCRAE, UWO.
C YOU KNOW WHAT COMPUTER, QUESTION MARK. THIS DAMN PROGRAM ACTUALLY WORKS
  DIMENSION DATA(50), A(28,28), E(3),COEFF(3),TEMP(20),TITLE(12),
  1 COMP(50), C(28,28)
  1,WT(50),B(3)
  2 ,          COEF(3)
COMMENT  READ NUMBER OF STANDARDS AND TITLE, ZERO IN COLUMN 4
COMMENT  TERMINATES PROGRAM
  1 READ(5,2) NDATA,TITLE
  2 FORMAT(14,12A6)
  IF(NDATA)3,3,4
  3 STOP
  4 WRITE(6,5) TITLE
  5 FORMAT(1H1,5X12A6/76X4HCOMP4X10HAVG COUNTS4X7HSTD DEV5X6HWHEIGHT/)
  NPNT= MIN0(NDATA-1,3)
  DO 8 I=1,NDATA
  READ(5,6) NPNT,COMP(I),(TEMP(J),J=1,NPNT)
  6 FORMAT(12,13F6.0)
COMMENT  CALCULATE AVERAGE AND WEIGHT
COMMENT  COMPUTER DEAR, YOU ARE VERY SMART
  SUM=0.0
  SUMS=0.0
  DO 7 J=1,NPNT
  SUM=SUM+TEMP(J)
  7 SUMS=SUMS+TEMP(J)**2
  DATA(I)=SUM/FLOAT(NPNT)
  SIG=SUMS/FLOAT(NPNT)-DATA(I)**2
  WT(I)=1.0/SIG
  SIG=SQRT(SIG)
  8 WRITE(6,9) COMP(I),DATA(I),SIG,WT(I)
  9 FORMAT(F10.1,F14.1,F11.3,F11.5)
COMMENT  CLEAR LEAST SQUARES MATRICES, THEN FORM MATRICES
  DO 10 I=1,3
  B(I)=0.0
  DO 10 J=1,3
  10 A(I,J)=0.0
  DO 12 I=1,NDATA
  DO 12 J=1,NPNT
  B(J)=B(J)+COMP(I)*WT(I)*DATA(I)**(J-1)
  DO 12 K=1,NPNT
  IJ=J+K-2
  12 A(J,K)=A(J,K)+WT(I)*DATA(I)**IJ
COMMENT  INVERT MATRIK
  DO 102 J=1,3
  DO 102 I=1,3
102  C(I,J)=A(I,J)
  CALL INVERT(A, 3)

```

```

DO 100 I=1,3
E(I)=0
DO 100 J=1,3
100 E(I)=E(I)+B(J)*A(I,J)
1000 FORMAT(1X, 10 E13.4)
COMMENT BACK CALCULATION
14 WRITE(6,15)
15 FORMAT(/10X27HRESULTS OF BACK CALCULATION//6X6HCOUNTS7X8HOBBS COMP
1 6X9HCALC COMP6X10HDIFFERENCE/)
DELT=0.0
DO 17 I=1,NDATA
SUM=0.0
DO 16 J=1,3
16 SUM=SUM+E(J)*DATA(I)**(J-1)
SUMS=COMP(I)-SUM
DELT=DELT+WT(I)*SUMS**2
17 WRITE(6,18) DATA(I),COMP(I),SUM,SUMS
18 FORMAT(F12.1,2F15.2,F16.3)
DELT=DELT/FLOAT(NDATA-NPOINT)
COMMENT MODIFY MATRIX TO VAR-COV.MATRIX
DO 20 I=1,3
DO 19 J=1,3
19 A(I,J)=A(I,J)*DELT
20 COEF(I)=SQRT(A(I,I))
WRITE(6,21) E,COEF,DELT
21 FORMAT(20X4HA(0)16X4HA(1)16X4HA(2)/1X4HCOEF10X3E20.10/1X7HSTD DEV
1 7X3E20.10/1X23HERROR SUM OF SQUARES = E20.10)
COMMENT START CALCUALTION OF UNKNOWNNS
WRITE(6,22)
22 FORMAT(1H1,10X8HUNKNOWNS//10X6HCOUNTS8X4HCOMP9X7HSTD DEV/)
23 READ(5,6) NPNT,(TEMP(I),I=1,NPNT)
IF(NPNT.EQ.13) GO TO 1
24 SUM=0.0
DO 25 I=1,NPNT
25 SUM=SUM+TEMP(I)
SUM=SUM/FLOAT(NPNT)
SUMS=0.0
DO 26 I=1,3
26 SUMS=SUMS+E(I)*SUM**(I-1)
TEMP(1)=1.0
TEMP(2)=SUM
TEMP(3)=SUM**2
TEMP(4)=E(2)+2.0*SUM*E(3)
DELT=0.0
DO 27 I=1,3
DO 27 J=1,3
27 DELT=DELT+TEMP(I)*TEMP(J)*A(I,J)
DELT=DELT+TEMP(4)**2*SUM
DELT=SQRT(ABS(DELT))
WRITE(6,28) SUM,SUMS,DELT
28 FORMAT(F16.1,F12.2,F16.3)
GO TO 23
END

```

## SIBFTC INVERT

```

SUBROUTINE INVERT (A,N)
C   HI COMPUTER.  WORKING VERY HARD TODAY, QUESTION MARK.
C   DOUBLE PRECISION D,HOLD,BIGA
C   DOUBLE PRECISION A(28,28)
   DIMENSION A(28,28)
   DIMENSION          L(28),M(28)
   D=1.0
   DO80 K=1,N
   L(K)=K
   M(K)=K
   BIGA=A(K,K)
   DO20 I=K,N
   DO20 J=K,N
   IF(ABS (BIGA)-ABS(A(I,J))) 10,20,20
10  BIGA=A(I,J)
   L(K)=I
   M(K)=J
20  CONTINUE
   J=L(K)
   IF(L(K)-K) 35,35,25
25  DO30 I=1,N
   HOLD=-A(K,I)
   A(K,I)=A(J,I)
30  A(J,I)=HOLD
35  I=M(K)
   IF(M(K)-K) 45,45,37
37  DO40 J=1,N
   HOLD=-A(J,K)
   A(J,K)=A(J,I)
40  A(J,I)=HOLD
45  DO55 I=1,N
46  IF(I-K)50,55,50
50  A(I,K)=A(I,K)/(-A(K,K))
55  CONTINUE
   DO65 I=1,N
   DO65 J=1,N
56  IF(I-K) 57,65,57
57  IF(J-K) 60,65,60
60  A(I,J)=A(I,K)*A(K,J)+A(I,J)
65  CONTINUE
   DO75 J=1,N
68  IF(J-K)70,75,70
70  A(K,J)=A(K,J)/A(K,K)
75  CONTINUE
   D=D*A(K,K)
   A(K,K)=1.0/A(K,K)
80  CONTINUE
   K=N
100 K=(K-1)
   IF(K) 150,150,103

```

```
103  I=L(K)
      IF(I-K) 120,120,105
105  DO110 J=1,N
      HOLD=A(J,K)
      A(J,K)=-A(J,I)
110  A(J,I)=HOLD
120  J=M(K)
      IF(J-K) 100,100,125
125  DO130 I=1,N
      HOLD=A(K,I)
      A(K,I)=-A(J,I)
130  A(J,I)=HOLD
      GO TO 100
150  RETURN
      END
```

Fig. D-2: Sample Input for CURVFT Program

```

$ENTRY
  19 TIO2 FOR C-6,C-14,C-18, CORRECTED FOR DRIFT, BACKGROUND
  3 15.24 336 374 328
  3 15.24 389 375 393
  3 16.84 485 440 482
  3 20.56 519 501 507
  3 20.56 513 533 533
  3 20.56 591 580 571
  3 27.0 747 671 708
  3 48.25 1392 1351 1437
  3 48.25 1360 1338 1322
  3 49.25 1393 1454 1444
  3 49.25 1334 1397 1413
  3 49.71 1179 1297 1533
  3 49.71 1303 1377 1358
  7 49.71 1369 1411 1369 1320 1307 1309 1399
  3 49.71 1381 1410 1408
  3 51.68 1352 1400 1451
  9 51.68 1365 1381 1474 1443 1464 1470 1363 1402 1383
  4 51.68 1439 1417 1353 1421
  3 52.65 1402 1479 1461
  3 1360 1324 1340
  3 1171 1245 1318
  3 1381 1303 1315
  3 400 386 410
  4 400 445 475 483
  4 1249 1181 1174 1371
  3 1213 1129 1061
  3 1394 1373 1400
  4 1268 1268 1306 1300
  4 1343 1422 1356 1315
  5 1275 1197 1188 1228 1157
  5 1173 1169 1171 1260 1197
$IBSYS

```

CD TOT 0034

Fig. D-3: Sample Output for Determination of  $TiO_2$  in Rhombohedral  
Phases

$TiO_2$  FOR C-6,C-14,C-18, CORRECTED FOR DRIFT, BACKGROUND

COMP	AVG COUNTS	STD DEV	WEIGHT
15.2	346.0	20.067	0.00248
15.2	385.7	7.717	0.01679
16.8	469.0	20.543	0.00237
20.6	509.0	7.483	0.01786
20.6	526.3	9.428	0.01125
20.6	580.7	8.179	0.01495
27.0	708.7	31.031	0.00104
48.3	1393.3	35.122	0.00081
48.3	1340.0	15.577	0.00412
49.3	1430.3	26.713	0.00140
49.3	1381.3	34.101	0.00086
49.7	1336.3	147.172	0.00005
49.7	1346.0	31.379	0.00102
49.7	1354.9	39.837	0.00063
49.7	1399.7	13.226	0.00572
51.7	1401.0	40.423	0.00061
51.7	1416.1	43.758	0.00052
51.7	1407.5	32.538	0.00094
52.7	1447.3	32.887	0.00092

RESULTS OF BACK CALCULATION

COUNTS	OBS COMP	CALC COMP	DIFFERENCE
346.0	15.24	14.43	0.811
385.7	15.24	15.65	-0.408
469.0	16.84	18.24	-1.400
509.0	20.56	19.50	1.060
526.3	20.56	20.05	0.511
580.7	20.56	21.78	-1.222
708.7	27.00	25.94	1.064
1393.3	48.25	49.88	-1.628
1340.0	48.25	47.91	0.342
1430.3	49.25	51.25	-2.004
1381.3	49.25	49.43	-0.183
1336.3	49.71	47.77	1.936
1346.0	49.71	48.13	1.581
1354.9	49.71	48.46	1.255
1399.7	49.71	50.11	-0.403
1401.0	51.68	50.16	1.518
1416.1	51.68	50.72	0.956
1407.5	51.68	50.40	1.276
1447.3	52.65	51.89	0.761

	A(0)	A(1)	A(2)
COEF	0.42107849E 01	0.28462291E-01	0.30953670E-05
STD DEV	0.23679774E 01	0.65781286E-02	0.35585786E-05
ERROR SUM OF SQUARES =	0.45274906E-02		

Fig. D-3: (continued)

UNKNOWNNS		
COUNTS	COMP	STD DEV
1341.3	47.96	1.429
1244.7	44.43	1.382
1333.0	47.65	1.423
398.7	16.05	0.735
450.8	17.67	0.723
1243.8	44.40	1.381
1134.3	40.48	1.358
1389.0	49.72	1.472
1285.5	45.91	1.397
1359.0	48.61	1.443
1209.0	43.15	1.373
1194.0	42.61	1.369

00922 U KRETSCHMAR  
SIBSYS

030

000MIN 19SEC COST\$001.42

Appendix E: Recalculation Procedures for Electron Probe  
and Chemical Analyses

Since probe analyses and simple chemical analyses do not allow determination of the oxidation state of Fe, the Fe content of the analysed oxide minerals had to be apportioned between FeO and Fe<sub>2</sub>O<sub>3</sub>, using Carmichael's recalculation procedures which assume stoichiometric oxide phases (I.S.E. Carmichael, 1967). Examples of non-stoichiometry are known. Akimoto et al. (1957) produced one-phase spinels which seem to contain excess Ti; however, Akimoto and Katsura (1959) state that these phases are metastable and rare in nature. This was first suggested by Vincent et al. (1957) and has been accepted by many subsequent investigators including I.S.E. Carmichael (1967), Wright (1965), and Buddington and Lindsley (1964).

An example of the recalculation of rhombohedral phases is given in Table E-1 for the chemical analysis of hemo-ilmenite C-15. Before recalculation of the chemical analysis, corrections must be made for impurities in the mineral separates. A modal count of the impurities in C-15 hemo-ilmenite showed 1.4 volume % pyroxene and 1.0 volume % garnet. The composition of the garnet impurity was determined from optical properties and X-ray determination of the unit cell, using the determinative tables of Winchell (1961) to be approximately pure almandine. Subsequent chemical analysis of this garnet confirmed this identification (I. Mason, personal communication). The composition of

pyroxene in the outer mafic-rich margin of the anorthosite is very constant, judging from five chemical analyses of these pyroxenes (I. Mason, personal communication). The average of these five (column II, Table E-1) is thought to represent a valid approximation to the composition of the contaminating pyroxene. The corrected analysis of hemo-ilmenite C-15 is shown in Column IV, Table E-1. In Column V this analysis is recalculated to molecular proportion oxides.

The steps for recalculation of molecular proportions to molecular % hematite and ilmenite are as follows:

1. Ilmenite is formed by combining molecular proportions of  $\text{FeO} + \Sigma\text{RO}$  with  $\Sigma(\text{TiO}_2 + \text{SiO}_2)$  in the ratio 1:1 (where RO are MgO, MnO, CaO etc.).
2. The molecular proportion FeO used in step 1. is subtracted from the total FeO.
3. The FeO remaining is recalculated as equivalent  $\text{Fe}_2\text{O}_3$  by dividing the molecular proportion FeO by two (as in norm calculations). The ratio  $\text{FeO}/\text{Fe}_2\text{O}_3$  is thus  $339.07/269.09$ , which gives 24.36% FeO and 42.97%  $\text{Fe}_2\text{O}_3$  on back calculation to wt. %.

The recalculated analysis now totals 96.48% which is acceptable considering that MgO, which is at least 1.0 wt. % (see section V-2), was not determined. Also, the correction for impurities accounts for another 2% of the total. Since the chemical analysis was not complete, recalculation of the analysis to 100 wt. % is not warranted.

4. Using molecular proportions of oxides:

$$\frac{\Sigma\text{Fe}_2\text{O}_3 \text{ (including } \text{Fe}_2\text{O}_3\text{)}}{\Sigma\text{Fe}_2\text{O}_3 + \Sigma(\text{TiO}_2 + \text{SiO}_2)} \times 100 = \text{mol. \% hematite}$$

Table E-1: Analysis of C-15 hemo-ilmenite separate (wt.%) and  
recalculation to mol.% hem-ilm

	hematite- ilmenite (wt.%)***	average pyroxene	pure almadine	hem-ilm corrected for imp.	hem-ilm mol. prop. x 1000
SiO <sub>2</sub>	1.05	48.95	36.20	00.00	
TiO <sub>2</sub>	28.07	0.72		28.06	351.19
Al <sub>2</sub> O <sub>3</sub>	0.46	5.82	20.48	0.18	1.77
Fe <sub>2</sub> O <sub>3</sub>		2.98 <sup>++</sup>			
FeO	63.57 <sup>+</sup>	8.13	43.30	63.03	877.24
MnO	0.86	0.17	0.5*	0.86	12.12
MgO	**	10.73			
CaO	0.25	21.72		0.00	
Na <sub>2</sub> O		0.78			
K <sub>2</sub> O		0.05			
Cr <sub>2</sub> O <sub>3</sub>	0.05	0.02		0.05	0.33
Sum	94.31	100.07	100.48	92.18	

\* semi-quantitative probe analysis on some garnets in sample C-15 showed the presence of approx. 0.5% MnO.

+ all Fe determined as FeO

++ Fe<sub>2</sub>O<sub>3</sub> recalculated as equivalent FeO purposes of correction of C-15 analysis.

\*\* probe analysis shows approx. 1% MgO in ilmenite (see section V-2). MgO not determined.

\*\*\* Chemical analysis from Table V-1-2.

It is this value which is applied to the experimental data of Buddington and Lindsley.

Chemical analyses recalculated in this manner provide mol.% compositions that are probably precise to within  $\pm 5\%$ . For probe analyses precision is probably somewhat less (see section V-2).

Recalculation of probe analyses of homogeneous ilmenite and hematite-ilmenite (Table V-2-3 and V-2-4) proceed in a similar manner. The FeO of the analyses apportioned between FeO and  $\text{Fe}_2\text{O}_3$  in the above outlined manner is shown in columns III and IV of these tables.

It was noticed that the hematite content of homogeneous rhombohedral phases can be obtained very simply by referring the  $\text{TiO}_2$  content as determined either by electron probe analysis or chemical analysis to a theoretically calculated curve of wt.%  $\text{TiO}_2$  versus mol.% hematite in the rhombohedral phase. Such a curve can be represented by the equation:

$$y = -0.5265 x + 52.65 \quad (\text{E-1})$$

where  $x$  = mol.% hematite in rhombohedral phase

$y$  = wt.%  $\text{TiO}_2$  in the rhombohedral phase.

Testing of Carmichael's (1967) analyses of rhombohedral phases with this equation shows that the mol.% hematite obtained almost invariably agrees to within 1% of the value obtained by the more extensive recalculation procedures outlined above. Generally agreement is much better than 1%. For analyses containing large amounts of RO (up to 4%) other than FeO the agreement is not as good, but never differs by more than 1.9%.

For ulvospinel in magnetite, the theoretical equation is:

$$y = 0.3573 x \quad (E-2)$$

where  $x$  = mol.% usp in magnetite

$y$  = wt.%  $TiO_2$  in magnetite

Agreement between mol.% usp obtained by Carmichael's calculations and those obtained from equation E-2 is even better than for the rhombohedral phase.

These observations suggest that if  $TiO_2$  can be accurately determined, and the oxide phase does not contain too many impurities, equations E-1 and E-2 provide a rapid and convenient way of obtaining mol.% end members in homogeneous oxides. For comparative purposes column VI of Tables V-2-4 and V-2-3 presents mol.% hematite obtained in this manner.

## Appendix F: Electron Probe Data Corrections and Evaluations of Errors

Detailed calculations using the methods of Long and Reed (1964) and Reed (1965) were carried out in order to evaluate various uncertainties inherent in electron probe microanalysis of Fe-Ti oxides. The effect of absorption in particular was expected to be large, because of the low spectrometer takeoff angle of the Acton microprobe. Only a brief outline of the procedures for calculation of each correction are given because they are fairly involved. They are carried out for pure metal standards, because this maximizes the corrections. When standards whose composition is close to the unknowns are used, the corrections will be much smaller.

### I. Example of calculations for hematite-ilmenite grain from sample C-5B:

#### 1. Operating Conditions

Element Analysed	Radiation Used	Wavelength in $\text{\AA}$	Analysing crystal	d spacing in $\text{\AA}$
Fe	FeK $_{\alpha}$	1.94	10 $\bar{1}$ 1 qtz	3.343
Ti	TiK $_{\alpha}$	2.75	10 $\bar{1}$ 0 qtz	4.246

Beam current runoff on Fe metal: 150 microamps

Specimen Current: 80 nanoamps

Beam current: 16 KV

#### 2. Measured Intensities on Specimen and Standard (counts/sec)

		background
Fe metal standard	2348	3

		background
Fe on specimen	858	3
Ti metal	522	4
Ti on specimen	135	4

### 3. Dead Time Correction

For counting rates below 5000 counts/sec., dead time corrections are not significant (Adler, 1966; Keil, 1967; Reed and Long, 1964). Counting rates were always below this figure and consequently dead time corrections were not applied.

### 4. Background Correction

Background was measured by noting the counts obtained on a mineral containing none of the element being analysed for, e.g. Al background measured on magnetite 64019 (0.00 % Al). Also, counts for the element of interest were taken on pure metal standards that contained none of the element.

Background counts were subtracted only if they satisfied the more or less arbitrary criterion that peak to background ratio was greater than 20. Generally the ratio was much greater than this.

### 5. Calculation of apparent concentration (C)

$$\text{For Fe} \quad C = \frac{858}{2348} \times 100 = 36.54 \%$$

$$\text{For Ti} \quad C = \frac{135}{522} \times 100 = 25.86 \%$$

$$\text{Oxygen, by difference} \quad = 36.70 \%$$

### 6. Absorption Correction

The X-rays suffer partial absorption in emerging from the

specimen and this varies with the composition. It is therefore necessary to apply an absorption correction to compensate for differences between absorption coefficients of specimen and standard for the wavelength of the characteristic line used for analysis. Values of mass absorption coefficients of the elements were obtained from Heinrich (1966). For a compound, the mass absorption coefficient is:

$$\mu_{A,B,C,\dots}^A = \mu_A^A C_A + \mu_B^A C_B + \mu_C^A C_C + \dots, \quad (F-1)$$

(Adler & Goldstein, 1965)

where  $\mu_C^A$  is the mass absorption coefficient of element C for A radiation, and  $C_A$  is the wt. fraction of element A.

The parameter which determines X-ray absorption is:

$$\chi = \mu \operatorname{cosec} \theta, \text{ where } \theta \text{ is the takeoff angle (18}^\circ\text{).}$$

The next stage is to evaluate the function  $f(\chi)$  for specimen and standard, this quantity being the factor by which the X-ray intensity is reduced by absorption.

The formula for  $f(\chi)$  is:

$$f(\chi) = \left(1 + \frac{\chi}{\sigma}\right) \left(1 + \frac{h\chi}{\sigma}\right) \quad (F-2)$$

The quantity  $h$  is a function of the composition of the specimen.

The function ' $\sigma$ ' is mainly dependent of the accelerating voltage of the electron beam, but it is also somewhat dependent on the atomic number of the analysed element.

To correct for absorption the apparent concentration must be multiplied by the absorption correction factor which is equal to  $f(\chi_0)/f(\chi_1)$  where  $\chi_0$  and  $\chi_1$  are for standard and specimen res-

pectively. Assuming that only Fe and Ti are present in appreciable quantities the values listed in Table F-1 are obtained for the quantities mentioned above.

Table F-1: Values of critical parameters for absorption correction

Absorption coefficients		f (%)	original concentration	corrected concentration
$\mu_{\text{Ti}}^{\text{Fe}}$	71.0			
		for Fe 1.043	36.54	38.11
$\mu_{\text{hem-ilm}}^{\text{Fe}}$	134.1			
$\mu_{\text{Fe}}^{\text{Ti}}$	111.0			
		for Ti 1.010	25.86	26.11
$\mu_{\text{hem-ilm}}^{\text{Ti}}$	122.8			

Contrary to expectation, the effect of absorption on the composition of the hem-ilm grain is small.

## 7. Fluorescence Correction

Sometimes part of the measured characteristic intensity arises from fluorescence excited by other characteristic lines. This correction is necessary only if the lines emitted by the other elements lie on the short wavelength side of the absorption edge leading to the series line being measured. When K radiation is used for analysis, fluorescence may be excited by the K radiation from another element (K-K fluorescence) or by L radiation (L-K fluorescence). Similarly, when L radiation is used for analysis, either L-L or K-L fluorescence may occur. For a

given analysed element fluorescence is excited by radiation from elements with atomic numbers greater than or equal to a certain critical number. In the case of Fe (at. no. 26) and Ti (at. no. 22) the critical numbers are 28 and 24 respectively. Therefore only Ti must be corrected for fluorescence. The required correction factor is:

$1/1 + \gamma$ , in which  $\gamma$  is calculated from the formula:

$$\gamma = C_{Fe} \cdot F(A) \cdot D \cdot \frac{\mu_{Ti}^{Fe}}{\mu_{hem-ilm}^{Fe}} \quad (g(x) + g(y)) \quad (F-3)$$

The correction factor is that by which the uncorrected concentration must be multiplied. The terms in the formula are evaluated as follows:

- a)  $C_{Fe}$  is the mass concentration of the exciting element Fe.
- b)  $F(A)$  is a function of the analysed element Ti.
- c)  $D$  is a function of the accelerating voltage and of the difference in atomic numbers between Fe and Ti.
- d)  $\mu_{Ti}^{Fe}$  is the mass absorption coefficient of Ti for  $FeK_{\alpha}$  radiation.
- e)  $\mu_{hem-ilm}^{Fe}$  is the mass absorption coefficient of the specimen for the same radiation.
- f)  $g(x)$  and  $g(y)$  are functions of the absorption parameters 'x' and 'y'.

The absorption parameters are given by:

$$x = \frac{\mu_{Ti}^{Ti}}{\mu_{Fe}^{Ti}} \operatorname{cosec} \theta, \quad y = \frac{\sigma_{Fe}}{\mu_{Fe}^{Fe}}$$

In K-K fluorescence, the correction is largest when the exciting element is close to the analysed element in atomic number and is present in

large concentration. The correction is very small in analyses of the light elements (Na, Mg, Al ..... ) and can nearly always be neglected. In general it tends to increase with atomic number, becoming largest at the upper end of the range for which K lines are used.

In the case of hem-ilm grain from C-5B,  $1/1 + \gamma$  calculates to 0.973. The concentration of Ti corrected for fluorescence is thus 25.40 wt.%.

#### 8. Atomic Number Correction

The atomic number effect is roughly proportional to the difference in atomic number between specimen and standard. The factors involved are the rate of retardation of the incident electrons in the target and the loss of X-ray intensity due to some of the electrons leaving the target altogether. The phenomenon is complex and not completely understood (Adler, 1966, p. 203). Smith (1965) ignores this correction altogether. Because Fe and Ti are only a few atomic numbers removed, the effect is expected to be small.

## II. Conclusions:

Table F-2 summarizes the effect the various corrections had on the original concentration of Fe and Ti in a hem-ilm grain.

Table F-2: Effect of corrections on original concentration

Element	Concentration in Wt %			Difference between original estimate and final (wt %)
	Apparent	Corr. for Absorption	Corrected for Fluorescence	
Fe	36.54	38.11	38.11	+ 1.57
Ti	25.86	26.12	25.40	- 0.46
O	37.60	35.77	36.49	- 1.11

Recalculation of this analysis to mol % hematite-ilmenite by the methods outlined in Appendix E, shows that application of absorption and fluorescence corrections change the composition only from Hem<sub>24</sub> Ilm<sub>76</sub> to Hem<sub>27</sub> Ilm<sub>73</sub>. Random experimental error is expected to have a much greater effect than this, and therefore exact corrections are not warranted. The main sources of random error are counting statistics, probe current drift, focussing error, surface roughness, and fluorescence effects due to inhomogeneous areas in the specimen. Counting statistics are such that for a total of N counts, the standard deviation is  $\sqrt{N}$ , therefore the relative error is reduced by increasing N. Minimization of the other sources of error has been dealt with in the sections on probe analyses, description of the CURVFT program and sample preparation.

Systematic errors arise mainly from the correction calculations not being completely accurate. These need not be dealt with further.

Appendix G : Plates & Figures

**Plate 1**

EXPLANATION OF PLATE 1

Fig. 1. Feldspar with minute inclusions of oxides, remobilized oxides at grain boundaries; and euhedral garnet.

Sample C-2. Magnification 100X.

Fig. 2. (O) Dendritic oxides in cracks in feldspar.  
(P) Pyroxene with minute rods of oxides.  
(A) Amphibole.

Sample C-2. Magnification 250X.

Plate 1

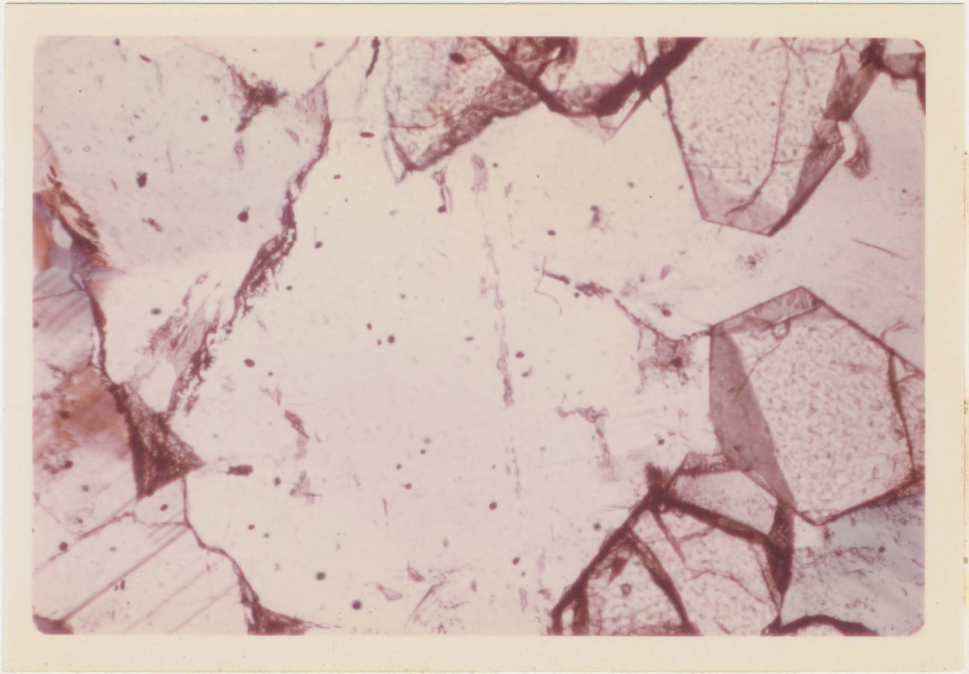


Fig. 1



Fig. 2

**Plate 2**

EXPLANATION OF PLATE 2

Fig. 1. Rods of oxide mineral in pyroxene and incipient alteration of pyroxene.

Sample C-5B. Magnification 400X.

Fig. 2. Opaque mineral in cleavage plane of amphibole. Composite photo was taken by focusing through the mineral along an inclined cleavage plane at three different positions and joining the photos so obtained.

Sample C-5B. Magnification 640X.

Plate 2

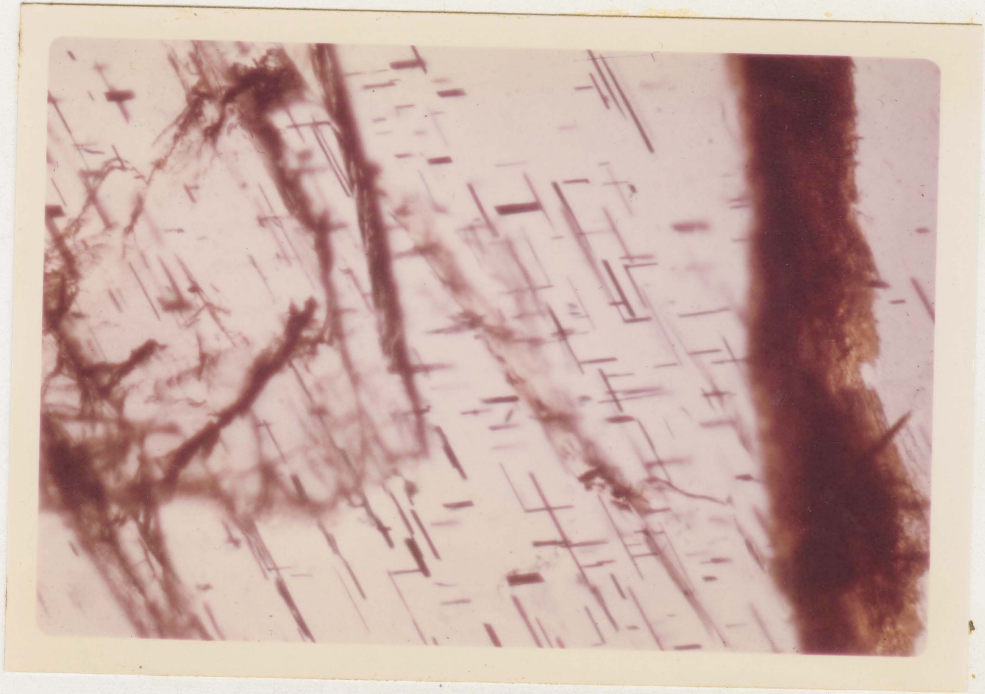


Fig. 1



Fig. 2

Plate 3

### EXPLANATION OF PLATE 3

Fig. 1. Photomicrograph of representative portion of polished thin section of sample C-5B showing:

1. Polishing appearance and irregular cracks in euhedral magnetite.
2. Reaction rim where hemo-ilmenite is in contact with magnetite.
3. Typical exsolution texture in the hemo-ilmenite.
4. Appearance of euhedral, altered, interstitial pyrite.

Magnification 32X.

Line on photo indicates a possible electron beam traverse that would produce trace closely similar to Fig. V-2-1, A.

Fig. 2. Thin slivers of magnetite replacing ilmeno-hematite along the (001) plane in hemo-ilmenite.

Sample C-14. Magnification 400X.

Plate 3



Fig. 1

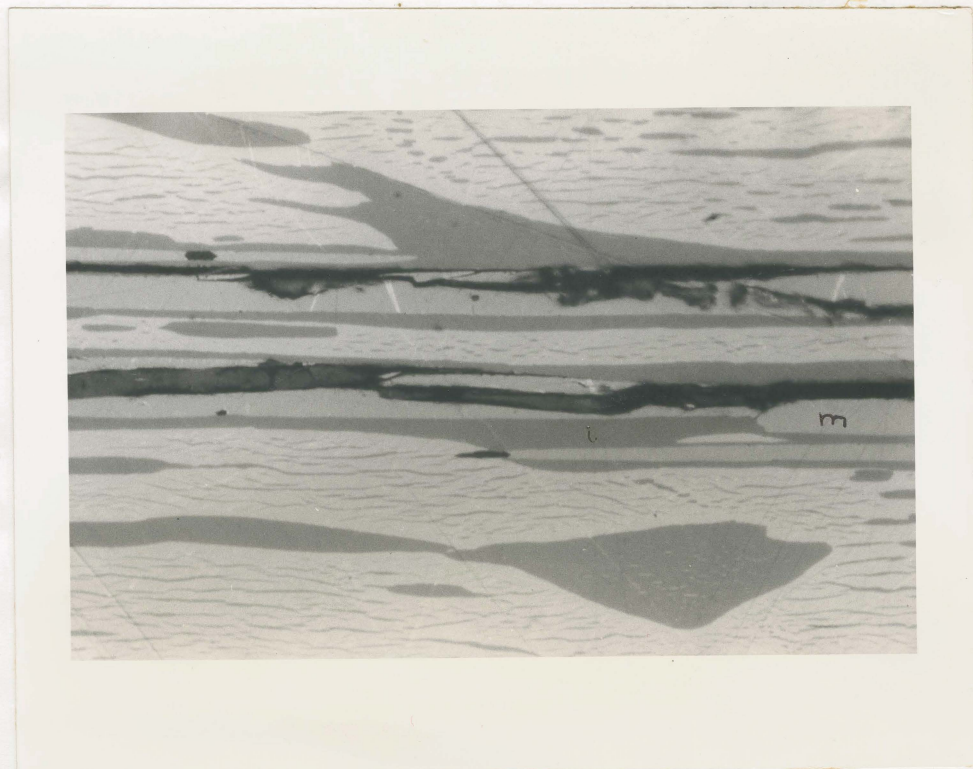


Fig.2

Plate 4

EXPLANATION OF PLATE 4

Fig. 1. Typical hematite exsolution lamellae in hemo-ilmenite, showing reaction relationship with magnetite.

Sample C-4A. Magnification 32X.

Fig. 2. Appearance of typical hemo-ilmenite with maximum amount of ilmeno-hematite exsolved from it.

Sample C-15. Magnification 32X.

Plate 4

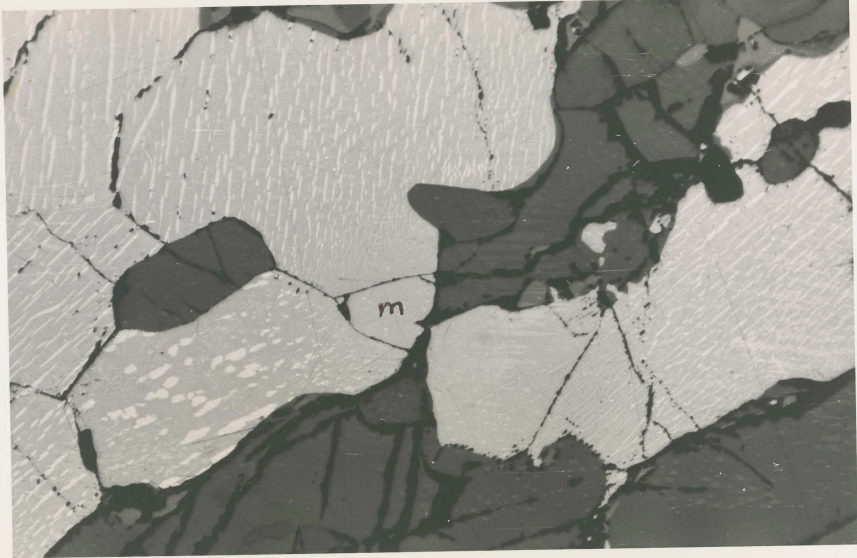


Fig. 1

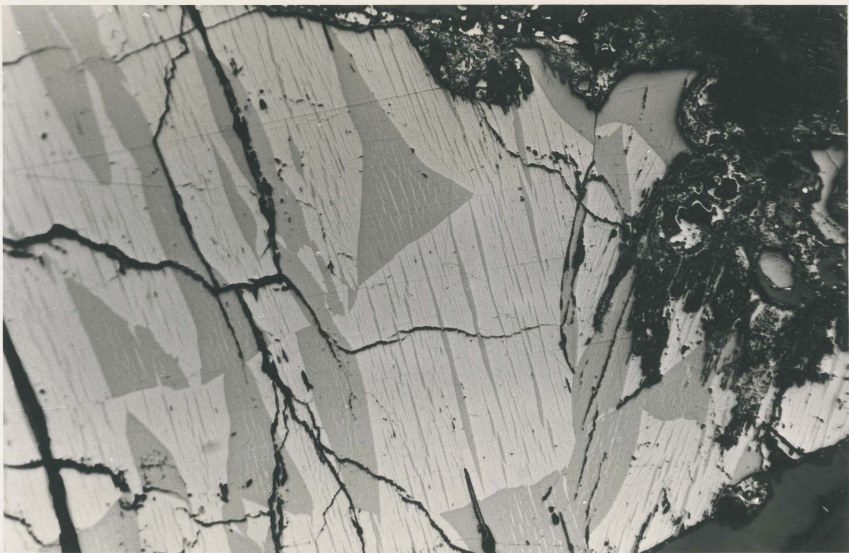


Fig. 2

Plate 5

EXPLANATION OF PLATE 5

Fig. 1. Skeletal-graphic intergrowth of ilmenite with garnet.

Sample C-9. Magnification 32X.

Fig. 2. Sulfide minerals almost completely altered to secondary iron minerals.

Sample C-9. Magnification 160X.



Fig. 1

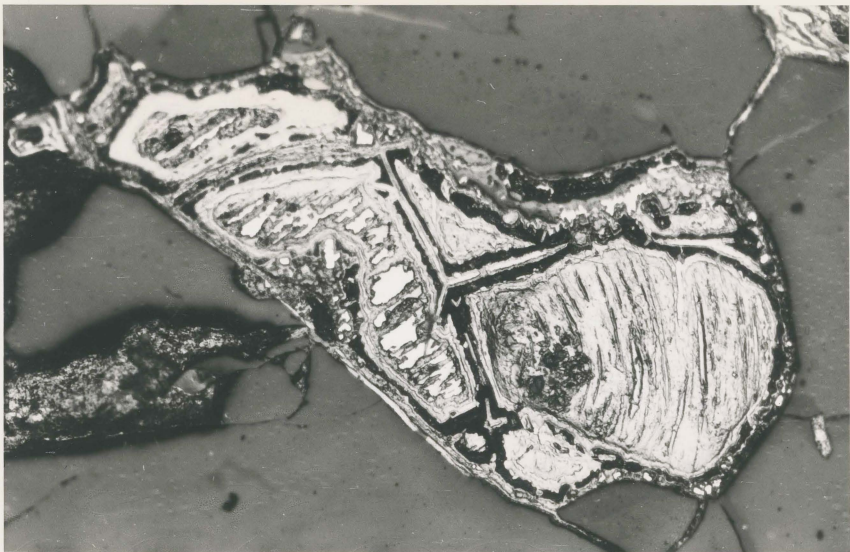


Fig. 2

Plate 6

EXPLANATION OF PLATE 6

Fig. 1. Remobilized hemo-ilmenite injected along cleavage planes of amphibole.

Sample C-4. Magnification 50X.

Fig. 2. Magnetite-hemo-ilmenite contact with polishing imperfections.

Sample C-5. Magnification 640X.

Plate 6

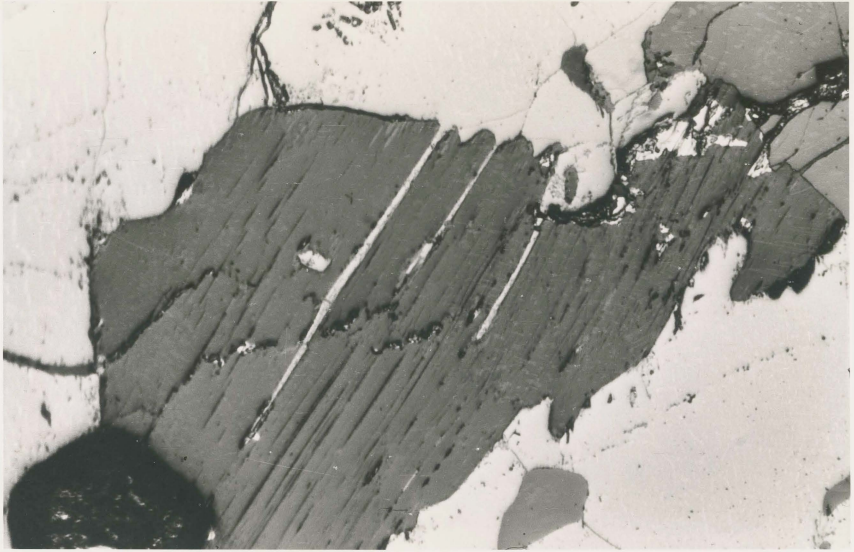


Fig. 1

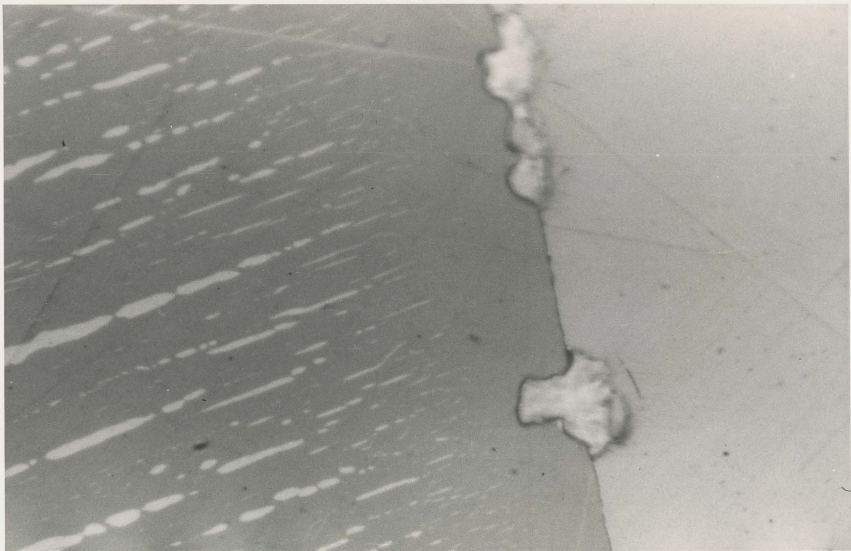


Fig. 2

#### BIBLIOGRAPHY

- Abdullah, Mohamed I., 1965: The Fe-Ti Oxide Phases in Metamorphism, in: Controls of Metamorphism, W.S. Pitcher, G.W. Flinn, eds., Oliver and Boyd; Edinburgh and London, p. 274-280.
- \_\_\_\_\_ & Atherton, M.P., 1964: The Thermometric Significance of Magnetite in Low Grade Metamorphic Rocks, Am. J. Sci., v. 262, p. 904-917.
- Ade-Hall, J.W., 1964: Electron-Probe Microanalyser Analyses of Basaltic Titanomagnetites and their Significance to Rock Magnetism, J. Roy. Astronom. Soc., v. 8, no. 3, p. 301-312.
- Adler, I., 1966: X-Ray Emission Spectrography in Geology, Elsevier Publishing Co.; N.Y., 258 p.
- \_\_\_\_\_ & Goldstein, J., 1965: Absorption Tables for Electron Probe Microanalysis, N.A.S.A. Tech. Note D-2984: Goddard Space Flight Centre, 276 p.
- Akimoto, S., Katsura, T. & Yoshida, N., 1957: Magnetic Properties of  $TiFe_2O_4 - Fe_3O_4$  System and their Change with Oxidation, J. Geomag. and Geoelectr., v. 9, p. 165-178.
- \_\_\_\_\_, Nagata, T. & Katsura, T., 1957 a: The  $TiFe_2O_5 - Ti_2FeO_5$  Solid Solution Series, Nature, v. 179, p. 37-38.
- \_\_\_\_\_ & Katsura, T., 1959: Magneto-Chemical Study of the Generalized Titanomagnetite in Volcanic Rocks, J. Geomag. and Geoelectr., v. 10, p. 60-90.

- Anderson, A. T., 1965: Electron Microprobe Analyses of Magnetite and Ilmenite in five dike rocks, (Abstr. only), Trans. Am. Geophys. Union, 47th Ann. Mtg., p.210.
- \_\_\_\_\_, 1965a: The Crystallization Differentiation of the Labrieville Anorthosite in Terms of T and  $f_{O_2}$ , (Abstr. only), Trans. Am. Geophys. Union, 47th Ann. Mtg., p. 209.
- \_\_\_\_\_, 1966a: Mineralogy of the Labrieville Anorthosite, P.Q., Am. Min., v. 51, p. 1671-1712.
- \_\_\_\_\_, 1966b: Microprobe analysis of magnetite and ilmenite (unpublished report), Written communication, 1966, 15 p.
- Aoki, K., 1966: Phenocrystic spineliferous titanomagnetites from trachyandesites, Iki Island, Japan, Am. Min., v. 51, p. 1799-1805.
- Baird, D. C., 1962: An Introduction to Measurement Theory and Experiment Design, Prentice-Hall, Inc.; Englewood Cliffs, N. J., 198 p.
- Basta, E. Z., 1957: Accurate Determination of the Cell Dimensions of Magnetite, Min. Mag., v. 31, p. 431-442.
- \_\_\_\_\_, 1960: Natural and Synthetic Titanomagnetites (The System  $Fe_3O_4$ - $Fe_2TiO_4$ - $FeTiO_3$ ), N. Jahrbuch Min., Abh., v. 94<sup>2</sup> p. 1017-1048.
- Best, M. G. & Mercy, E. L. P., 1967: Composition and Crystallization of Mafic Minerals in the Guadalupe Igneous Complex, Calif., Am. Min., v. 52, p. 436-474.

- Bolfa, J., de la Roche, H., Kern, R. & Capitant, M., 1961:  
Sur la nature minéralogique exacte d'exsolutions dans les  
"ilménites" de Vohibarika (Madagascar) déterminée à la  
microsonde électronique, Bull. Soc. franc. Miner. Crist.,  
v. 84, p. 400-401.
- Bowes, D.R. & Park, R.G., 1966: Segregation Banding in the Lewisian  
of Gairloch, Ross-Shire, J. Petrol., v. 7, p. 306-330.
- Buddington, A.F., 1961: The Origin of Anorthosite Re-evaluated,  
Geol. Surv. of India Records, v. 86, p. 421-432.
- \_\_\_\_\_, 1964: Distribution of MnO Between Coexisting Ilmenite and  
Magnetite, in: Advancing Frontiers in Geology and Geo-  
physics; Hyderabad, India, p. 233-248.
- \_\_\_\_\_ & Balsley, J.R., 1961: Microintergrowths and Fabric of Fe-Ti  
Oxide Minerals in some Adirondack Rocks, in: Mahadevan Vol.,  
M.S. Krishnan, ed., Osmania Press; Hyderabad, India,  
p. 1-16.
- \_\_\_\_\_, Fahey, J. & Vlisidis, A., 1955: The Thermometric and  
Petrogenetic Significance of Titaniferous Magnetite, Am.J. Sci.,  
v. 253, p. 497-532.
- \_\_\_\_\_, Fahey, J. & Vlisidis, A., 1963: Degree of Oxidation of  
Adirondack Fe Oxide and Fe-Ti Oxide Minerals in Relation  
to Petrogeny, J. Petrol. v. 4, p. 138-169.
- \_\_\_\_\_ & Lindsley, D.H., 1964: Iron-Titanium Oxide Minerals and  
their Synthetic Equivalents, J. Petrol., v. 5, p. 310-357.

- Carmichael, C. M., 1959: Remanent Magnetism of the Allard Lake Ilmenites, *Nature*, v. 183, p. 1239-1241.
- \_\_\_\_\_, 1961: The Magnetic Properties of Ilmenite-Hematite Crystals, *Proc. Royal Soc.*, v. 263A, p. 508-530.
- \_\_\_\_\_, 1965: The Present State of Rock Magnetism with Particular Reference to the Magnetite Ulvospinel System, *J. of Geomagnetism and Geoelectricity*, v. 17, p. 3-4.
- Carmichael, I. S. E., 1967: The Iron-Titanium Oxides of Salic Volcanic Rocks and their Associated Ferromagnesian Silicates, *Contr. Min. and Petr.*, v. 14, No. 1, p. 36-64.
- Chinner, G. A., 1960: Pelitic Gneisses with Varying Ferrous/Ferric Ratios from Glen Clova, Angus, Scotland, *J. Petrol.*, v. 1, p. 178-217.
- Deer, W. A., Howie, R. A. & Zussman, J., 1966: An Introduction to the Rock-forming Minerals, J. Wiley & Sons Inc.; New York, 528 p.
- Duchesne, J. C., 1966: Separation Rapide des mineraux des roches, *Annales de la Soc. Geol. de Belgique*, v. 89, Bull.#8, p. 347-356.
- Eugster, H. P., 1959: Reduction and Oxidation in Metamorphism, in: *Researches in Geochemistry*, v. 1, P. Abelson, Ed., J. Wiley & Sons; New York, p. 397-426.
- Evans, B. W., 1967: Mineralogy as a Function of Depth in the Prehistoric Makaopuhi Lava Lake, Hawaii, *Contr. Min. Petr.*, v. 17, p. 85-115 (pub. 1968).

- Evrard, P., 1944: (not consulted in original), Ann. Soc. Geol. Belgique, v. 66, p. 110.
- Freud, H., 1966: Applied ore Microscopy. Theory and Technique, Collier-Macmillan Ltd.; Toronto, 607 p.
- Girault, J. P., 1953: Sur un Spinelle Titanifère de Formule  $TiFe_2O_4$ , Provenant du lac de la Blache, Comté du Saguenay, Le Naturaliste Canadien, v. IX, No. 12, p. 307-311.
- Gjelsvik, T., 1957: Geochemical and Mineralogical Investigations of Titaniferous Iron Ores, W. Coast of Norway, Ec. Geol., v. 52, p. 482-498.
- Hagner, A. F. & Collins, L. G., 1967: Magnetite Ore Formed During Regional Metamorphism, Ausable Mte. District, N. Y., Ec. Geol., v. 62, p. 1034-1071.
- Hammond, 1952: Allard Lake ilmenite deposits, Ec. Geol., v. 47, p. 634-649.
- Hargraves, R. B., 1962: Petrology of the Allard Lake Anorthosite Suite, Quebec, in: Petrologic Studies: A Volume in Honour of A. F. Buddington, Geol. Soc. Am., 1962, p. 163-190.
- Haughton, D. R., 1967: A mineralogical Study of Scapolite, Unpublished M.Sc. thesis, McMaster University, 125 p.
- Heier, Knut, 1956: Thermometric and Petrogenic Significance of Titaniferous Magnetite - Discussion, Am. J. Sci., v. 254, p. 506-515.
- Heinrich, K. J. F., 1966: Mass Absorption Coefficients for  $K_{\alpha}$  Lines, in: The Electron Microprobe, McKinley, Heinrich & Wittry, eds., J. Wiley & Sons, Inc.; N. Y., p. 351-376.

- Hubaux, A., 1956: Différent types de minerais noirs de la région d'Egersund (Norvege): Ann. de la Soc. Géol. de Belg., t. 79, p. 203-215.
- James, R.S., 1965: The Properties of Sodalite and its Petrogenesis at the Princess Quarry, Bancroft, Ont., unpublished M.Sc. Thesis, McMaster University, 142 p.
- Keil, K., 1967: The Electron Microprobe X-Ray Analyzer and its Application in Mineralogy, Fortschr. Min., v. 44, p. 4-66.
- Klemm, D.D., 1965: Bemerkungen zur Quantitativen Messung von Diffusionsvorgaengen in Erzlagerstaetten mit Hilfe der Elektronen Mikrosonde, Geol. Rundschau, v. 55, p. 359-365.
- Klug, H.P. and Alexander, L.E., 1954:  
X-Ray Diffraction Procedures for Polycrystalline and Amorphous Materials, J. Wiley & Sons, Inc.; N.Y., 716 p.
- Kranck, E.H., 1961: The tectonic Position of the Anorthosites of Eastern Canada, 75 - Års Festskrift Suomen Geologinen Seura, p. 299-320.
- Krause, H., 1965: Mineralien und ihre Verteilung auf der Ilmenitlagerstaette von Abu Ghalaga, Aegypten, N. Jb. Miner. Abh., v. 104, p. 29-52.
- \_\_\_\_\_, 1967: Beobachtungen am Ilmenit Feingefuege, N. Jb. Miner. Mh., 1967, p. 179-183.
- Lacy, W.C., 1960: Geology of the Dunchurch Area, Geol. Soc. Am., Bull. v. 71, p. 1713-1717.

- Lindsley, D.H., 1962: Investigation in the System  $\text{FeO-Fe}_2\text{O}_3\text{-TiO}_2$ ,  
Geophys. Lab. Ann. Rept. (1961-1962), p. 100-106.
- \_\_\_\_\_ Equilibrium Relations of Coexisting Pairs of Fe-Ti Oxides,  
Geophys. Lab. Ann. Rept. (1962-1963), p. 60-66.
- Long, J.V.P., Reed, S.J.B., 1964: Calculating Corrections for Electron  
Probe Analysis, Private Instr. Manual, Dept. of Miner. &  
Petr., Cambridge Univ., 25 p.
- Marmo, V., 1959: On the  $\text{TiO}_2$ -Content of Magnetites as a Petrogenetic  
Hint, Am. J. Sci., v. 257, p. 144-149.
- Maucher, A. & Rehwald, G., 1961: Bildkartei der Erzmikroskopie,  
Umschau Vlg.; Frankfurt a.M., 1000 p.
- Naldrett, A.J., 1968: Melting Relations over a Portion of the Fe-S-O  
System and their Bearing on the Temperature of Crystallization  
of Natural Sulfide-Oxide Liquids, Geophys. Lab. Ann. Rept.  
(1966-1967), p. 419-422.
- Nichols, G.D., 1955: The Mineralogy of Rock Magnetism, Advances in  
Physics, v. 4, p. 113-190.
- Osborn, E.F., 1959: Role of Oxygen Pressure in the Crystallization  
and Differentiation of Basaltic Magma, Am. J. Sc., v. 257,  
p. 609-647.
- Petruk, W., 1964: The Analysis of Rocks and Ores by X-Ray Diffractometer,  
Can. Min., v. 8, Part 1, p. 68-85.
- Philpotts, A.R., 1966: Origin of the Anorthosite-Mangerite Rocks in  
Southern Quebec, J. Petrol. v. 7, p. 1-64.

- Philpotts, A.R., 1967: Origin of Certain Fe-Ti Oxide and Apatite  
Rocks, *Ec. Geol.*, v. 62, p. 303-315.
- Ramberg, H., 1952: *The Origin of Metamorphic and Metasomatic Rocks*,  
Univ. Chicago Press; Chicago, 317 p.
- Reed, S.J.B., 1965: Characteristic Fluorescence Correction in  
Electron Probe Microanalysis, *Br. J. Appl. Phys.*, v. 16,  
p. 913-926.
- Rose, E.R., 1960: Iron and Titanium in the Morin Anorthosite, Quebec,  
*Geol. Survey of Canada, Paper 60-11*, 12 p.
- \_\_\_\_\_, 1961: Iron and Titanium in the Anorthosite, St. Urbain, Que.,  
*Geol. Survey of Canada, Paper 61-7*, 25 p.
- Schwarcz, H.P., 1966: Chemical and Mineralogic Variations in an  
Arkosic Quartzite during Progressive Regional Metamorphism,  
*G.S.A., Bull.* v. 77, p. 509-532.
- Smith, J.V., 1965: X-Ray Emission Microanalysis of Rock-Forming  
Minerals I Experimental Techniques, *J. Geol.*, v. 73, p. 830-863.
- Stanton, R.L., 1964 a: Mineral Interfaces in Stratiform Ores,  
*Inst. Min. Met. Trans.*, v. 74, pt. 2, p. 45-79.
- \_\_\_\_\_, 1964 b: Textures of Stratiform Ores, *Nature*, v. 202, no. 4928,  
p. 173-174.
- Tatlock, D.B., 1966: Rapid Modal Analysis of some Felsic Rocks from  
Calibrated X-Ray Diffraction Patterns, *U.S. Geol. Surv.*,  
*Bull.* 1209, 41 p.
- Verhoogen, J. 1962 a: Oxidation of Iron-Titanium Oxides in Igneous Rocks,  
*J. Geol.*, v. 70, p. 168-181.

- Verhoogen, J. 1962 b: Distribution of Titanium between Silicates and Oxides in Igneous Rocks, *Am. J. Sci.*, v. 260, p. 211-220.
- Vincent, E.A., Wright, J.B., Chevallier, R., and Mathieu, S., 1957: Heating Experiments on some Natural Titaniferous Magnetites, *Mineralog. Mag.*, v. 31, p. 624-655.
- Winchell, A.N. & Winchell, H., 1961: Elements of Optical Mineralogy, Part II: Descriptions of Minerals. J. Wiley & Sons, Inc.; N.Y., 551 p.
- Wright, J.B. & Lovering, J.F., 1965: Electron-Probe Micro-Analysis of the Fe-Ti Oxides in some New Zealand Ironsands. *Min. Mag.* v. 35, p. 604-621.
- Zeller, C. & Babkine, J., 1965: Mise en évidence d'une loi reliant le paramètre cristallin au chimisme des titanomagnétites. *C.R. Acad. Sci. Paris*, t. 260, p. 1375-1379.

## ADDENDUM TO BIBLIOGRAPHY

- Eugster, H. P., Skippen, G. B., 1967: Igneous and Metamorphic Reactions Involving Gas Equilibria, *Researches in Geochemistry*, Vol. 2, . Abelson, ed., J. Wiley and Sons; New York, p. 492-520.
- Fyfe, W. S., Turner, F. J., Verhoogen, J., 1958: *Metamorphic Reactions and Metamorphic Facies*, Geol. Soc. America, New York, Memoir 73, 259 p.
- Speidel, D. H., 1965: Effect of MgO on Hem-Ilm, Mte-Usp Equilibria (Abstract), Am. Geophys. Union, Trans. 47th Ann. Meeting.
- Uyeda, S., 1958: *Jap. J. Geophys.* Vol. 2, 1-123; quoted in Carmichael, 1961.